

8-2017

Pharmacologic and Genetic Manipulations of Angiotensin Signaling in Thoracic Aortic Disease Models

Andrew M. Peters

Follow this and additional works at: https://digitalcommons.library.tmc.edu/utgsbs_dissertations



Part of the [Cell Biology Commons](#), [Medicine and Health Sciences Commons](#), and the [Pharmacology Commons](#)

Recommended Citation

Peters, Andrew M., "Pharmacologic and Genetic Manipulations of Angiotensin Signaling in Thoracic Aortic Disease Models" (2017). *The University of Texas MD Anderson Cancer Center UTHealth Graduate School of Biomedical Sciences Dissertations and Theses (Open Access)*. 801.
https://digitalcommons.library.tmc.edu/utgsbs_dissertations/801

This Dissertation (PhD) is brought to you for free and open access by the The University of Texas MD Anderson Cancer Center UTHealth Graduate School of Biomedical Sciences at DigitalCommons@TMC. It has been accepted for inclusion in The University of Texas MD Anderson Cancer Center UTHealth Graduate School of Biomedical Sciences Dissertations and Theses (Open Access) by an authorized administrator of DigitalCommons@TMC. For more information, please contact digitalcommons@library.tmc.edu.

PHARMACOLOGIC AND GENETIC MANIPULATIONS OF ANGIOTENSIN
SIGNALING IN THORACIC AORTIC DISEASE MODELS

by

Andrew Milton Peters, B.S.

APPROVED:

Dianna M. Milewicz, M.D., Ph.D.
Advisory Professor

Carmen W. Dessauer, Ph.D.

Edgar T. Walters, Ph.D.

Heinrich Taegtmeyer, M.D., D.Phil.

Jay Humphrey, Ph.D.

APPROVED:

Dean, The University of Texas
MD Anderson Cancer Center UTHHealth Graduate School of Biomedical
Sciences

PHARMACOLOGIC AND GENETIC MANIPULATIONS OF ANGIOTENSIN
SIGNALING IN THORACIC AORTIC DISEASE MODELS

A

DISSERTATION

Presented to the Faculty of

The University of Texas

MD Anderson Cancer Center UTHealth

Graduate School of Biomedical Sciences

in Partial Fulfillment

of the Requirements

for the Degree of

DOCTOR OF PHILOSOPHY

by

Andrew Milton Peters, B.S.
Houston, Texas

Date of Graduation *May, 2017*

Dedication

This is for my Grandpa (Russell Milton Peters), my Mammaw (Carolyn Rummel), and my Uncle John Rummel. I miss you all very much. I miss you too, Doris Taylor.

Acknowledgments

I would first like to say thank you to Dr. Milewicz. I am sorry I was such a pain. Thank you so much for your patience, mentorship, and guidance. You have an uncanny ability to push people to the limit and judge character (except perhaps me). You let me struggle, and I often stumbled. Your door was always open, but at times I was too determined to do it on my own. I need to get better at learning when to ask for help. I hope I make you proud someday. Please forgive me for my failures and wasting any of your time. Again, thank you.

Thank you to my many committee members and mentors. You are all saints. I cannot thank you enough for your time, patience, and guidance. I hope I have a shard of your wisdom and knowledge someday. I once told a friend in a moment of stress, "I am walking in the footsteps of giants." I still feel like that every day. I hope that I make you all proud as well.

I would like to thank my colleagues that have helped me along the way. There are too many of you to count, but three stand out. Thank you to Callie, Jiyuan, and Zhen. Callie, you kept me sane. Your advice always helped and reassured me. Jiyuan, thank you for all of your help, advice, and input. Your calm demeanor always helped me zone in. Zhen, thank you for all of your assistance and input. You often offered a fresh perspective on many of my later studies. I really appreciated it, and I could not have done it without your help.

I would like to thank my parents Mary Jo (Rummel) Peters and Douglas Andrew Peters. Your love, support, and teachings are major reason I have made it here. You two are an inspiration to me, and I hope that I have your strength and faith in the future. To my siblings, Derek, Julia, Jana, and Josh, you all inspire me to be better, and I am proud of each of you. I cannot thank you enough for your love and support.

To my grandparents, godparents, aunts, uncles, and cousins, family has always been important to me. You all helped me. I started unknowingly down this path with the death of my Grandpa, Russell Milton Peters, whose strength astounded me. Thank you, Grandpa. I also had a few other close family members pass away since then. I miss your compassion, Mammaw, (Carolyn Rummel), and your humor and wisdom Uncle John (Rummel), my Godfather. You were driving forces that kept me up at night. Also, thank you to my Granny (Frances Peters) and Grandpa (Kenneth Rummel). Thank you to my Godmother (Judy), and other Aunts and Uncles: Mike, Jeff, KK, Sally, Gaye-Ann, Jim, Adam, and Jody. You all lifted me up at some point on the way, and usually more than once. I would not be here if it were not for your support.

To my friends, thank you. You reminded me that it was OK to be human. Otherwise, I would have crumbled a long time ago. I hope to return the many favors.

To Jo, Betsy, and Melisa, God bless you. Thank you so much for all you have done.

Finally, I met you so late on this journey, but, Kendall Wright, thank you. I will always appreciate your strength, your courage, and your love. You understand me, and I do not know how. I love you.

AP

PHARMACOLOGIC AND GENETIC MANIPULATIONS OF ANGIOTENSIN SIGNALING IN THORACIC AORTIC DISEASE MODELS

Andrew Milton Peters, B.S.

Advisory Professor: Dianna M. Milewicz, M.D., Ph.D.

Thoracic aortic aneurysms and dissections (TAAD) are a major cause of morbidity and mortality in patients. Many different risk factors have been associated TAAD, but hypertension is the largest risk factor. Subsets of TAAD patients have identifiable syndromic genetic diseases, yet a number of genetic non-syndromic patients have been identified. Infusion of angiotensin II into mouse models causes aortic disease through inflammation and fibrosis. An angiotensin type I receptor (AT1R) blocker (ARB) or an angiotensin converting enzyme (ACE) inhibitor (ACEi) can reverse aortic pathology in some mouse models. I set out to better understand the relationship between angiotensin and TAAD in our mouse models, and hypothesized **that angiotensin II signaling through the AT1R contributes to thoracic aortic aneurysm formation in multiple model systems of disease, and that blocking related receptors in addition to the AT1R, such as the AT2R and Mas receptor, may have negative consequences.** Previously identified genetic variants in the gene encoding smooth muscle alpha-actin, *ACTA2*, were modeled with *Acta2*^{-/-} mice.

I found that the ascending aorta and aortic root in these mice become significantly dilated over time. *Acta2*^{-/-} mice are hypotensive, and increasing the blood pressure with a pharmaceutical and diet based regimen significantly accelerated and worsened the aortic phenotype. Treatment with losartan, an ARB, attenuated the aortic dilation, but captopril, an ACEi, did not decrease aortic growth and worsened the disease. Transverse aortic constriction (TAC) was used to study the ascending aorta and aortic root in response to increased biomechanical forces. Losartan attenuated the histologic and inflammatory changes associated with TAC, but captopril was again unable to rescue the phenotype. To understand why, I investigated other receptors blocked by ACEis: the angiotensin II type 2 receptor (AT2R) and the Mas receptor, a receptor for the Ang1-7 peptide. I found that cotreatment with captopril and an agonist for the AT2R had similar physiologic effects as the AT1R blocker despite being unable to prevent the fibrotic and inflammatory remodeling. In contrast, cotreatment with captopril and an agonist for the Mas receptor blocked remodeling but did not rescue aneurysm formation. My results, coupled with clinical data, indicate that fibrosis may be beneficial in the aorta, and show we must expand our understanding of the angiotensin system in aortic disease.

Table of Contents

Signature page -----	i
Title page -----	ii
Dedication -----	iii
Acknowledgment -----	iv
Abstract -----	vi
Table of contents -----	ix
List of figures -----	xiii
List of tables -----	xv
List of abbreviations -----	xvi
Chapter 1: Introduction -----	1
1.1 Structure of the aorta -----	2
1.2 Thoracic aortic disease and pathology -----	7
1.3 Angiotensin system -----	12
1.4 Angiotensin in animal models -----	14
1.5 Hypothesis tested -----	17
Chapter 2: Methods -----	18

2.1 Introduction -----	19
2.2 Mouse models -----	19
2.3 Transverse aortic constriction -----	20
2.4 Echo & Doppler studies -----	21
2.5 Non-invasive blood pressure monitoring and blood pressure measurements -----	24
2.6 Drug administration -----	25
2.7 Histomorphometric study -----	26
2.8 ImageJ analysis -----	28
2.9 Measurement of ROS in aortas by dihydroethidium (DHE) -----	29
2.10 RNA extraction and qPCR -----	30
2.11 2D-gel electrophoresis -----	31
2.12 NADPH oxidase activity assay -----	31
2.13 Calcium imaging -----	32
2.14 Statistical analysis -----	32
 Chapter 3: The <i>Acta2</i>^{-/-} mouse model of thoracic aortic disease: source of increased AngII signaling and pharmacologic manipulation of AngII signaling -----	 34
3.1 Introduction -----	35

3.2 Results	37
3.2.1 <i>Acta2</i> ^{-/-} mice and losartan treatment over time	37
3.2.2 Long term captopril treatment incapable of reversing pathological changes associated with <i>Acta2</i> ^{-/-} mouse model	44
3.2.3 L-NAME and NAC in <i>Acta2</i> ^{-/-} mice	53
3.2.4 <i>Agtra1</i> ^{-/-} and <i>Acta2</i> ^{-/-} cross	54
3.3 Discussion	57
Chapter 4: Pharmacologic manipulation of AngII signaling in the TAC mouse model of thoracic aortic aneurysm formation	63
4.1 Introduction	64
4.2 Results	67
4.2.1 Treatment with captopril fails to rescue remodeling associated with TAC	67
4.2.2 C21 is beneficial in biomechanical stress model	76
4.2.3 Knock out of Agtr1a does not alter vascular inflammation	86
4.3 Discussion	90
Chapter 5: Discussion and Conclusions	97
5.1 Introduction	98

5.2 Role of angiotensin in TAAD -----	99
5.3 Angiotensin signaling through AT1R-----	101
5.4 Clinical relevance-----	101
5.5 The fibrotic response -----	104
5.6 Angiotensin signaling through AT2R -----	106
5.7 Study limitations -----	106
5.8 Future directions -----	107
References -----	109

List of Figures

Chapter 1

Figure 1.1 ----- 3

Figure 1.2 ----- 6

Figure 1.3 ----- 7

Figure 1.4 ----- 8

Figure 1.5 ----- 12

Figure 1.6 ----- 14

Chapter 2

Figure 2.1 ----- 21

Figure 2.2 ----- 23

Chapter 3

Figure 3.1 ----- 38

Figure 3.2 ----- 40

Figure 3.3 ----- 41

Figure 3.4 ----- 43

Figure 3.5 ----- 45

Figure 3.6 ----- 47

Figure 3.7 ----- 50

Figure 3.8 ----- 51

Figure 3.9 ----- 52

Figure 3.10 ----- 54

Figure 3.11 ----- 56

Figure 3.12 ----- 59

Chapter 4

Figure 4.1 ----- 69

Figure 4.2 ----- 71

Figure 4.3 ----- 74

Figure 4.4 ----- 75

Figure 4.5 ----- 77

Figure 4.6 ----- 79

Figure 4.7 ----- 80

Figure 4.8 ----- 81

Figure 4.9 ----- 83

Figure 4.10 ----- 84

Figure 4.11 ----- 85

Figure 4.12 ----- 86

Figure 4.13 ----- 87

Figure 4.14 ----- 88

Figure 4.15 ----- 89

Figure 4.16 ----- 90

Figure 4.17 ----- 92

Chapter 5

(None)

List of Tables

Chapter 1

(None)

Chapter 2

Table 2.1 ----- 27

Table 2.2 ----- 31

Chapter 3

(None)

Chapter 4

(None)

Chapter 5

(None)

List of abbreviations

AngI – Angiotensin I

AngII – angiotensin II

AT1R – angiotensin receptor, type 1

AT2R – angiotensin receptor, type 2

At1a – angiotensin receptor, type 1a

At1b – angiotensin receptor, type 1b

ACE – angiotensin converting enzyme, one

ACE2 – angiotensin converting enzyme, two

ACEi – angiotensin converting enzyme inhibitor(s)

ARB – angiotensin receptor blocker

EM – electron microscopy

FAK – focal adhesion kinase

H&E – hematoxylin and eosin

IHC – Immunohistochemistry

L-NAME - L-NG-nitroarginine methyl ester

MMP – Meta-metalloprotease

NAC – N-acetyl cysteine

PDGF – platelet derived growth factor

pH3 – phospho-histone H3

ROS – reactive oxygen species

SM α -actin –smooth muscle specific α -actin

SMC – smooth muscle cell

SM-MHC – smooth muscle myosin heavy chain

WT – Wild type (C57BL6 background)

IL6 – Interleukin-6

MCP-1 – monocyte chemoattractant protein, one

TGF β – transformation growth factor β

eNOS – endothelial nitric oxide synthase

TAAD – thoracic aortic aneurysm or dissection

ERK – extracellular signaling regulating kinases

pERK – phosphorylated extracellular signaling regulating kinases

Chapter 1 – Introduction

1.1 – Structure of the aorta

The aorta is the largest vessel in the body, originating from the heart and serving as a conduit for blood flow to the rest of the body. Anatomically, it is divided into multiple sections, starting with the aortic valve (aortic annulus), then the aortic root with the sinuses of Valsalva, where the left and right coronary arteries branch off to provide blood to the heart (**Figure 1.1**). The junction between the root and ascending aorta is the sinotubular junction, and the tubular ascending aorta extends to the arch. The innominate artery branches off the aortic arch and divides into the right subclavian artery and right common carotid artery. The segment through the aortic arch is also known as the transverse aorta, and the left common carotid artery branches off this segment of the aorta followed by the left subclavian artery. The descending thoracic aorta runs along the spine and is where the intercostal arteries originate. Once the aorta passes the diaphragm, it becomes the suprarenal abdominal aorta and, eventually, the infrarenal abdominal aorta below the branches of the left and right renal arteries. The aorta ends where it branches into the left and right iliac artery (1, 2). The sections of the aorta arise from distinct embryologic origins, experience distinct biomechanical pressures, and as a result may respond differently to different stimuli (3, 4). In the ascending aorta, all the smooth muscle cells are of neural crest cell origin. In the aortic root, these cells are derived from the second heart field (3). In the research presented here, the focus is on the aortic root and ascending aorta.

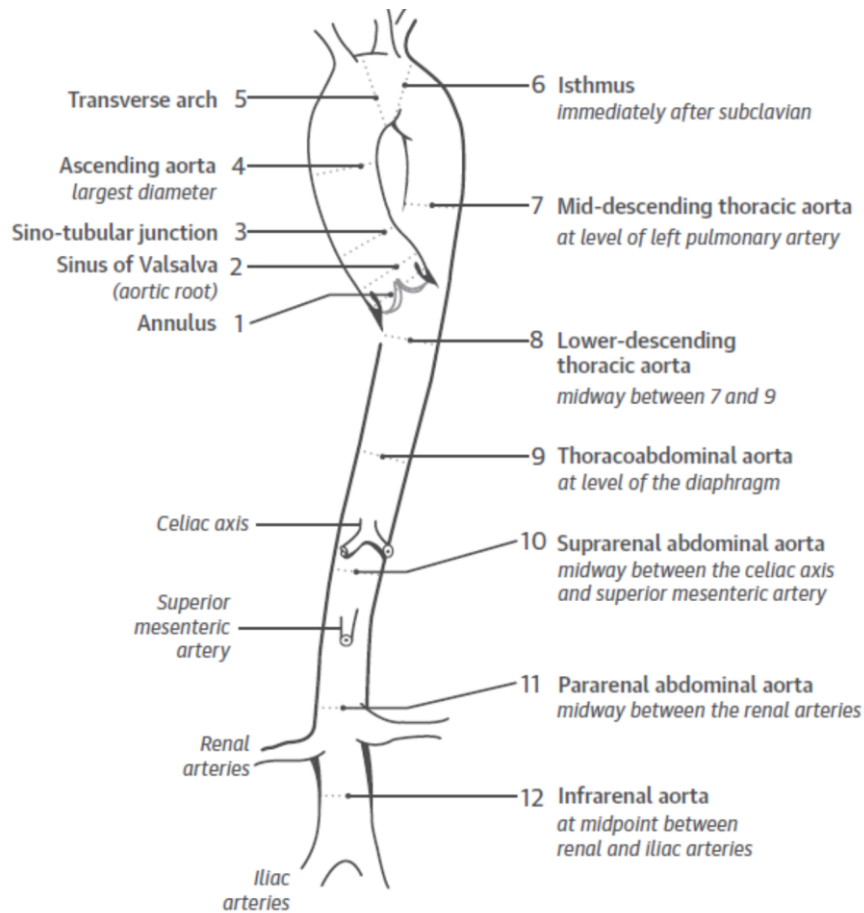


Figure 1.1 – Anatomical figure of the aorta from the heart to the pelvis starting from the aortic valve annulus where the blood leaves the heart through the aortic valve. The focus of the research presented here is primarily at the aortic root, which includes the sinuses of Valsalva, and the ascending aorta. The pathology associated with each segment of the aorta can be different, in part due to the different developmental origin of the SMCs and the hemodynamic flow patterns. Reprinted with permission from Journal of the American College of Cardiology (Weinsaft JW, Devereux RB, Preiss LR, Feher A, Roman MJ, Basson CT, Geevarghese A, Ravekes W, Dietz HC, Holmes K, Habashi J, Pyeritz RE, Bavaria J, Milewski K, LeMaire SA, Morris S, Milewicz DM, Prakash S, Maslen C, Song HK, Silberbach GM, Shohet RV, McDonnell N, Hendershot T, Eagle KA, Asch FM, Investigators GR. Aortic Dissection in Patients With Genetically Mediated Aneurysms: Incidence and Predictors in the GenTAC Registry, 2016) (1)

The aortic is an elastic artery and the aortic wall is composed of three layers: the tunica intima, tunica media, and tunica adventitia. As shown in **Figure 1.2**, the tunica intima

is composed of a single layer of endothelial cells that, under normal physiologic conditions, rests on the internal elastic lamina and signals changes in sheer stress to the cells underneath (5-7). Between the internal elastic lamina and the external elastic lamina lies the tunica media which is the layer containing the smooth muscle cells. In the aorta, the tunica media is composed of layers of elastin with smooth muscle cells (SMCs) in between, with all layers laid down during development. In humans, there are approximately 50 layers. The number of layers varies in different species, and this number has been shown to depend on multiple factors like weight, diameter, and pressure (6). The number of elastin lamellae/SMCs can also vary in genetically-engineered mouse models (6, 8-11). The layers of elastin provide the aorta with the elasticity required to store the energy of the heart beat when the aortic valves close and maintain the blood pressure for continuous blood flow. This is referred to as the Windkessel effect. Approximately 50% of the stroke volume has been reported to be stored in the aorta and proximal blood vessels to perfuse the peripheral tissues, but some reports indicate that pharmaceuticals can manipulate it (12).

In the aorta, the SMCs are arranged in concentric rings between the elastin layers. Microfibrils, in which the major protein is fibrillin, are at the tips of elastin extensions extend from the elastin lamellae and bind to dense plaques or focal adhesions on SMCs (13) (**Figure 1.3**). At the cell surface, dense plaques or focal adhesions connect the microfibrils to the cellular network of contractile filaments, which are made up of the smooth muscle specific isoforms of α -actin (SM α -actin) and myosin heavy chain (SM-MHC). Together, this apparatus of connecting cells and matrix has been termed the

“elastin-contractile unit,” (9, 14) and as discussed below, perturbations in this unit may be an important cause of thoracic aortic disease.

The outer layer of the aorta, the tunica adventitia, is composed of fibroblasts and can contain inflammatory cells with some diseases. In addition, this layer also contains stem cells capable of differentiating into multiple cell types in the vessel wall but their significance, function, and origin are still under debate (15-19). From a clinical and physiological perspective, the extracellular matrix in the adventitia is composed mostly of collagen, which provides the vessel with the structural integrity to support the wall of the vessel against high intraluminal pressures. In humans, this layer is also where the vasa vasorum (blood vessels of the blood vessel) reside, providing oxygen and nourishment to the vessel wall (13, 20).

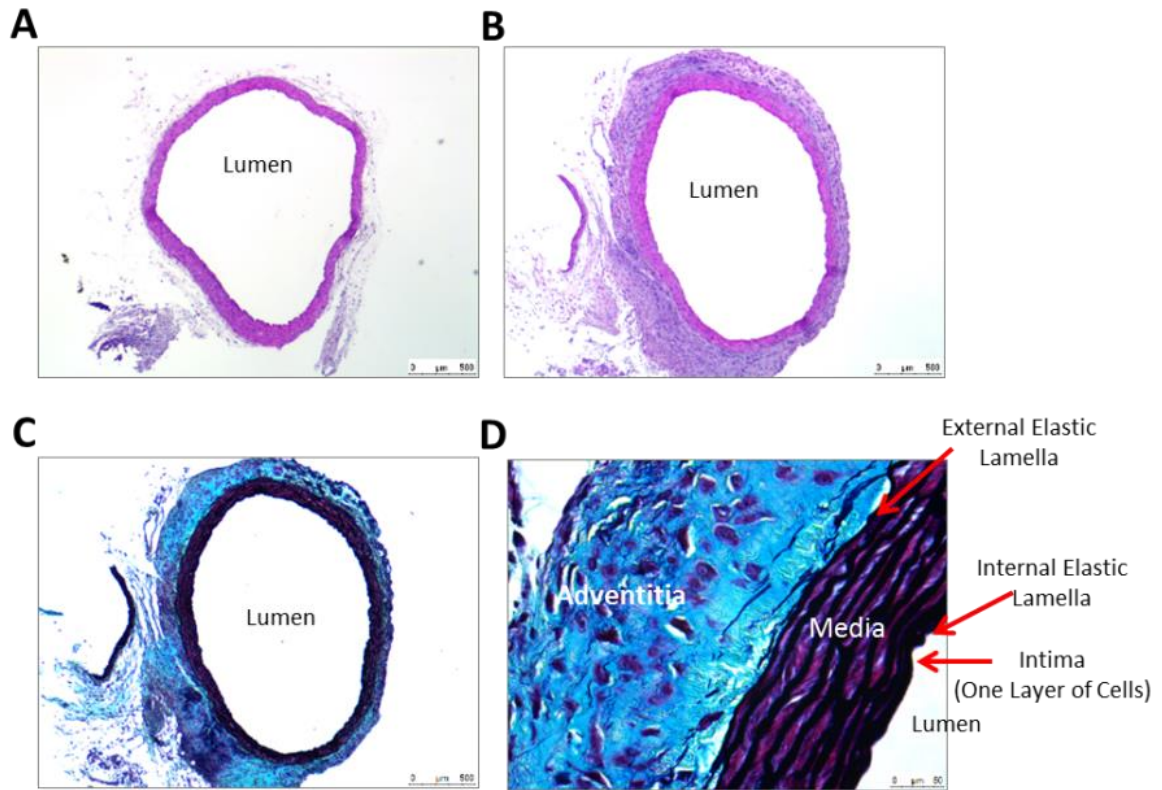


Figure 1.2 – Histology of the aortic wall. A) A hematoxylin and eosin (H&E) stain of a wild type (WT) mouse aorta. Most of the vessel wall observed is the media with minimal adventitia and a single layer of endothelial cells. Normally, in mice there is not a sizeable amount of adventitial layer. B) The adventitial layer is much larger with some forms of aortic pathology. H&E stain of biomechanically stressed ascending mouse aorta to show the expansion of the adventitia. C) A Movat stain of the stressed aorta demonstrating the lumen, media (dark), and adventitial layer, which is composed of cells (red), collagen (yellow, poorly visualized due to the proteoglycan deposition), and proteoglycans (blue). D) At higher magnification, the elastin fibers can be seen in black in the medial layer. While not present in mice, the adventitia would be the location of the small arteries of the vasa vasorum.

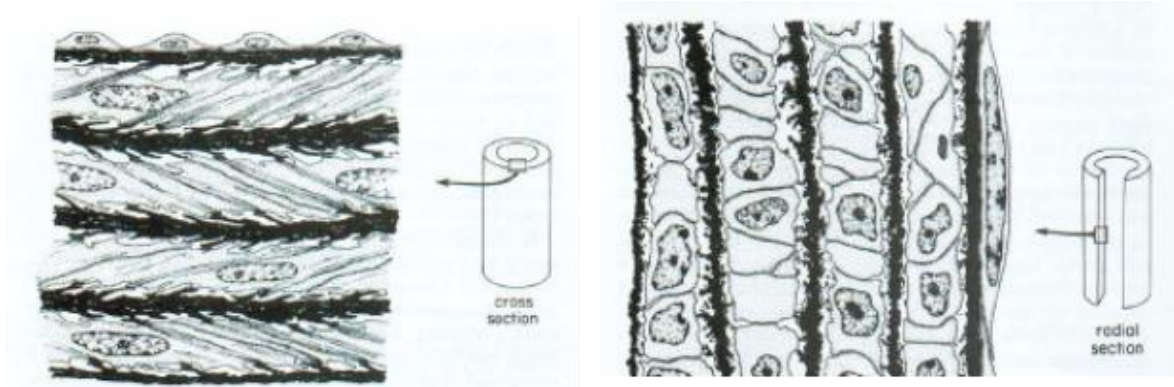


Figure 1.3 – A drawing of the transverse and longitudinal cross section of the vessel wall demonstrating the contractile unit. Elastin layers (dense black) are arranged between the smooth muscle cells, and the contractile fibrils are connected to them in the cell. Reprinted with permission from Lab Invest (Davis EC. Smooth muscle cell to elastic lamina connections in developing mouse aorta. Role in aortic medial organization, 1993) (14)

1.2 – Thoracic aortic disease and pathology

Thoracic aortic aneurysms and dissections are a major clinical concern, and constitute some of the most devastating pathologies plaguing patients. The natural history of thoracic aortic aneurysms is that they enlarge over time, and with this expansion, are predisposed to acute aortic dissections. With multiple possible presentations, the diagnosis of thoracic aortic dissections is often missed by physicians. Acute pain in the upper thorax radiating to the back or to other parts of the chest can often be mistaken for a minor ailment, when, in fact, it is an aortic dissection and a clinical emergency.

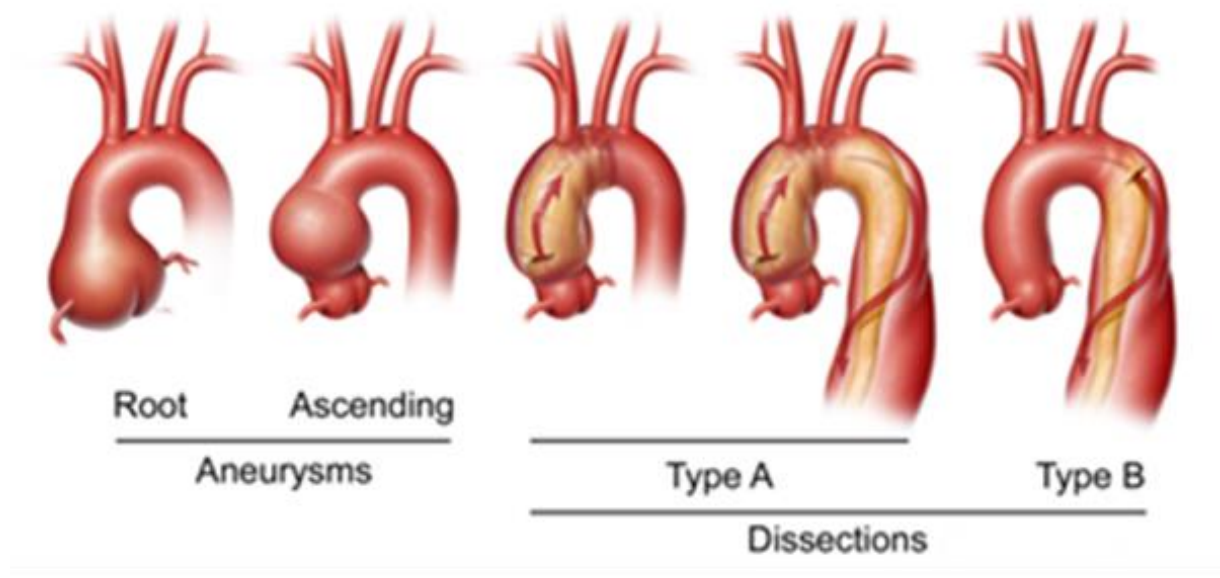


Figure 1.4 – Aortic aneurysm formation can lead to aortic rupture or dissection. Far left is an illustration of a root aneurysm and ascending aortic aneurysm. Stanford Type A dissections are depicted in the middle. They encompass the ascending aorta and are considered a clinical emergency. A Stanford Type B dissection is anything distal of the left subclavian artery (depicted far right). Uncomplicated dissections are medically managed and electively repaired.

Thoracic aortic aneurysms are closely monitored in patients because they are often the precursor to an aortic dissection or aortic rupture. A rupture of the vessel wall results in blood leaving the vascular system causing a patient to bleed out or, depending on the location, compromise other organs near the structure. A dissection is more complex. The structure of the vessel (aorta) becomes compromised as the aorta enlarges, and a tear in the intima allows blood to enter the vessel wall. The blood separates the vessel wall creating a true and false lumen with the false lumen often being located in the medial layer

of the wall. Blood pressure builds in the false lumen, and the increase in pressure can cause the dissection to progress proximally or distally down the vessel wall. The pressure in the false lumen can often collapse or restrict the blood flow in the true lumen causing distal malperfusion with clinical symptoms. Furthermore, a dissection can lead to rupture and a patient exsanguinates out if the vessel ruptured is in a large enough compartment of the body (21, 22).

Aortic aneurysms and dissections are commonly classified by the Stanford Classification System, which identifies the need for immediate surgical intervention. Other classification systems of dissection, such as the DeBakey Classification System are also used (23). Any dissection between the aortic valve and the left subclavian artery is considered a Stanford Type A dissection. This is considered a surgical emergency as the dissection can cause a stroke distally or a hemo-pericardium proximally. Normally, these dissections require emergent replacement of the vessel or more depending on the patient. Stanford Type B dissections are distal to the left subclavian artery. Often, these cases are medically managed but closely monitored. They are only surgically addressed if there are complications such as mesenteric ischemia, paralysis, or untreatable pain (23).

A vascular aneurysm is defined by a ballooning of a vessel to 1.5 times its normal size, and indicates a weakening of the vessel wall. Aneurysm formation is accompanied by pathologic changes that strain the wall, alter its structure, and in theory change the flow mechanics (24-27). In the aortic root and ascending thoracic aorta, the pathology associated with aneurysms is usually characterized by a disordering and fragmentation of

the elastic fibers along with an increase in inflammation. Inflammatory markers produced by vascular SMCs and fibroblasts, such as *IL6* and *MCP1*, signal inflammatory macrophages to invade the vessel wall. The macrophages then recruit fibroblasts to begin remodeling the medial layer and alter the extracellular matrix (28). While the origin of the fibroblast have been debated (17), they differentiate into myofibroblasts and induce the remodeling process, including the production of matrix metalloproteases (*MMPs*), to alter the vessel wall by cleaving multiple target proteins in the extracellular matrix (29). The remodeling includes changes in the extracellular matrix with alterations or fragmentation of elastin fibers, the production of proteoglycans, and the production of adventitial collagen (28, 30). These changes lead to a loss of the highly structured matrix organization described above. The resulting disruption of the “elastin-contractile unit” structure can cause aberrant changes in smooth muscle cells such as apoptosis (31) or hyper-proliferation (5, 9, 11).

By far the most important risk factor for thoracic aortic aneurysms and dissection (TAAD) is hypertension. Other factors that increase blood pressure and biomechanical forces on the ascending aorta are body building, weight lifting, and illegal drug use (cocaine, methamphetamines). Approximately 75% of patients with TAAD have elevated blood pressure, making it the most significant co-factor in the disease (32). Other factors that increase the risk for thoracic aortic disease include age and the presence of a bicuspid aortic valve (8). The disease is significantly more common in males than females. In the studies reported here, Chapter 4 describes the role of increased biomechanical forces on the ascending aorta in aortic aneurysm formation.

There are also multiple genetic changes that predispose to thoracic aortic disease. Clinical studies have shown that up to 25% of TAAD patients have a first degree relative with the disease (33-35). These cases with an inherited predisposition can have syndromic forms of the disease, including Marfan syndrome or Loeys-Dietz syndrome, or can lack syndromic features. Genetic variants leading to TAAD are typically inherited in an autosomal dominant pattern with reduced penetrance and variable expression (36). Mutations contributing to the disease have been found in cell adhesion proteins (*FBN1*, *COL3A1*) (37, 38), transforming growth factor-beta (*TGF- β*) pathway genes (*TGFBR1*, *TGFBR2*, *SMAD3*, *TGFB2*) (5, 39, 40), genes encoding proteins involved in SMC contraction (*ACTA2*, *MYH11*, *MYLK*) (41-44), and genes associated with survival and metabolism(*FOXE3*, *MAT2A*)(8, 45). Marfan syndrome is caused by mutations in *FBN1*, which encodes fibrillin-1, the major component in the microfibrils that link elastin with SMCs in the aorta. Many of these genes have been extensively studied for their relationship to the canonical *TGF- β* pathway. The data presented in this dissertation will focus on mutations in the gene encoding SM α -actin (*ACTA2*), which were identified by our lab in 2007 (41).

1.3 Angiotensin system

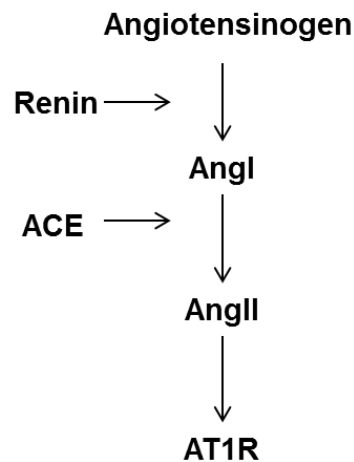


Figure 1.5 –Angiotensinogen is converted to angiotensin I, which is then converted to angiotensin II via angiotensin converting enzyme (ACE). There are multiple therapeutics developed that alter this pathway, such as ACE inhibitors and AT1R blockers.

The renin-angiotensin system (RAS) is a system that regulates blood pressure. In response to changes in blood pressure, angiotensinogen, an α_2 -globulin, is produced by the liver and converted by renin to angiotensin I (AngI). An angiotensin converting enzyme (ACE) on the surface of pulmonary and renal endothelium then converts angiotensin I to angiotensin II (AngII) which binds to AngII receptors to alter multiple cells in the body and adjust blood pressure. Through the angiotensin II type 1 receptor (AT1R) it leads to the release of a mineralocorticoid, aldosterone, from the adrenal glands which increase sodium reabsorption in the kidneys to help control blood pressure (46, 47). There are two

pharmaceutical strategies to alter this pathway that are currently used extensively in patients, one via inhibition of ACE inhibitor (ACEi) the second blocking the AT1R (24). However, the angiotensin system is much more complex. There is more than one receptor for angiotensin II (48-51). The AT2R has different effects in cells than the AT1R. Additionally, there is more than one ACE. The second ACE, ACE2, can convert angiotensin I and angiotensin II to smaller peptides Ang1-9 and Ang1-7, respectively, which lead down a different pathway triggering the Mas receptor. Additionally, Ang1-9 is converted by ACE to Ang1-7, which is the ligand for the Mas receptor. These pathways are further discussed below and shown in **Figure 1.6**.

The AT2R has been known to counter the effects of the AT1R downstream in multiple systems. In the vascular SMCs, the AT1R increases proliferation, fibrosis, MMP2, and MMP9 expression (52), while the AT2R decreases proliferation, fibrosis, and MMP9 expression (48). However, in some models the AT2R has been thought to affect smooth muscle cell apoptosis (53, 54). Evidence indicates that Ang1-9 is converted by ACE to Ang1-7. With Ang1-7 binding to the Mas receptor on cardiomyocytes, it increases heart function improving cardiac output, cardiac index, and fractional shortening. It also reduces cardiomyocyte hypertrophy, fibrosis, and inflammation, but the Ang1-7 peptide and AngII have been viewed as having different effects on different physiologic systems, commonly focused on inflammation and fibrosis (55, 56).

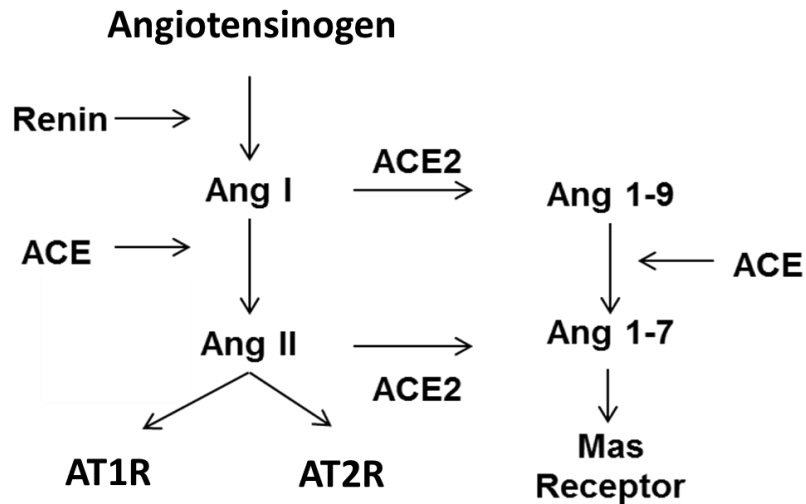


Figure 1.6 – The revised view of the renin-angiotensin system. AngII can activate both the AT1R and AT2R receptors. AngI and AngII can both be metabolized by a second ACE enzyme into angiotensin peptides Ang1-9 and Ang 1-7, respectively.

1.4 Angiotensin in animal models

The role of the angiotensin system in aortic disease has been studied extensively in mouse models. The infusion of AngII into a mouse at a high enough dose can cause aortic disease. Most of the studies on angiotensin infusions focus on abdominal aortic aneurysms, since this and increased blood pressure are the most common presentations with this model, but expansion and dilation of the ascending aorta coupled with structural changes are also seen (57). AngII infusion causes medial expansion via hypertrophy or hyperplasia in both the abdominal and the thoracic aorta. Additionally, it has been shown to increase inflammation with the secretion of inflammatory cytokines by fibroblast and cells in the adventitia to recruit monocytes which further stimulate fibroblasts to remodel and increase cytokine production. Of note, however, blood pressure does not play the only role

as an increase in blood pressure with norepinephrine does not have the same effects (28, 30, 58).

There have been multiple studies using manipulation of the angiotensin system in genetic models of aneurysm formation to study the role of this pathway in driving the disease. There are a few different mouse models of Marfan syndrome which have variable effects on pathology and survival. These models include models that are deficient in fibrillin-1 (*Fbn1*^{-/-}) (59) or express only a small percentage of normal fibrillin *Fbn1*^{mgR/mgR} (8, 60). One of the most established models is the *Fbn1*^{C1039G/+} mouse model (61, 62), which is viable and exhibits slow aortic growth. This mouse is heterozygous for a missense mutation that results in production of mutant fibrillin-1. In these mice, it was shown that the traditional beta-blocker (propranolol) and TGFβ neutralizing antibodies were able to reverse some of the aortic pathology. The idea was that propranolol would decrease blood pressure and stress on the aortic wall and the TGFβ neutralizing antibodies would block pathologic TGFβ signaling. However, an Angiotensin II type I receptor blocker (ARB), losartan, had a more drastic effect altering the structure of the aortic wall with decreased elastin fiber disruption, decreased wall thickening, and decreased distance between the elastic fibers (61). This echoes multiple studies showing the beneficial effects of blocking the AT1R or knocking it out in mice not just in the aorta, but also the heart (63, 64).

One study also focused on the effects of the AT2R. *Agtr2*^{-/-} mice were crossed with *Fbn1*^{C1039G/+} mice, which lead to an increase in pERK signaling, a downstream indicator of AT1R signaling (48). These results indicated that the AT2R may counter many of the

intracellular effects of the AT1R. Another mouse model of TAAD with a deletion in fibulin-4 (*Fbln4*^{-/-} mice) causes aneurysm formation with severe medial degeneration along with a loss of SMC differentiation and hyper proliferation. In these *Fbln4*^{-/-} mice, the angiotensin converting enzyme inhibitor captopril was shown to be just as effective as losartan: initiating treatment with either drug in the first month of life attenuated the growth of the aorta and reduced pathologic changes in this model (65).

Our lab developed a more acute biomechanical model, in which I focused on hyper-acute aortic remodeling model using transverse aortic constriction (TAC) (52). The model was originally designed to mimic congestive heart failure and has been studied extensively in congestive heart failure and left ventricular hypertrophy (66). Over two weeks I saw an increase in proximal aortic size of 23%. There was an increase in the thickness of the media and adventitia. Medial cell density did not change, but cell density did increase in the adventitia. Inflammatory markers rose significantly as indicated by expression of *IL6* and *MCP-1*. Additionally, I observed an increase in matrix remodeling genes *MMP2* and *MMP9*. I also observed evidence of increased TGFβ signaling. As in other studies, losartan attenuated many of the pathophysiologic changes associated with this model. Specifically, losartan attenuated aortic growth, reduced medial thickening, and blocked the inflammatory response including the infiltration of macrophages. However, losartan was not able to completely reverse the changes in the adventitial layer, including thickening, collagen production, and signaling changes (52). Our data, combined with the prior studies by other labs (61, 65), indicate that AT1R may be a therapeutic target in ascending aortic disease.

1.5 Hypothesis tested

I hypothesize that angiotensin II signaling through the AT1R contributes to thoracic aortic aneurysm formation in multiple model systems of disease, but that blocking related receptors in addition to the AT1R, such as the AT2R and Mas receptor, may have no effects or negative consequences.

Herein, I demonstrate that losartan prevents aortic aneurysms in a mouse model of *ACTA2* mutations, *Acta2*^{-/-} mice, but captopril increases the growth of the aorta. Instead of increased production of AngII in the aorta, I determined that the loss of α -actin filaments in aortic SMCs increases NF- κ B signaling, thus driving increased expression of AT1R receptor, sensitizing the cells to exogenous AngII. Furthermore, I show that in an acute biomechanical stress model, blocking AngII production using an ACE inhibitor (captopril) is not sufficient to reverse the aortic enlargement associated with the increased pressure. The addition of an AT2R agonist coupled with captopril prevented aortic growth in a manner similar to losartan. Lastly, unrecognized congenital abnormalities in the aorta of the *Agtr1*^{-/-} mice prevented the use of this model to confirm that losartan prevention of aortic enlargement with increased biomechanical forces was specifically due to blocking the AT1R receptor. This is an unexpected, totally novel observation.

Chapter 2 – Methods

2.1 Introduction

Similar methods are used in all projects and will be described in this section. When I chose to make small adjustments from these approaches in different projects, I will mention those accordingly.

2.2 Mouse models

Mice were housed either at the animal care facility (CLAMC) at The University of Texas Health Science Center McGovern Medical School Building or in the Mouse Cardiovascular Phenotyping Core at Baylor College of Medicine. Wild type (WT) mice for transverse aortic constriction (TAC) were all acquired from Jackson Labs (Bar Harbor, ME, C57BL/6J Stock No:000664) at 10-12 weeks of age. Upon arriving, mice were quarantined, and the TAC surgery was performed at 12-14 weeks of age. Mice were sacrificed two weeks post-operatively as described below. Our lab had previously obtained frozen embryos of the *Acta2*^{-/-} mouse from Dr. Warren Zimmer at Texas A&M, originally designed by Schildmeyer et al and bred into a C57BL6 background (67). *Acta2*^{-/-} mice were then bred in house for our studies. In our *Agtr1a*^{-/-} studies, mice were acquired from Jackson Labs (*B6.129P2-Agtr1a*^{Tm1Unc/J}, Stock No: 002682). Studies with TAC and *Acta2*^{-/-} treated with captopril were all male while the other studies consisted of both male and female mice.

2.3 Transverse aortic constriction (TAC)

All mouse experimental procedures were approved by the Animal Welfare Committee at The University of Texas Health Science Center McGovern Medical School and the Animal Welfare Committee at Baylor College of Medicine Mouse Phenotyping Core. C57BL/6J mice were purchased from Jackson Laboratories (Bar Harbor, ME) at 10-11 weeks of age. As previously described in Kuang et al (52), mice were administered buprenorphine preoperatively (0.1 - 2.5 mg/kg subcutaneous injection). Mice were then given 2 – 2.5% isoflurane with 0.5 to 1.0 L/min of 100 % oxygen via a nose cone. Neck and chest hair was removed and the surgical site was prepared with chlorohexidine and 70% ethanol. Surgical instruments were sterilized chemically or by steam autoclave and the surgical area prepared accordingly. Sterile technique was used throughout. For surgery, the mouse was placed in a supine position. After administering bupivacaine, a midline incision was made and superficial tissues were divided to expose the trachea to intubate the trachea using an 18 – 21 gauge catheter. The catheter was then connected to a rodent ventilator (MiniVent, Type 845) administering 100% oxygen and 2 – 2.5% isoflurane. Mice were kept at a respiratory rate of 100-125 breaths per minute with a tidal volume of approximately 0.15-0.25 mL. A partial sternotomy was performed to the second rib and the thymus divided to expose the transverse aorta. A blunt 27 gauge needle was placed on the transverse aorta between the right innominate and left carotid artery. Constriction was then made by tying a 6-0 non-absorbable braided black silk suture around the transverse aortic arch and needle. The needle was removed yielding the constriction. The chest was closed with two interrupted vicryl 5-0 sutures after the lungs were re-inflated by closing of the outflow on

the rodent respirator. The skin was closed using 5-0 non-absorbable suture which was removed 10 days post-operatively. Anesthesia was discontinued and the animal extubated once it resumed spontaneous breathing. Mice were monitored closely post-operatively for signs of distress and discomfort. The sham group underwent an identical procedure but no suture was tied to the aorta. Adequacy of the constriction was confirmed by Doppler flow studies, echocardiography, and catheter measurements described below.

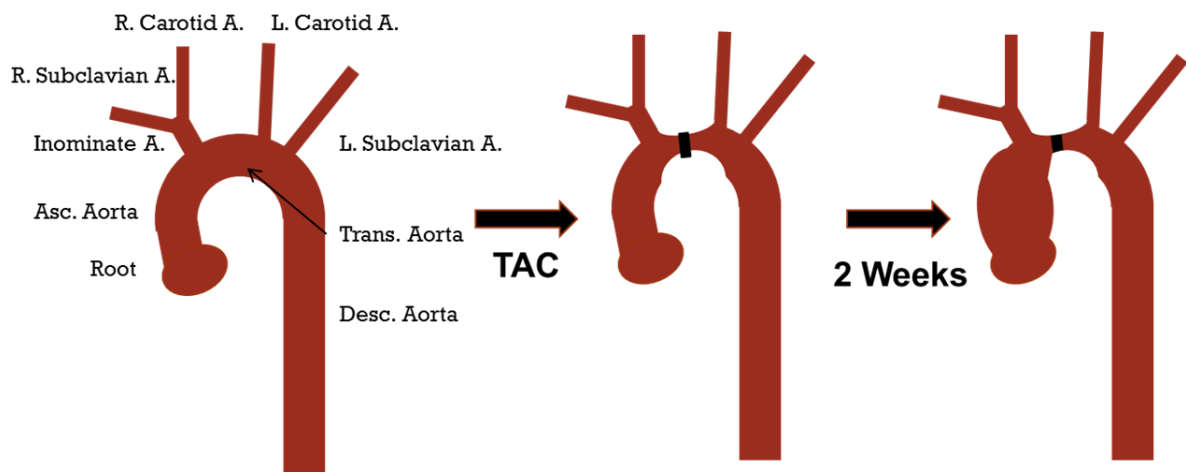


Figure 2.1 –The mice are constricted at the site of the transverse aorta leading to an increase in ascending aorta and aortic root size at two weeks. With the proximal increase in pressure, flow in the right carotid would increase significantly compared to the left carotid and there would be a significant pressure drop across the site of the constriction.

2.4 Echo & Doppler studies

Echocardiographic, Doppler, and blood pressure studies were all done in accordance with protocols previously described (11, 52). Under anesthesia, measurements were performed with a Vevo700, Vevo2100, Vevo3100, or an Indus Instruments Doppler system. Briefly, for all echo studies the mice were weighed and placed under anesthesia

with isoflurane administered and maintained via nose cone with a dose of 1 – 2% isoflurane at a rate of 0.5 to 1.0 L/min of 100 % oxygen. Mice were maintained under anesthesia for the duration of the experiment with a goal heart rate of 300 to 400 bpm. Heart rate and temperature were continuously monitored, and the temperature maintained within normal limits using the Indus Instruments pad and system. I observed some variability in response to anesthesia even within groups, with some mice appearing more sensitive to the anesthesia. Therefore, anesthesia was adjusted accordingly. All images were obtained in a parasternal long-axis view with 40 MHz ultrasonic probes.

With all experiments performed with the Vevo700 and Vevo2100 systems (VisualSonics, Toronto, Ontario, Canada), the mice were placed in a supine position on the monitoring pad angled slightly to the mouse's left side. Images of the ascending aorta and aortic root were then obtained and multiple videos recorded for each mouse. Under similar monitoring and anesthesia, Doppler measurements were made with the Indus Instruments Doppler probe one week post-operatively and recorded with their Doppler Signaling Processing Workstation with the mouse supine.

The same procedures were performed using the Vevo3100 (VisualSonics, Toronto, Ontario, Canada) for ascending and aortic root measurements. However, with the 3100 system, with the mice still sedated, I also assessed cardiac function and flow across the constriction at the transverse aorta, left common carotid artery, and right common carotid artery. Flow across the transverse aorta was obtained with the mouse still in the supine position. Cardiac function was assessed by obtaining both longitudinal and transverse

views across the left ventricle with the animal tilted slightly to its right in the supine position. Images over the left common carotid artery and right common carotid were obtained with the mouse in the Trendelenburg position.

All mice were removed from isoflurane and allowed to recover. Flow studies of the common carotid arteries using the Vevo3100 correlated with the Indus Instruments Doppler studies. These studies were done using similar techniques, but the mice were not required to have their hair removed.

Images of the ascending aorta and aortic root were then obtained, recorded, and later analyzed using VevoLAB 1.7.1 (VisualSonics, Toronto, Ontario, Canada) or Sante DICOM Editor 3.1 (Santesoft) (**Figure 2.2**). Carotid Doppler measurements were also analyzed with the VevoLAB 1.7.1 when obtained with either the Vevo 3100 or the Doppler Signal Processing Workstation, Ver 1.624 (Indus Instruments, Houston, Texas).

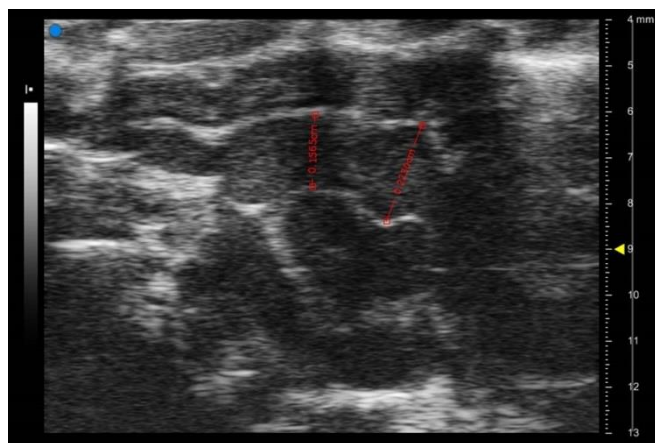


Figure 2.2 – Echo image of the aorta in the longitudinal view. Measurements were taken at the ascending aorta and the aortic root. Images taken using the Vevo 700 and analyzed in the SanteDICOM Software. The red lines designate the measurements for the ascending aorta (left) and aortic root (right). The heart would be to the right of the image.

2.5 Non-invasive blood pressure monitoring and blood pressure measurements

Non-invasive blood pressure monitoring was performed via a tail cuff system and were not utilized in TAC experiments. Briefly, awake mice were immobilized, and a blood pressure cuff placed over the tail. Mice were then placed on a heating pad and the blood pressure was recorded for five minutes with a CODA Noninvasive Blood Pressure system (Kent Scientific Corporation, Torrington, CT). This procedure was repeated multiple days in a row in order to acclimate the mouse to the testing environment and technique. Only the measurements on day five were utilized for analysis.

For TAC studies I utilized an invasive, non-survival catheterization technique with a SPR-1000 1F Catheter (AD Instruments, Sydney, Australia), a Pressure Control Unit PCU-2000 (Millar, Houston, TX), a PowerLab 4/35 DAQ device (AD Instruments), and LabChart software (AD Instruments). Prior to the procedure, all surgical instruments and supplies were sterilized by steam autoclave, and the surgical field prepared in a sterile fashion. The 1F pressure catheter probes were presoaked in saline or distilled water for 30 second before catheterization. Mice were anesthetized with isoflurane via nose cone using the same method previously described for echocardiography (Section 2.4). Ketoprofen was given subcutaneously at a dose of 2.5 mg/kg. Hair on the chest and throat was removed, and the skin was prepared with povidone iodine and alcohol. A longitudinal incision was made approximately 2 mm to the right of the midline of the throat, from the lower jaw to the sternum. The skin and overlying tissue was gently divided and the right carotid artery

exposed. Ligatures were then placed on the right common carotid artery at the proximal and distal sites. The knot on the distal site was made tight, while that on the proximal location site was made loose around the artery. Using a hemostat, the artery was clamped proximal to the more proximal ligation site. A 27 G needle was then used to create a small hole near the distal ligation site. The catheter probe was then inserted and advanced past the proximal knot, and the knot tightened down around the probe. For reference, the depth to insert the probe into a carotid for an 11-week-old mouse would be about 12 mm. Next, the hemostat was removed and the blood pressure recorded for a 5-10 minutes. Afterwards, the mouse was euthanized, while still sedated, for studies described below.

2.6 Drug administration

Captopril and Losartan are orally administered drugs used in both our TAC and *Acta2*^{-/-} trials. Captopril (Cat# sc-200566A, Santa Cruz Biotechnology) was administered at 75 mg/L and Losartan Potassium (Cat# sc-204796A, Santa Cruz Biotechnology) was administered at 600 mg/L in the drinking water, as previously (52). For the studies using AVE0991 (Sanofi, Paris, France), captopril was given in the drinking water and AVE0991 given by intraperitoneal (IP) injection at a dose of 576 ug/kg/d. Similarly, Compound 21 (C21, Vicore, Moelndal, Sweden) was administered by IP injection at a dose of 300 ug/kg/d with or without captopril in the drinking water.

For the *Acta2*^{-/-} studies, mice were treated long term with captopril via drinking water at a dose of 75 mg/L starting at four weeks of age. The mice remained on this dose until they were sacrificed at 13 months of age, for a total of 12 months of treatment.

Similarly, mice treated with losartan, were given 600 mg/L in the drinking water starting at 4 weeks of age (11). Losartan treatment was continued for 10 months until sacrifice at 11 months of age. Some mice were also treated long term with doxycycline for approximately 12 months starting at 4 weeks of age. Doxycycline was administered in their drinking water with 1% sucrose. Controls for all of these experiments were untreated mutant and WT littermates given drinking water, except in the doxycycline trial in which the control mice were given 1% sucrose water. The doxycycline doses were based on previous studies (63, 68).

Additional cohorts of *Acta2*^{-/-} mice were treated short-term with L-NG-nitroarginine methyl ester (L-NAME) in their drinking water (3 g/L) in conjunction with a high salt diet (8% NaCl diet, Harlan), to make the mutant mice normotensive. Mice were started on L-NAME and high salt diet at 4 weeks for age and treated for 3 months prior to sacrifice at 4 months of age.

2.7 Histomorphometric study

Following completion of the echo, Doppler, and catheterization studies, animals were sacrificed. After anesthetization with 2.5% avertin, transcardiac perfusion was performed with 10 mL of PBS for 5 minutes followed by fixation with 10 mL of formalin for 5 minutes. The heart, aortic root, ascending aorta, descending thoracic, and left and right carotid arteries were then carefully removed and placed in 10% formalin overnight. On the next day, the tissue was cleaned, processed and embedded in paraffin wax in a transverse orientation. Tissues were cut into 4 µm sections using a microtome and mounted on slides

for staining. Hematoxylin and eosin (H&E) staining was performed via standard protocols. Pictures of the vessel cross-sections were taken at 40x, 50x, 200x, and 400x magnification. The luminal, medial, and adventitial areas were measured for each vessel in ImageJ. In addition, cell density was also assessed utilizing ImageJ. Movat staining was used to assess the structure, elastin breaks, and the amount of elastin and proteoglycan in the vessel wall. Additional staining of Mac-2 cells (anti-Mac-2 monoclonal antibody for macrophages), Sirius Red, and α -actin (anti-SMC α -actin specific antibody) were also obtained to look at inflammation, collagen production, and smooth muscle cells/fibroblast. TUNEL and PH3 staining was also performed to analyze apoptosis and proliferation, respectively. Five or more mice were analyzed for each group and averaged, but the number of mice depended on the specific study. Some of the preliminary studies have smaller “n” sizes. **Table 2.1** shows the stains and antibodies utilized for these studies.

IHC Stain	Company	Catalog Number
Hematoxylin	Stat Lab	SL-100
Eosin	Stat Lab	SL-104
Movat	ScyTek Labs	MPS-1
Actin	Sigma-Aldrich	A2547
Mac-2	Cedarlane	CL8942B
PH3	Millipore	06-570
TUNEL	Millipore	S7100
1A 280 Sirius Red	Chroma-Gesellschaft	35780

Table 2.1 – Antibodies and stains utilized for IHC studies including their company and catalog number.

2.8 ImageJ analysis

Images were recorded with a DP71 light microscope (Olympus, courtesy of Blackburn Lab) at 40x and 400x magnification, and all analysis was performed using ImageJ 1.47v (NIH). I utilized 40x magnification as a baseline and method of orientation for analysis. Cross-sectioned H&E's at 40x were used to measure luminal area, vascular wall area, medial area, and adventitial area. Luminal area was defined as the area contained within the endothelium. However, in reality it is best measured to the internal elastic lamina, and echo measurements are considered a more physiologic standard. Vascular area was defined as everything from the internal elastic lamina to the tunica externa, the outer most defined layer of the vessel wall. Medial area was defined as the area between the internal elastic lamina and external elastic lamina. The adventitial area was defined as the area between the external elastic lamina and the tunica externa. Note this area was often omitted in the sham treated mice because it is very small and more difficult to quantify. In all mice, the endothelium is omitted since it is a single layer of cells and also difficulty to quantify.

The 40x images were used to select sections at equivalent locations that were appropriately distributed throughout the aortic wall for analysis. The majority of the analysis was done at 400x. On H&E stained sections, cell nuclei were counted using a cell counter and individually the cellular density of the media and adventitia was determined in

each image. Over 6 images were analyzed for each section and averaged to calculate, which I once normalized to the area of each image. Measurements were verified by looking at multiple cuts of the same aorta.

Images for Movat analysis were taken in a similar fashion at 400x magnification and analyzed in ImageJ. All components stained by Movat (elastin, collagen, proteoglycan, fibrin and smooth muscle cells) were assessed and presented as percentages registered pixels of the segment of interest for quantification. I focused primarily on elastin (black), proteoglycans (blue), and the cells which stained (red). A band pass filter was used for analysis, which allowed us to identify color thresholds for hue, saturation, and brightness for each measured component (i.e. elastin, proteoglycan, and smooth muscle cells). The resulting images were then used for quantification by the number of pixels.

Mac-2 staining was quantified by manually counting the total number of Mac-2 positive cells in each section. The sirius red, TUNEL, and PH3 stains and images were not quantified for the purpose of these studies.

2.9 Measurement of ROS in aortas by dihydroethidium (DHE)

Descending aortas were harvested, rinsed immediately in cold PBS, placed in Tissue-Tek OCT compound (Miles Laboratories), and snap frozen in liquid nitrogen. Blocks were cut to 30 μm -thick cryosections on a cryostat. Frozen sections were fixed in 4% PFA at room temperature for 15 minutes and rinsed 3x with PBS. DHE (Invitrogen, Cat#C10422)

stock at 2.5 mM was diluted for a final concentration of 10 μ M in PBS and applied to each tissue section. Slides were incubated in a light-protected humidified incubator at 37°C for 30 minutes. DHE was counterstained with DAPI. Sections were imaged within 8 hours of staining with a fluorescent ZEISS AXIOSKOP 40 microscope. Identical acquisition settings were used for tissue from wild-type or mutant animals. Fluorescence images were quantified with ImageJ. Integrated fluorescence intensity (IFI) was calculated by integrating the area and strength of red staining within the aortic wall in each image. Error bars represent standard error.

2.10 RNA extraction and qPCR

Following the echo, Doppler, and catheterization studies, RNA was extracted from the ascending and descending aorta of a subset of the mice. For RNA extraction, the mice were perfused with saline and the tissue harvested, cleaned, and then flash frozen. Trizol (Invitrogen) was used for the extraction of RNA. RNA was then reverse transcribed using the cDNA Archive Kits (Life Technologies) or iScript cDNA synthesis kit (Bio-Rad) following the manufacturer protocols. For real-time PCR analysis of mRNA expression, I utilized both TaqMan (Applied Biosystems, Foster City CA) and SyberGreen primers. SybrGreen probes were designed as described in the **Table 2.2** with references. When mentioned, I acknowledge the catalog number for the Taqman probes that were used. Experiments were performed in triplicate, and Gapdh was used as an endogenous control for each run.

Gene	Forward Primer (5'-3')	Reverse Primer (5'-3')
Agt	cgagtgggagaggttctcaatag	gacgtggctcggctgttctt
Ren	ggatcaggagagagtcacaggttt	tcacagtgttccaccacagt
Ace	gggcattgacctagagactgatg	cttgggctgtccggtcata
Enpep	cccatgatagagacgtactttca	cctgccatcccagcaaatac
Agtr1a	actcacagcaaccctccaag	ctcagacactgttcaaatgcac
Agtr1b	cgccagcagcactgtaga	ggaggggggtgaattcaaaa
At2	ccctctctgggcaacctattact	atcgacactcatgcaggtataaaaa
Gapdh	caaaatggtgaaggtcggtgtg	tgatgttagtggggtctcgctc

Table 2.2 – Primers designed from SybrGreen utilized in our studies.

“2.11 2D-gel electrophoresis

Cultured SMCs or freshly isolated ascending aortic tissue were homogenized in urea sample buffer, containing 8M urea, 20mM Tris, 23mM glycine, 0.2mM EDTA, 5% saturated sucrose, and 10mM DTT. Three micrograms of cell lysates mixed with or without 200ng of purified SM α -actin or SM γ -actin (provided by Dr. Kathleen Trybus from the University of Vermont) were added into 450 μ L of Rehydration/Sample buffer (Bio-Rad). Samples were loaded onto 24 cm, pH 4–7, immobilized pH gradient strips (Bio-Rad) overnight and focused in a PROTEAN® i12™ IEF System (Bio-Rad) for 60kVh. Then, the strips were equilibrated in Equilibration Buffer I and II (Bio-Rad), the center third parts were cut out and saved, and the strips were gently inserted into a 8-12% SDS-PAGE mini-gel (Bio-Rad). Then, the gel was run, transferred to nitrocellulose membrane, blotted with anti-pan actin antibody (MA5-11869, Sigma), and visualized as described in routine immunoblotting. The calculated isoelectric points for α -, β -, and γ -actin are 5.24, 5.29, and 5.31, respectively.

2.12 NADPH oxidase activity assay.

Aortic tissues harvested from 2 months old mice (n=4 per group) were ground in chilled grinding vials and were homogenized in lysis buffer (20 mmol/l KH_2PO_4 , 1 mmol/l EGTA, and protease inhibitors cocktail; pH 7.4) and sonicated for 5s (3x with 10s interval). The homogenates were then centrifuged at 750 *g* for 5 min. The pellet was discarded and the supernatant was collected and subjected to a lucigenin-enhanced luminescence assay as described before to determine NADPH oxidase activity in the aortic tissue homogenate (69). Protein content was measured in an aliquot of homogenate by Bradford assay.

NADPH oxidase activity was measured by chemiluminescence in a well containing assay phosphate buffer (50 mM KH_2PO_4 , 1 mM EGTA, and 150 mM sucrose; pH 7.4), 5 μM lucigenin (Sigma), and the sample (50 μl). Reactions (final volume, 250 μl) were initiated by addition of 100 μM NADPH (Sigma). Luminescence was measured every second for 5 min in a luminometer (BioTek Synergy™ HT; BioTek Instruments, Inc., Winooski, VT). A background value was subtracted from each reading. Activity was calculated from the ratio of mean light units to total protein level and expressed as arbitrary units (relative light unit).

2.13 Calcium imaging

Cells were seeded on 25mm coverslips and pretreated with the indicated drugs for the indicated times. Cells were loaded with Fura-2AM for 10-15 minutes and then placed in the imaging chamber with 0.5mL of culture medium. Coverslips were mounted for viewing on a Nikon TE200 microscope, and imaging was performed with Incytm2 software (Intracellular Imaging, Inc.). Measurements were taken using excitation wavelengths of 343/380 nm and emission wavelength of 520 nm. Basal Ca^{++} was assessed for 20 seconds, then 0.5mL of medium containing the indicated amounts of AngII was added to the chamber. Imaging continued until Ca^{++} levels returned to baseline. Data is represented as F_{max}/F_0 where F_{max} represents the highest 340/380 ratio and F_0 represents the baseline 340/380 ratio for each cell.”

Quoted text reprinted from Supplemental Information with minimal modification with permission from Wolters Kluwer Health (Chen J, Peters AM, Papke CL, Villamizar C, Ringuette LJ, Cao JM, Wang S, Ma S, Gong L, Byanova K, Xiong J, Zhu MX, Madonna R, Kee P, Geng YJ, Brasier A, Davis EC, Prakash SK, Kwartler CS, Milewicz DM. Loss of Smooth Muscle alpha-actin Leads to NF-kappaB-Dependent Increased Sensitivity to Angiotensin II in Smooth Muscle Cells and Aortic Enlargement *Circ Res* 2017). See reference (11)

2.14 Statistical analysis

All data are expressed as mean \pm standard deviation. Multiple groups were analyzed assuming unpaired, non-parametric analysis (Kruskal-Wallis). Differences between specific

groups were analyzed assuming unpaired, non-parametric analyses (Mann-Whitney U). All groups included 4 or more male mice depending on the study. I was limited by survival rates in some of the long term treated *Acta2*^{-/-} mice although, the analysis consists of 5 or more animals for most of the studies. Statistical analysis and graphs were all produced with GraphPad Prism 6 (Version 6.03) or with Microsoft Excel. Differences were considered significant when $p < 0.05$. However p values approaching the 0.05 limit may be reported if I felt that it was due to that experiment being underpowered. The Bonferroni correction was not performed. When shown in the figures, a * indicates $p \leq 0.05$, ** indicates $p \leq 0.01$, *** indicates $p \leq 0.001$, and **** indicates $p \leq 0.0001$.

Chapter 3 –The *Acta2*^{-/-} mouse model of thoracic aortic disease: source of increased AngII signaling and pharmacologic manipulation of AngII signaling

3.1 Introduction

As mentioned earlier, in patients with thoracic aortic aneurysm or dissection (TAAD), it has been shown that up to 20% of them have a genetic predisposition for the disease (33, 34). Although many of those patients have syndromic features such as Marfan syndrome, the majority do not have features of a syndrome. These patients show no specific distinguishable features to identify them to be at risk for thoracic aortic disease other than a family history of the disease. In these cases, *ACTA2* is the most frequently mutated gene, accounting for 12-20% of the familial mutations making it a specific clinical concern. *ACTA2* encodes the SMC-specific isoform of α -actin (SM α -actin), which makes up to 40% of SMC cellular protein. SMCs major function is contracting in response to stimuli, such as cyclic strain or neurostimulation. This cyclic contraction is mediated by sliding thin filaments composed of α -actin filaments over the thick filaments, composed of SMC-specific β -myosin heavy chain and other proteins. *ACTA2* variants causing thoracic aortic disease are missense mutations inherited in an autosomal dominant pattern, which have been shown *in vitro* to cause a dominant negative effect on SMC α -actin filament formation (5, 41). It is notable that *ACTA2* is a highly conserved and invariable gene with essentially no variation in the general population. Missense variants throughout the protein have been identified and strong associations exist between specific genotypes and phenotypes (5). Recurrent mutations disrupting specific amino acids, such p.R179, p.R258, and p.R149, have sufficient clinical data to identify distinctive clinical phenotypes associated with each variant and allow for personalized management of the vascular disease associated with these variants (70-73).

To model vascular disease in patients with ACTA2 mutations, we used a mouse model with knock out of SMC α -actin, *Acta2*^{-/-} mice. Prior studies had shown that *Acta2*^{-/-} mice have normal vascular development, but the mice are hypotensive and aortic segments contract less with agonist stimulation (67). Work in our lab initially focused on characterizing the SMC phenotype and determined that *Acta2*^{-/-} SMCs were hyperplastic due to activation of cellular pathways, involving FAK, platelet-derived growth factor signaling, and reactive oxygen species (ROS) (9).

In the studies described below, we sought to characterize aortic pathology in *Acta2*^{-/-} mice and determine whether treatment with modulators of the angiotensin system could alter the pathology. I show that *Acta2*^{-/-} mice have aortic enlargement, but this enlargement does not progress to dissection. Furthermore, the aortic enlargement is attenuated by losartan treatment but exacerbated by captopril treatment. These results once again emphasize the complex role of angiotensin signaling in aortic disease. Through my investigations of the cellular mechanisms of aneurysm formation, we identified that increased NF- κ B signaling is responsible for increased expression of *Agtr1*. The overexpression of *Agtr1* leads to increased sensitivity of the aortic SMCs to endogenous AngII levels and drives enlargement of the aorta. My results show a completely novel mechanism by which angiotensin signaling can be increased in cells without an increase in local or systemic levels of AngII.

3.2 Results

3.2.1 *Acta2*^{-/-} mice and losartan treatment over time

There was no difference in the size of the aortic root or the ascending aorta between *Acta2*^{-/-} and WT mice at 4 weeks of age (**Figure 3.1 A**). By 6 months of age, a significant increase in the size of the aortic root in *Acta2*^{-/-} mice was evident when compared to WT mice, and the aortic diameter continued to increase at 7 months of age (**Figure 3.1 B**). Interestingly, we observed these changes despite the fact that the *Acta2*^{-/-} mice were significantly hypotensive compared to the WT mice (11). Importantly, there was no significant difference in mouse survival between the mutant and WT mice (**Figure 3.1 C**).

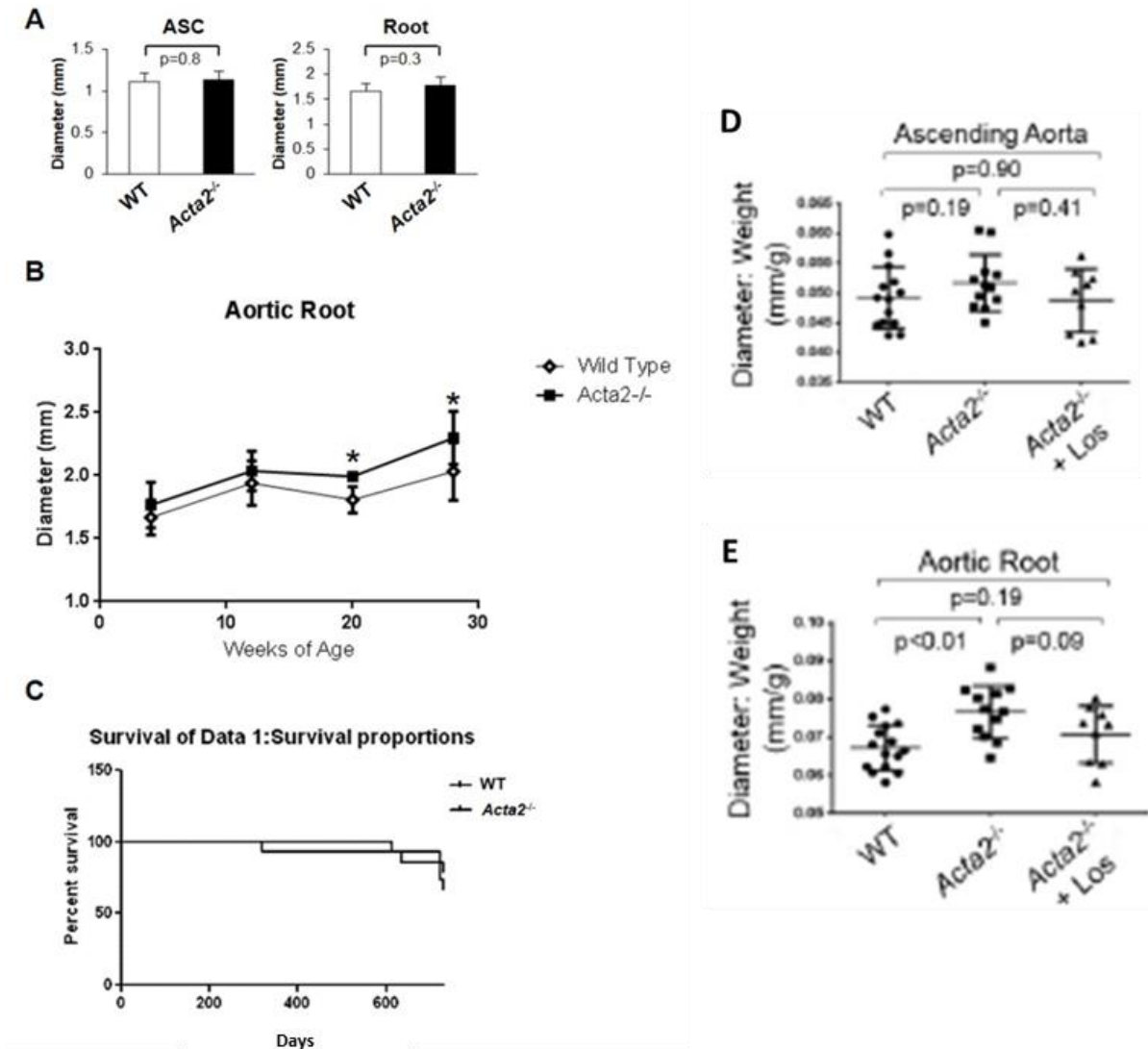


Figure 3.1 – A) At four months of age there was no significant difference between the size of the ascending aorta and the aortic root between the WT and $Acta2^{-/-}$ mice. B) Over time the aortic root became significantly larger in the $Acta2^{-/-}$ by 20 weeks of age. C) There was no difference significant in survival between these mice and their WT littermates. D & E) Ascending aorta and the aortic root measurements at seven months of age in the $Acta2^{-/-}$ with and without treated with losartan. Losartan was able to attenuate the growth of the aortic root. Note that the ascending aorta is not significantly enlarged in the $Acta2^{-/-}$ mice. Modified and reprinted with permission from Circulation Research (Chen J, Peters AM, Papke CL, Villamizar C, Ringuette LJ, Cao JM, Wang S, Ma S, Gong L, Byanova K, Xiong J, Zhu MX, Madonna R, Kee P, Geng YJ, Brasier A, Davis EC, Prakash SK, Kwartler CS, Milewicz DM. Loss of Smooth Muscle alpha-actin Leads to NF-kappaB-Dependent Increased Sensitivity to Angiotensin II in Smooth Muscle Cells and Aortic Enlargement. Circ Res 2017). See reference (11)

I also observed an increase in the number of elastin lamellae in the *Acta2*^{-/-} postnatal aortas when compared to WT aortas ($p < 0.05$, **Figure 3.2 A, B**). Elastic lamellae are laid down during development (7, 74), and the increased layers in the aorta can be observed in the histologic sections at every time point regardless of the treatments or procedures the mice went through postnatally. A similar phenotype is seen in mice deficient in elastin, *Eln*^{-/-} mice (10). At 4 weeks of age *Acta2*^{-/-} aortas also have an increase in the density of cells staining positive for a calponin, a SMC marker (**Figure 3.3 A, C**). However, the cell density normalizes to the same density as WT by 8 weeks of age, and the density remains the same as WT at all other time points assessed (**Figure 3.2**). This data suggests that the cellular proliferation phenotype and pathways that were previously identified in *Acta2*^{-/-} SMCs do alter the development of aortic disease in this mouse. The pathophysiologic changes seen between the observed groups were consistent with what we had previously observed in this model. In early studies, we found that there was a significant increase in the medial area of the *Acta2*^{-/-} mice while there was no significant difference in medial cell density at older age. This would possibly indicate some form of cellular hypertrophy (**Figure 3.5**). However, the significant difference in medial cell density at a younger mouse age without increase in medial area may indicate that the cellular hyperplasia already exist after development.

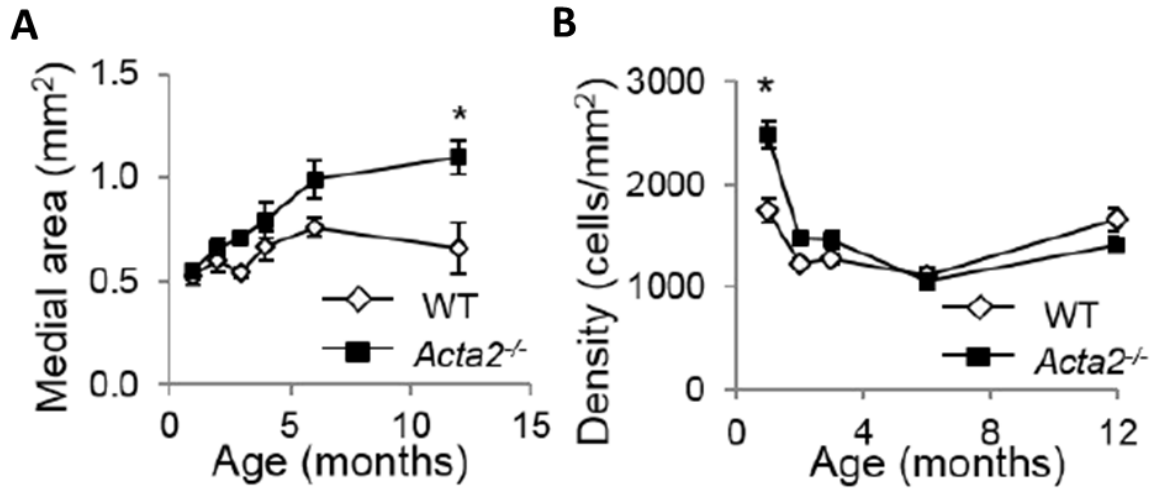


Figure 3.2 – A) Aortic medial area increases significantly over time in the *Acta2*^{-/-} mice compared to WT mice. B) Medial cell density was significantly higher in *Acta2*^{-/-} mice compared to WT shortly after birth, however, the cell density between the mutant and WT were similar by 3 weeks of age. Modified and reprinted with permission from Circulation Research (Chen J, Peters AM, Papke CL, Villamizar C, Ringuette LJ, Cao JM, Wang S, Ma S, Gong L, Byanova K, Xiong J, Zhu MX, Madonna R, Kee P, Geng YJ, Brasier A, Davis EC, Prakash SK, Kwartler CS, Milewicz DM. Loss of Smooth Muscle alpha-actin Leads to NF-kappaB-Dependent Increased Sensitivity to Angiotensin II in Smooth Muscle Cells and Aortic Enlargement, Circ Res 2017). See reference (11)

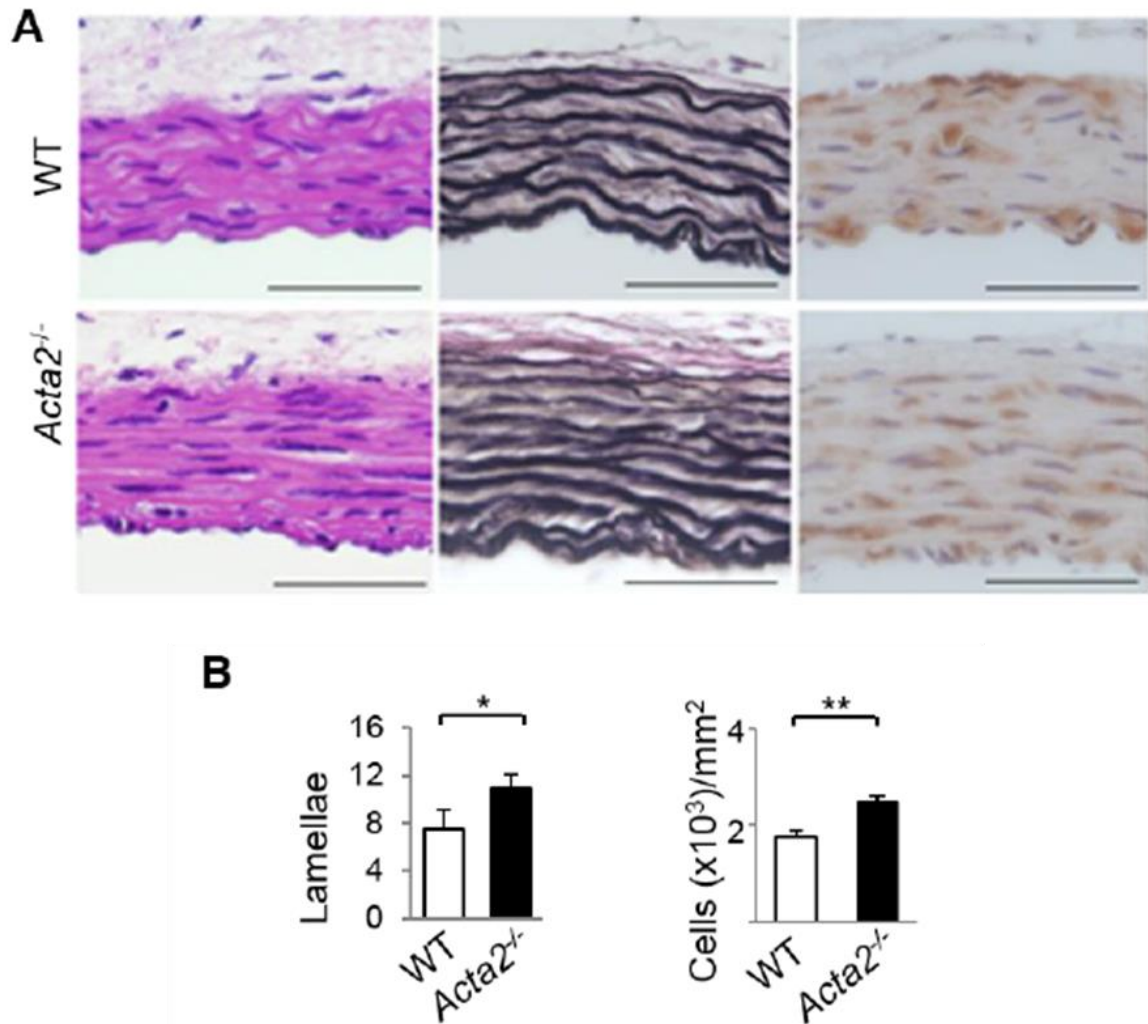


Figure 3.3 – Histologic analysis of the ascending aortas in mice at four weeks of age. A,B) Representative H&E, Movat, and calponin stains of the WT and *Acta2*^{-/-} mice. (A) Show the increase in elastic lamellae and cells staining positive for calponin (quantified in B). Modified and reprinted with permission from Circulation Research (Chen J, Peters AM, Papke CL, Villamizar C, Ringuette LJ, Cao JM, Wang S, Ma S, Gong L, Byanova K, Xiong J, Zhu MX, Madonna R, Kee P, Geng YJ, Brasier A, Davis EC, Prakash SK, Kwartler CS, Milewicz DM. Loss of Smooth Muscle alpha-actin Leads to NF-kappaB-Dependent Increased Sensitivity to Angiotensin II in Smooth Muscle Cells and Aortic Enlargement, 2017) (11).

Given that losartan blocked aortic enlargement in other mouse models of thoracic aortic disease (61, 63), we assessed whether losartan treatment could rescue the aortic

dilation and pathology in *Acta2*^{-/-} mice. The mice were treated with losartan starting at 4 weeks of age, and treatment continued for six months. The growth of the aortic root was attenuated with losartan treatment in the *Acta2*^{-/-} mice compared to WT mice, indicating that losartan can partially prevent the age-dependent aortic growth (Fig 3.1-D,E). *Acta2*^{-/-} aortas have minimal medial degeneration and the only significant change in aortic pathology in the mutant aortas compared with WT aortas was an increase in proteoglycan deposition in the medial layer, and this deposition was prevented by losartan. There were no significant differences in elastin breaks between *Acta2*^{-/-} and WT mice. However, collagen deposition in the adventitial layer was borderline increased (p=0.07) and attenuated by losartan (p=0.08) (**Figure 3.4**).

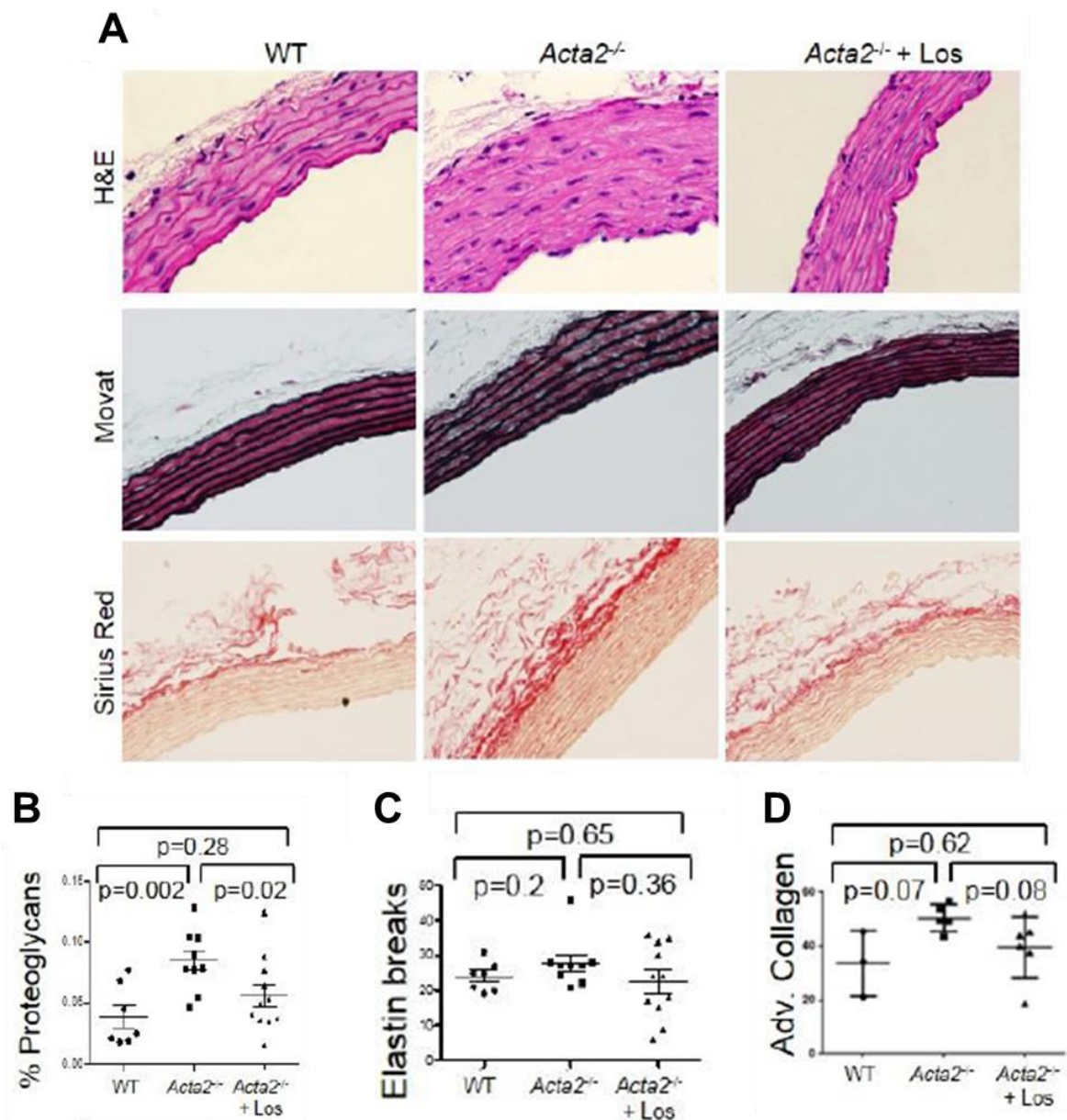


Figure 3.4 – A) The H&E, Movat, and Sirius Red stains of the WT, *Acta2*^{-/-}, and *Acta2*^{-/-} losartan treated mice. The Movat stain colors indicate elastin (black), proteoglycans (blue), and the cells which stained (red). B) Analysis showed that there was a significant increase in the amount of proteoglycan in the wall of the *Acta2*^{-/-} mice while there was significantly less with losartan treatment. C & D) showed that there is no difference in elastin breaks between the groups. It appears that adventitial collagen is increased, but our study is underpowered. Modified and reprinted with permission from Circulation Research (Chen J, Peters AM, Papke CL, Villamizar C, Ringuette LJ, Cao JM, Wang S, Ma S, Gong L, Byanova K, Xiong J, Zhu MX, Madonna R, Kee P, Geng YJ, Brasier A, Davis EC, Prakash SK, Kwartler CS, Milewicz DM. Loss of Smooth Muscle alpha-actin Leads to NF-kappaB-Dependent Increased

Sensitivity to Angiotensin II in Smooth Muscle Cells and Aortic Enlargement, Circ Res 2017). See reference (11) .

3.2.2 Long term captopril treatment incapable of reversing pathological changes associated with *Acta2*^{-/-} mouse model

Losartan was able to attenuate aortic enlargement in the *Acta2*^{-/-} mice. We therefore we wanted to further define the role of the angiotensin system in aneurysm formation and explore whether other therapeutic targets within this system might be effective. ACE inhibitors (ACEi) are upstream in the AngII signaling pathway of AngII receptor blockers, like losartan (**Figure 1.5**), we tested the use of an ACEi, captopril, in blocking aortic enlargement in the *Acta2*^{-/-} mice. Habashi et al. found that they were able to inhibit aneurysm formation and the angiotensin pathway (65). This captured our interest given the clinical use of ACEi's despite the fact that others noted that ACEi (enalapril) were not as effective in treating aortic aneurysm in *Fbn1*^{C1039G/+} (48). ACE inhibitors have been studied extensively in other tissues (75, 76). For this study, male *Acta2*^{-/-} mice were treated for 10 months with captopril, with treatment beginning at 1 month of age. By 11 months of age, there was no difference in the aortic diameters between the *Acta2*^{-/-} mice and WT mice. Surprisingly, there was a significant increase in both the ascending aorta and aortic root diameter in the *Acta2*^{-/-} mice treated with captopril compared to WT and untreated *Acta2*^{-/-} littermates (**Figure 3.4 A & B**). Because larger mice tend to have larger aortas, we also analyzed the data normalizing the aortic size to the weight for all mice. There was no significant difference in the weight of WT and *Acta2*^{-/-} mice, but treatment with captopril

significantly decreased their weight (**Figure 3.4 C**). As a result, when we normalized to weight, the difference between the ascending aorta and aortic root size between the mice becomes more significant even in the ascending aorta (**Figure 3.4 D & E**).

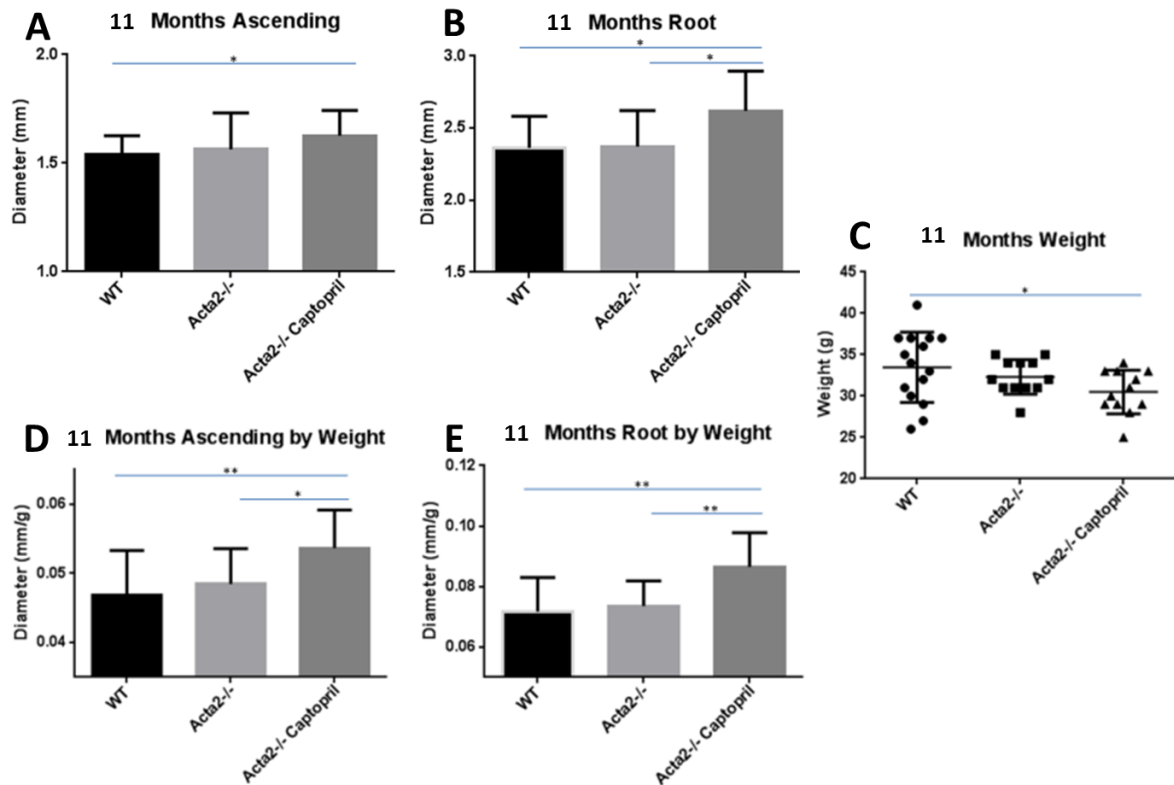


Figure 3.5 – A, B) Ascending aortic (A) and aortic root (B) measurements at 11 months of age and 10 months of treatment show that captopril treatment exacerbates the phenotype of *Acta2*^{-/-} mice. C) *Acta2*^{-/-} mice treated with captopril weigh significantly less than wild-type. D, E) Normalizing to weight increases the significant differences between the groups. * indicates $p \leq 0.05$ and ** indicates $p \leq 0.01$ in the analysis. (Andrew M. Peters, Zhen Zhou, Jiyuan Chen, Alexandra Janda, Corey L. Reynolds, Shao-Qing Kuang, Shanzhi Wang, Siddharth Prakash, GenTAC Consortium, Callie S. Kwartler, Dianna M. Milewicz Pharmacologic Manipulation of the Angiotensin System Affects Aortic Remodeling and Aneurysm Development: Cautions for Clinical Practice, Submitted 2017) See reference (77).

Despite exacerbating the dilation of the aorta, captopril treatment did reverse some of the pathologic changes associated with *Acta2*^{-/-} aortas. Specifically, the increased medial and adventitial areas were decreased with captopril treatment. These results suggest that the thickening of the adventitia and the media is actually protective. Captopril treatment had no effect on proteoglycan deposition but did increase elastin content in the aortic wall. The cellular hypertrophy that causes the medial thickening over time does not happen in the captopril treated aortas, so while elastin content remains constant, the amount of cells in the wall is lower in the captopril treated mice (**Figure 3.6**).

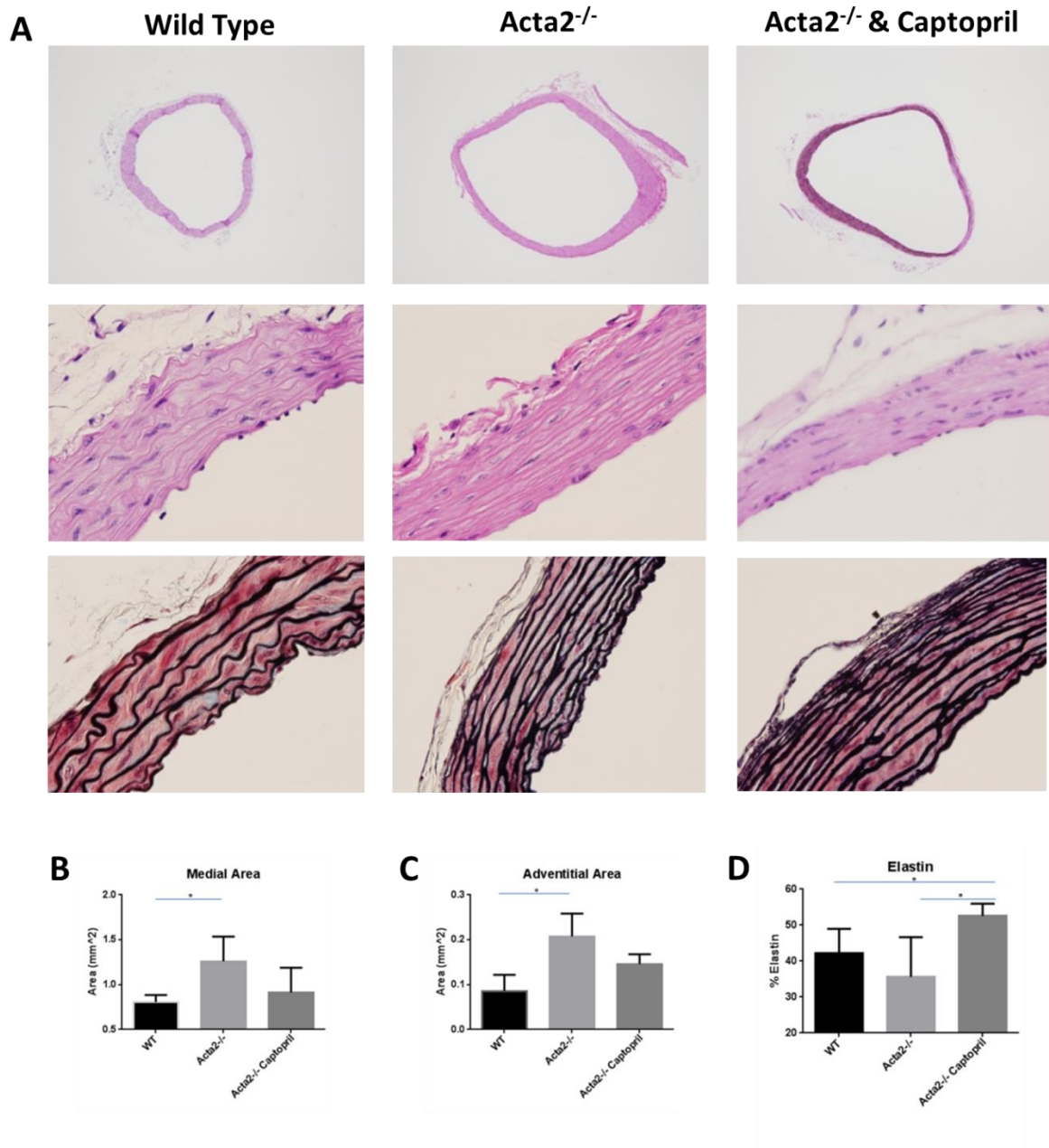


Figure 3.6 – A) H&E and Movat stains of the WT, *Acta2*^{-/-}, and *Acta2*^{-/-} mice treated with captopril. B & C) Analysis indicates that the *Acta2*^{-/-} mice have a significant increase in the medial area and the adventitial area. These increases are not seen in the *Acta2*^{-/-} captopril treated mice. D) There was a significant increase in the amount of elastin in the medial wall of the captopril treated mice compared to both the WT and untreated *Acta2*^{-/-} mice. (Andrew M. Peters, Zhen Zhou, Jiyuan Chen, Alexandra Janda, Corey L. Reynolds, Shao-Qing Kuang, Shanzhi Wang, Siddharth Prakash, GenTAC Consortium, Callie S. Kwartler, Dianna M. Milewicz Pharmacologic Manipulation of the Angiotensin System Affects Aortic

“To investigate the increased signaling through the *Agtr1a* in *Acta2*^{-/-} mice, SMCs were explanted from the ascending aorta. Our previous studies determined that *Acta2*^{-/-} SMCs have increased levels of cellular ROS and ERK1/2 signaling (9). To determine whether *Acta2*^{-/-} SMCs are more responsive to exogenous AngII, we assessed pRelA levels. Surprisingly, *Acta2*^{-/-} SMCs show activated pRelA in the absence of AngII, whereas WT SMCs do not (**Figure 3.7 A**), and this increased pRelA signaling correlates with increased *Il6* expression in the *Acta2*^{-/-} SMCs [data not shown]. Furthermore, the *Acta2*^{-/-} SMCs showed increased sensitivity to AngII and prolonged signaling. In the *Acta2*^{-/-} SMCs, pRelA levels increase at 10 nmol/L AngII, whereas pRelA levels do not increase in WT SMCs until a 100-fold higher dose of AngII is used (1000nmol/L; **Figure 3.7 A**; [data not shown]). The *Acta2*^{-/-} SMCs are also more sensitive than WT SMCs to exogenous AngII based on intracellular Ca²⁺ assays (**Figure 3.7 B**). The *Acta2*^{-/-} SMCs show earlier and more prolonged increases in pRelA levels than WT SMCs when exposed to 1 μ mol/L AngII [data not shown]. Similar to the *Acta2*^{-/-} aortas, expression of *Agtr1a* is increased >8-fold in the *Acta2*^{-/-} SMCs (**Figure 3.7 D**). For all cellular studies, *Agtr1b* expression followed the same pattern as *Agtr1a* but is \approx 10-fold lower (data not shown).

We sought to determine the signaling pathway responsible for increased *Agtr1a* expression and AngII sensitivity in the *Acta2*^{-/-} SMCs. Inhibition of the *Agtr1a* using losartan effectively blocks the increase of pRelA in response to exogenous AngII but does not decrease the basal level of pRelA in *Acta2*^{-/-} SMCs; *Il6* expression with these treatments correlates with pRelA levels[data not shown]. AngII-induced NF- κ B activation in SMCs is mediated by RhoA/ROCK phosphorylation of Ser536 of RelA (78). Therefore, *Acta2*^{-/-} SMCs were exposed to *Clostridium botulinum* exoenzyme C3 exotoxin to block Rho activation, which blocks AngII-inducible pRelA as expected, but does not decrease baseline activation of RelA in the *Acta2*^{-/-} SMCs [data not shown]. ROS is a known activator of NF- κ B signaling, and we previously found increased cellular ROS levels in the *Acta2*^{-/-} SMCs (9).

Blocking cellular ROS using [N-acetylcysteine (NAC)] decreases the baseline pRelA levels in the *Acta2*^{-/-} SMCs and

reduces the sensitivity of these cells to exogenous AngII (**Figure 3.7 C**; [data not shown]). NAC treatment also decreases the expression of *Agtr1a*, *Il6*, and *Mmp2* in the mutant SMCs to levels similar to WT SMCs (**Figure 3.7 D**). Finally, pre-treatment of cells with NAC abolishes the increase in intracellular calcium in response to exogenous AngII in both WT and *Acta2*^{-/-} SMCs (**Figure 3.7 E**). To confirm that NF- κ B signaling is responsible for the hypersensitivity of the *Acta2*^{-/-} SMCs, these cells were treated with an NF- κ B inhibitor anatabine, which partially blocked phosphorylation of RelA (**Figure 3.8 A**) and also reduced expression of *Il6*, *Agtr1a*, and *Mmp2* to levels similar to WT cells (**Figure 3.8 B**). Helenalin, an inhibitor of NF- κ B DNA binding activity, which does not affect RelA phosphorylation, also significantly blocks expression of *Il6*, *Agtr1a*, and *Mmp2* [data not shown] (79, 80). In addition, pre-treatment of cells with either anatabine or helenalin abolishes the increase in intracellular calcium in response to exogenous AngII in both WT and *Acta2*^{-/-} SMCs (**Figure 3.8 C**).

To identify the source of increased ROS, the expressions of the nicotinamide adenine dinucleotide phosphate (NADPH) oxidases were assessed, and expressions of *Nox4* and *p22phox*, along with a known activator of Nox4, *Poldip2*, are all significantly increased in the *Acta2*^{-/-} SMCs (**Figure 3.8 D**) (81, 82). There is no significant change in expression of *Nox1* or *Nox2* [data not shown]. Furthermore, a specific inhibitor of Nox4, VCC588646, reduces ROS levels in *Acta2*^{-/-} SMCs and also significantly decreases expression of *Il6*, *Mmp2*, and *Agtr1a* (**Figure 3.8 E & F**) (83). NF- κ B has been previously shown to directly induce *Nox4* expression,(84) and treatment with helenalin significantly reduces expression of *Nox4*, *Poldip2*, and *p22phox* in *Acta2*^{-/-} SMCs. Taken together, our data suggest a feedback loop in which increased ROS levels drive NF- κ B signaling that increases *Nox4*, *p22phox*, and *Poldip2* expression and ROS accumulation. This feedback loop increases expression of *Agtr1a* leading to increased AngII sensitivity in the aortic SMCs."

Quoted text reprinted with minimal modification with permission from Wolters Kluwer Health (Chen J, Peters AM, Papke CL, Villamizar C, Ringuette LJ, Cao JM, Wang S, Ma S, Gong L, Byanova K, Xiong J, Zhu MX, Madonna R, Kee P, Geng YJ, Brasier A, Davis EC, Prakash SK, Kwartler CS, Milewicz DM. Loss of Smooth Muscle alpha-actin Leads to NF-kappaB-Dependent Increased Sensitivity to Angiotensin II in Smooth Muscle Cells and Aortic Enlargement. 2017) (11)

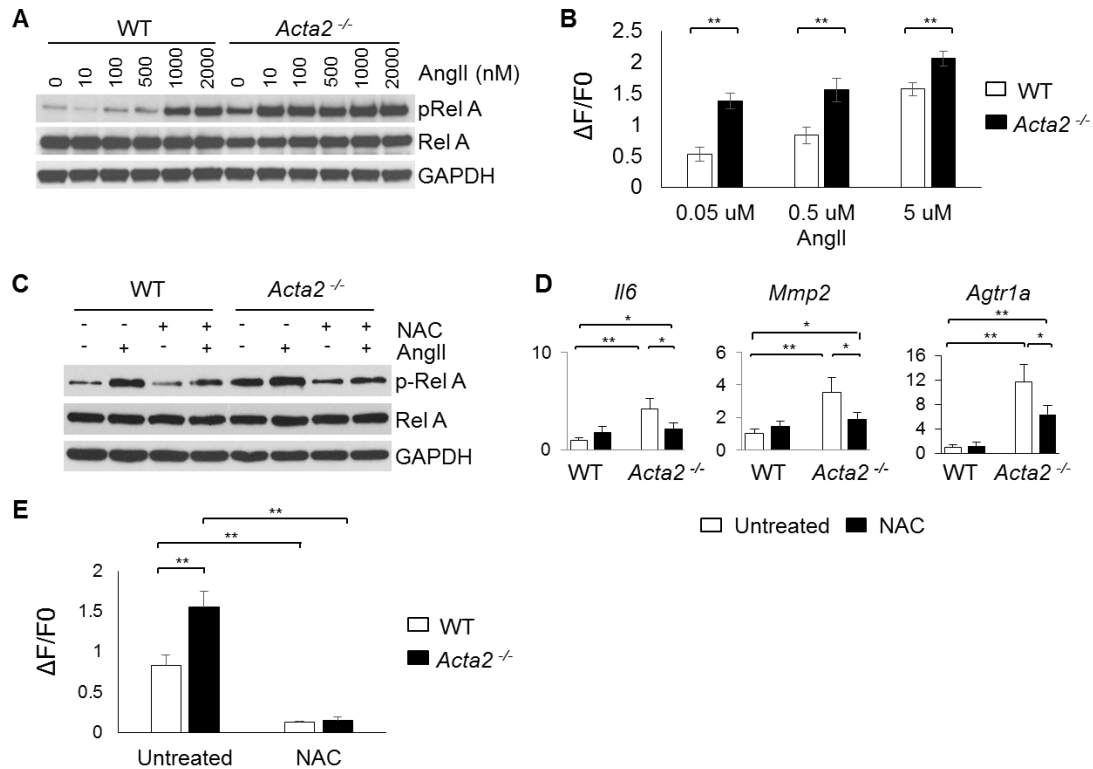


Figure 3.7 – Increased sensitivity to angiotensin II (AngII) in *Acta2*^{-/-} smooth muscle cells (SMCs) is driven by reactive oxygen species (ROS). A) Dose–response curve after 20 min of AngII treatment shows that *Acta2*^{-/-} SMCs have increased baseline phosphorylate RelA (pRelA) that increases with exposure to AngII concentrations as low as 10 nmol/L, compared with 1000 nmol/L in wild-type (WT) SMCs. B) Immediately after stimulation with various doses of AngII, *Acta2*^{-/-} SMCs have increased intracellular Ca²⁺ levels when compared with WT cells. At least 30 cells were measured for each group. C) Treatment with N-acetyl cysteine (NAC) reduces baseline pRelA in *Acta2*^{-/-} SMCs and reduces AngII-induced phosphorylation of RelA in both genotypes. D) *Acta2*^{-/-} SMCs, like the aortic tissue, have increased expression of *Il6*, *Agtr1a*, and *Mmp2*. NAC treatment significantly reduces expression of all 3 genes but not to WT levels. E) Pre-treatment with NAC for 12 h abolishes the increase in intracellular Ca²⁺ levels after stimulation with 0.5 μmol/L AngII in both WT and *Acta2*^{-/-} SMCs. Modified and printed with permission from Circulation Research (Chen J, Peters AM, Papke CL, Villamizar C, Ringuette LJ, Cao JM, Wang S, Ma S, Gong L, Byanova K, Xiong J, Zhu MX, Madonna R, Kee P, Geng YJ, Brasier A, Davis EC, Prakash SK, Kwartler CS, Milewicz DM. Loss of Smooth Muscle alpha-actin Leads to NF-kappaB-Dependent Increased Sensitivity to Angiotensin II in Smooth Muscle Cells and Aortic Enlargement. Circ Res 2017). See reference (11) ”

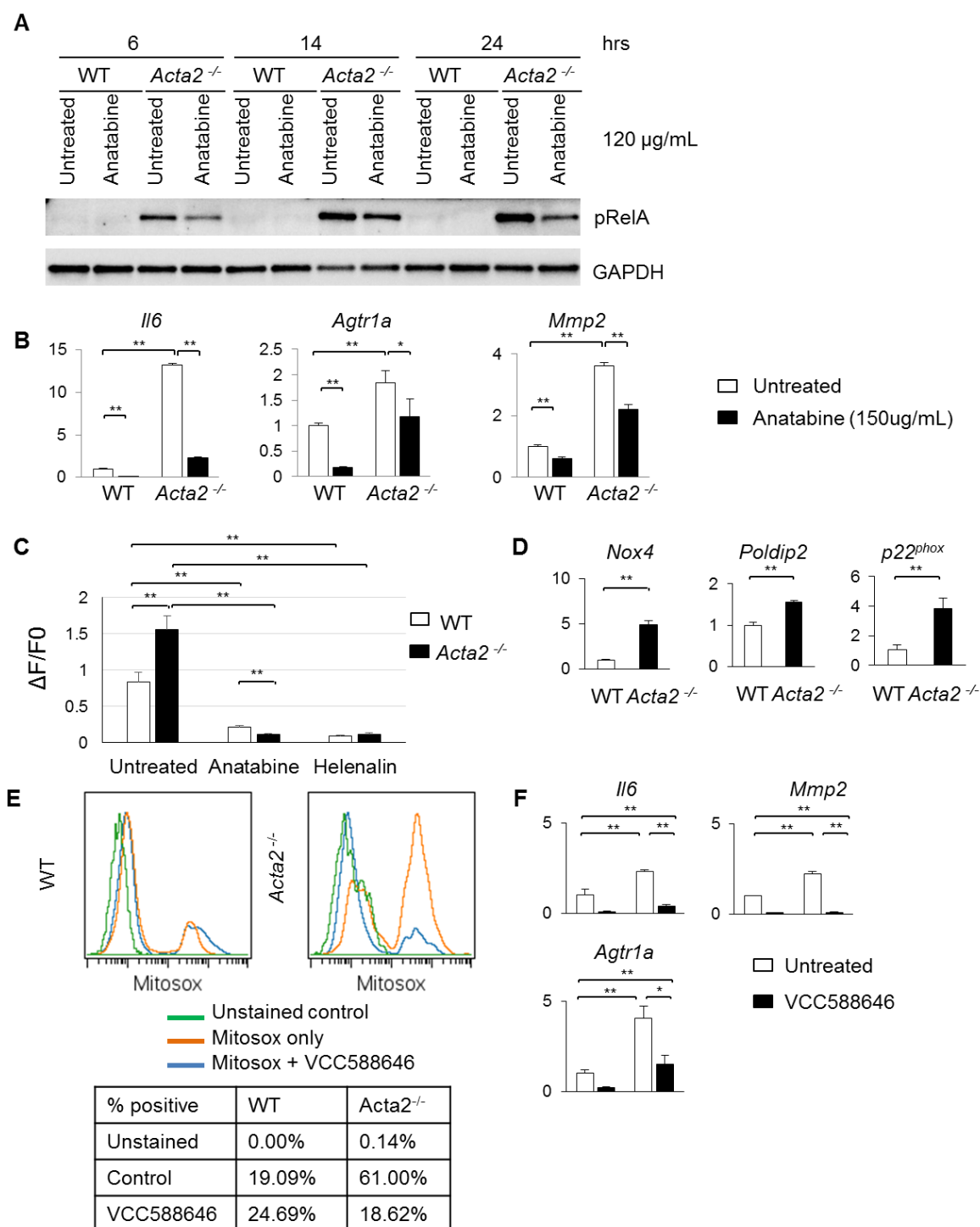


Figure 3.8 – Inhibition of either nuclear factor (NF)- κ B signaling or Nox4 reduces *Agtr1a* expression and decreases sensitivity to angiotensin II (AngII) in *Acta2*^{-/-} smooth muscle cells SMCs. A) Helenalin, an inhibitor of NF- κ B signaling, reduces expression of *Il6*, *Mmp2*, and *Agtr1a* after 6 h of treatment. B) Twelve- hour pre-treatment with helenalin or a second NF-

κB inhibitor anatabine abolishes the increase in intracellular Ca^{2+} with 0.5 $\mu\text{mol/L}$ AngII stimulation in both wild-type (WT) and *Acta2*^{-/-} SMCs. C) *Acta2*^{-/-} SMCs have increased expression of *Nox4*, *Poldip2*, and *p22phox* when compared with WT SMCs. D) A specific inhibitor of Nox4, VCC588646, reduces reactive oxygen species in *Acta2*^{-/-} SMCs to WT levels. E) VCC588646 treatment reduces expression of *Il6*, *Mmp2*, and *Agtr1a* in WT and *Acta2*^{-/-} SMCs. F) Treatment with the NF-κB inhibitor helenalin for 6 h reduces expression of *Nox4*, *Poldip2*, and *p22phox* in *Acta2*^{-/-} SMCs. Modified and reprinted with permission from Circulation Research (Chen J, Peters AM, Papke CL, Villamizar C, Ringuette LJ, Cao JM, Wang S, Ma S, Gong L, Byanova K, Xiong J, Zhu MX, Madonna R, Kee P, Geng YJ, Brasier A, Davis EC, Prakash SK, Kwartler CS, Milewicz DM. Loss of Smooth Muscle alpha-actin Leads to NF-kappaB-Dependent Increased Sensitivity to Angiotensin II in Smooth Muscle Cells and Aortic Enlargement, Circ Res 2017). See reference (11) .

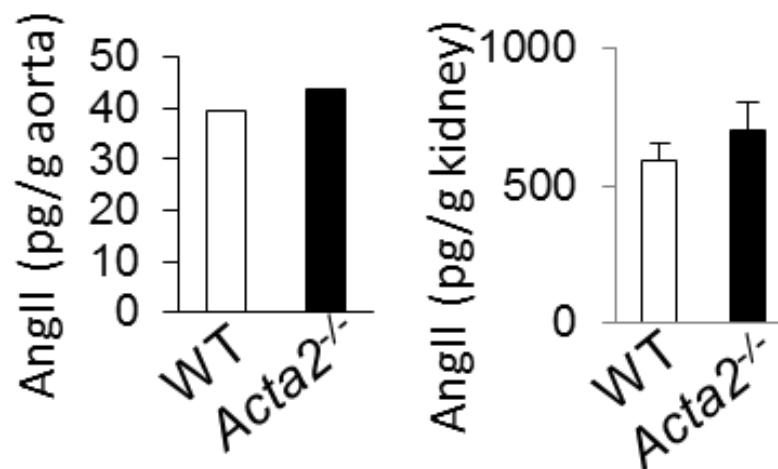


Figure 3.9 – Levels of AngII in *Acta2*^{-/-} aortas and kidneys are not significantly different from WT. Measurements were made at 3 mo of age (n=20 aortas per genotype, 4 kidneys per genotype). Modified and reprinted with permission from Circulation Research (Chen J, Peters AM, Papke CL, Villamizar C, Ringuette LJ, Cao JM, Wang S, Ma S, Gong L, Byanova K, Xiong J, Zhu MX, Madonna R, Kee P, Geng YJ, Brasier A, Davis EC, Prakash SK, Kwartler CS, Milewicz DM. Loss of Smooth Muscle alpha-actin Leads to NF-kappaB-Dependent Increased Sensitivity to Angiotensin II in Smooth Muscle Cells and Aortic Enlargement. Circ Res 2017.) See reference (11)

3.2.3 L-NAME and NAC in *Acta2*^{-/-} mice

Many of the studies in our lab have focused on the role of blood pressure in aortic disease. We and others have done numerous studies on mechanical stress and blood pressure in mouse models. I specifically discuss how we investigate this model in a hyper acute setting in Chapter 4 (52). Others have also shown that mechanically stressing the vessels can influence the angiotensin system through a β -arrestin and G-protein mediated pathway (85).

Given these ideas, we decided to significantly increase the biomechanical stress on the ascending aorta in the *Acta2*^{-/-} mice by utilizing a nitric oxide synthase inhibitor, L-NG-nitroarginine methyl ester (L-NAME), coupled with a high salt diet (8% NaCl in chow, Harlan). The regimen made the hypotensive *Acta2*^{-/-} mice normotensive (**Figure 3.10 A**) (11). With the increase in blood pressure, the studies showed that the increase in biomechanical stress in these mice could lead to a significant increase in aortic root size by just three months of age compared to the untreated WT and *Acta2*^{-/-} mice. The ascending aorta was also significantly enlarged in the normotensive *Acta2*^{-/-} mice by 3 months of age (**Figure 3.10 B & C**). These data show that the forces associated with increased blood pressure increase the growth rate of the ascending aorta and aortic root in the *Acta2*^{-/-} mice.

We initiated a treatment trial with N-acetyl cysteine (NAC), a broad spectrum antioxidant, to determine whether reducing ROS could prevent aortic dilation. To better observe any decrease in phenotype, we chose to use the *Acta2*^{-/-} mice treated with L-

NAME and high salt diet as these mice have accelerated aortic enlargement. Co-treatment with L-NAME, high salt diet, and NAC in *Acta2*^{-/-} mice attenuated the enlargement of the ascending aorta when compared with WT aortas, but the aortic root still significantly enlarged (**Figure 3.10 B & C**). These results suggest that ROS plays a greater role in the development of ascending aortic enlargement than aortic root enlargement.

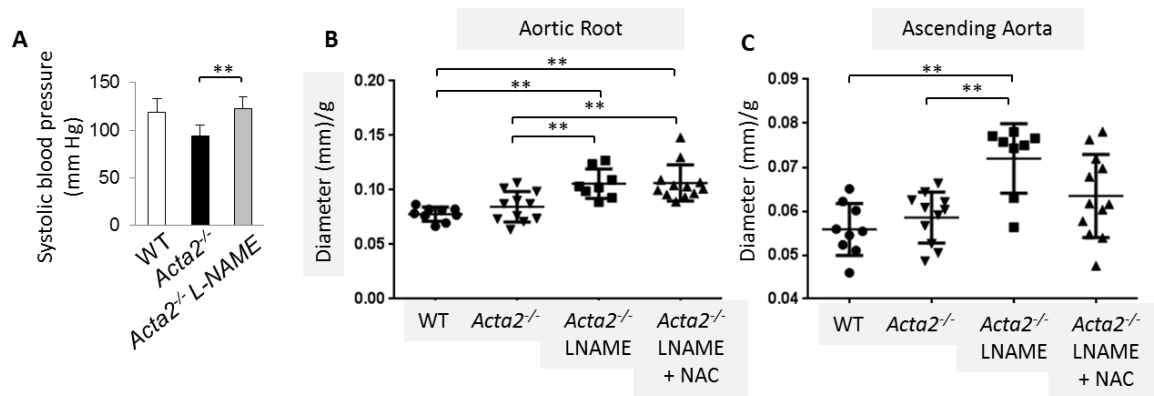


Figure 3.10 – A) All tail cuff blood pressure measurements taken in WT mice, *Acta2*^{-/-} mice and *Acta2*^{-/-} treated over the course of the study. *Acta2*^{-/-} had significantly lower blood pressure than WT mice. L-NAME and a high salt diet were able to increase the blood pressure in *Acta2*^{-/-} back to normal. B & C) Treatment with L-NAME and high-salt diet significantly increases aortic root dilation at 3 months of age. Treatment with L-NAME, NAC, and high salt diet reduces ascending aortic enlargement. Modified and reprinted with permission from Circulation Research (Chen J, Peters AM, Papke CL, Villamizar C, Ringuette LJ, Cao JM, Wang S, Ma S, Gong L, Byanova K, Xiong J, Zhu MX, Madonna R, Kee P, Geng YJ, Brasier A, Davis EC, Prakash SK, Kwartler CS, Milewicz DM. Loss of Smooth Muscle alpha-actin Leads to NF-kappaB-Dependent Increased Sensitivity to Angiotensin II in Smooth Muscle Cells and Aortic Enlargement. Circ Res 2017). See reference (11) .

3.2.4 *Agtr1*^{-/-} and *Acta2*^{-/-} cross

Since AngII signaling increases superoxide production by activating NADPH oxidases in SMCs (86), we crossed the *Acta2*^{-/-} mice and the *Agtr1a*^{-/-} mice to determine if ROS are increased in the *Acta2*^{-/-} aortas without AngII signaling from the *Agtr1a* receptor. *Agtr1a*^{-/-}

mice are hypotensive and have thinner aortic walls than WT, but do not develop aneurysms. The aortic tissue is more friable and falls apart easily on dissection, making it difficult to work with these mice. I was unable to determine whether aortic dilation was decreased or pathologic endpoints were altered in the *Acta2*^{-/-} *Agtr1a*^{-/-} double mutant mice because the significant hypotension complicated interpretation of the data. Instead, we hypothesized that we would not block the increased ROS signaling in the aorta if the Agtr1a receptor was not present, i.e., ROS would still be increased due to the loss of SM α -actin. *Acta2*^{-/-} *Agtr1a*^{-/-} double mutant mice were born in the expected Mendelian ratio, despite having lower blood pressures than the *Acta2*^{-/-} mice (**Figure 3.11 C**). Both DHE staining and lucigenin assays indicate decreased ROS in *Acta2*^{-/-} *Agtr1a*^{-/-} mice compare to the *Acta2*^{-/-} mice, suggesting that Agtr1a activity is partially, but not completely, responsible for the increased ROS. Importantly, the *Acta2*^{-/-} *Agtr1a*^{-/-} aortas still have significantly higher ROS levels than WT. Furthermore, the expression of *Il6* and *Mmp2* remains higher in the *Acta2*^{-/-} *Agtr1a*^{-/-} double mutant aortas than WT aortas, suggesting that pathways other than Agtr1a contribute to the activation of these genes. Expression of other renin-angiotensin system components was not significantly different in *Acta2*^{-/-} *Agtr1a*^{-/-} mice compared with the single mutants (**Figure 3.11**).

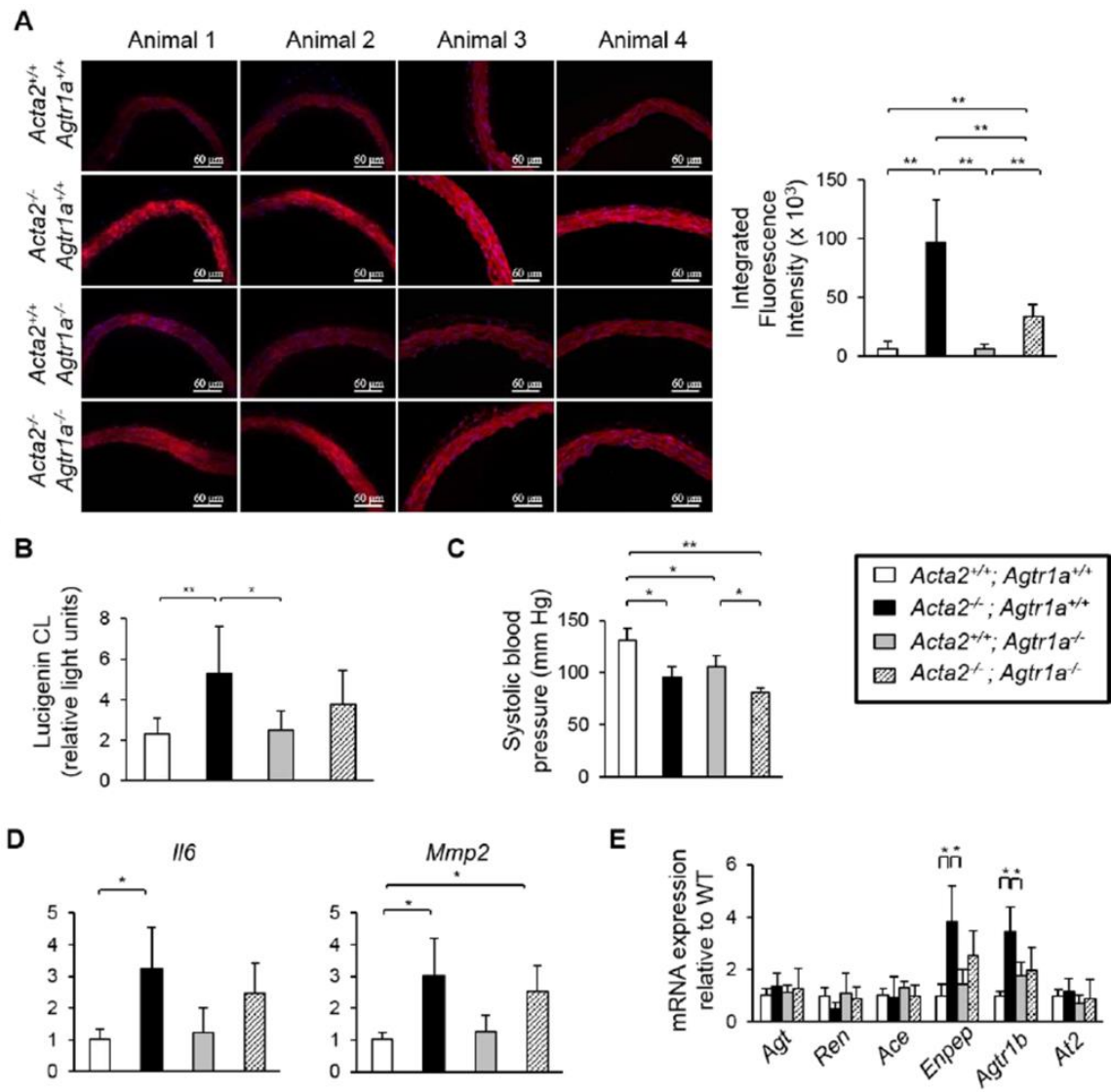


Figure 3.11 – Addition of the *Agtr1a*^{-/-} allele into *Acta2*^{-/-} mice does not completely prevent increased ROS A) frozen DHE staining of aortic sections indicate that ROS levels in the aortas of *Acta2*^{-/-} *Agtr1a*^{-/-} mice are higher than in WT mice, but lower than in *Acta2*^{-/-} mice. B) NADPH oxidase activity in the *Acta2*^{-/-} *Agtr1a*^{-/-} is not different compared to *Acta2*^{-/-} and WT mice. C) *Acta2*^{-/-} *Agtr1a*^{-/-} mice have significantly lower systolic blood pressure than *Acta2*^{-/-} mice. D) Expression of *Mmp2* is elevated in the *Acta2*^{-/-} *Agtr1a*^{-/-} mice compared to WT. E) Components of the RAS system appear to not be affected by the loss of *Agtr1a*. Modified and reprinted with permission from Circulation Research (Chen J, Peters AM, Papke CL, Villamizar C, Ringuette LJ, Cao JM, Wang S, Ma S, Gong L, Byanova K, Xiong J, Zhu MX, Madonna R, Kee P, Geng YJ, Brasier A, Davis EC, Prakash SK, Kwartler CS, Milewicz DM. Loss of Smooth Muscle alpha-actin Leads to NF-kappaB-Dependent Increased Sensitivity to Angiotensin II in Smooth Muscle Cells and Aortic Enlargement, Circ Res 2017). See reference (11) .

3.3 Discussion

I found that NF- κ B signaling driven by increased cellular ROS leads to an increase in expression of the *Agtr1a*. The increased expression of *Agtr1a* in aortic SMCs then leads to activation of AngII-dependent signaling at AngII levels that were 100 fold lower than that required in WT SMCs *in vitro*, as assessed by phosphorylation of RelA and increased intracellular Ca^{2+} . *Acta2*^{-/-} aortas have increased levels of ROS and phosphorylated RelA. Increased expression of *Agtr1a* is also observed. When the *Agtr1a* receptor is deleted in the *Acta2*^{-/-} mice, ROS levels remain elevated. This result indicates that increases in ROS and downstream molecular changes do not completely depend on exogenous AngII signaling through *Agtr1a* in the *Acta2*^{-/-} aortic SMCs. Exogenous AngII further augments both ROS and NF- κ B signaling in the mutant cells. In turn, this drives a feedback loop resulting in further increases in ROS and NF- κ B signaling (**Figure 3.12**). Others groups have shown that when ROS is increased in SMCs by overexpression of p22^{phox}, an important subunit for all NADPH oxidases, SMC hypertrophy driven by AngII is potentiated, making ROS a potential therapeutic target (87). My results indicate that increased cellular ROS in the p22^{phox}-overexpressing SMCs could activate NF- κ B signaling, increasing the expression of *Agtr1a*. This ends up potentiating AngII signaling in aortic SMCs.

The *Acta2*^{-/-} mice develop dilation of the aortic root by 6 months of age. This is similar to the aortic root enlargement observed in patients with *ACTA2* mutations (70), and aortic root dilation is attenuated with losartan, an *Agtr1a* and *Agtr1b* blocking agent (ARB). However, aortic growth is not completely reversed. Losartan treatment attenuates pRelA

signaling but not through ERK1/2 signaling, suggesting that ERK1/2 activation is driven by other pathways. Knocking out *Agtr1a* in *Acta2*^{-/-} mice does not decrease ROS levels to those of WT. This suggests that increased ROS and downstream molecular changes are not dependent on exogenous AngII signaling through the *Agtr1a* in the *Acta2*^{-/-} aortic SMCs *in vivo*. The baseline increase in ROS and/or the pathways driving ERK1/2 signaling may be responsible for losartan not completely reversing aortic enlargement. We note that significant hypotension in *Acta2*^{-/-} mice limits forces on the ascending aorta thereby attenuating aortic enlargement in this mouse model. L-NAME and a high salt diet increased the blood pressure to levels similar to the WT mice and also significantly increased the aorta growth rate. This is consistent with current data that suggests blocking nitric oxide (NO) signaling protects the aorta from enlargement in mouse models of aneurysms (88), and excessive signaling through a target downstream of NO signaling, type I cGMP-dependent protein kinase, can drive thoracic aortic disease (89). Therefore, the significantly increased growth rate of the aorta in the *Acta2*^{-/-} mice after L-NAME treatment is due to increased biomechanical stress on the aorta not inhibition of NO-synthase.

There was a significant increase in elastic lamellae in our mice in addition to an increase in SMCs, similar to what is reported with the *Eln*^{-/-} mice (10). I note that patients with *ELN* hemizygosity show a similar phenotype with supravalvular aortic stenosis and an increase in elastic lamellae (90, 91). As stated previously, the number of lamellar units is based biomechanical properties (6), and *Eln*^{+/-} mice are hypertensive. The increased lamellae in these mice are likely due to the increased blood pressure and increased biomechanical stress in the wall (92). The same cannot be said in the hypotensive *Acta2*^{-/-}

mice, but in culture *Acta2*^{-/-} SMCs are stiffer than WT SMCs (11), so cellular stiffness, rather than global wall, stress could be responsible for the increase in lamellar units in the *Acta2*^{-/-} aortas. Alternatively, the increased elastin lamellae laid down during development could be due to increased proliferation of the mutant SMCs. It is known that *Acta2*^{-/-} SMCs proliferate more rapidly than the WT SMCs *in vivo* and *in vitro* (9). *Eln*^{+/-} SMCs also proliferate more rapidly than WT cells (13). Therefore, it is possible that the increased elastin lamellae laid down in both mouse models may be a result of the increased proliferative capacity of these mutant cells.

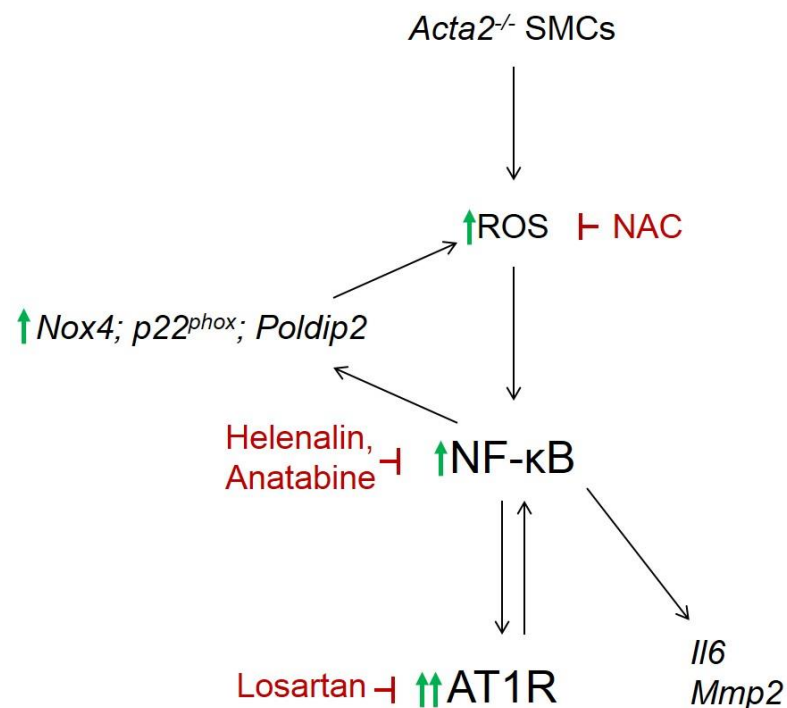


Figure 3.12 - Model of dysregulated signaling in *Acta2*^{-/-} SMCs showing the feedback loop linking reactive oxygen species with angiotensin signaling in *Acta2*^{-/-} SMCs. Reprinted with permission from Circulation Research (Chen J, Peters AM, Papke CL, Villamizar C, Ringuette LJ, Cao JM, Wang S, Ma S, Gong L, Byanova K, Xiong J, Zhu MX, Madonna R, Kee P, Geng YJ, Brasier A, Davis EC, Prakash SK, Kwartler CS, Milewicz DM. Loss of Smooth Muscle alpha-actin Leads to NF-kappaB-Dependent Increased Sensitivity to Angiotensin II in Smooth Muscle Cells and Aortic Enlargement, Circ Res 2017) See reference (11) .

The use of an ACEi, captopril, did not inhibit aneurysm formation in these mice. Instead it exacerbated the phenotype. My results differ from studies using other mouse models of thoracic aortic disease. Long-term treatment with captopril reversed aortic pathology, aortic growth, and aortic rupture in the *Fbln4*^{-/-} mouse (65). Additionally, aortic disease in the *Fbn1*^{C1039G/+} mouse was attenuated by treatment with another ACEi, enalapril. My cellular studies suggest that AngII signaling in SMCs could be increased without increased exogenous AngII, which may partially explain the failure of captopril treatment to attenuate growth. However, the exacerbation of the aortic enlargement in the *Acta2*^{-/-} mice when these mice were treated with captopril has thus far not been explained. The next chapter (pg. 55) will further explore pharmaceutical manipulation of the AngII signaling pathway in another model of thoracic aortic disease.

We also tested whether the MMP inhibitor, doxycycline, could alter aortic pathology in *Acta2*^{-/-} mice (data not shown). In the hypomorphic Marfan mouse model, *Fbn1*^{mgR/mgR} mice, doxycycline was able to increase their lifespan by about 53 days with decreased elastin breaks and levels of *Mmp2* and *Mmp9* expression (68). Another group showed that combining losartan and doxycycline could synergistically prevent thoracic aortic aneurysms in *Fbn1*^{C1039G/+} mice by down regulating *Mmp2* and *Mmp9* and restoring the structural integrity of the wall (63). However, my results were inconclusive as to whether doxycycline decreased aortic enlargement in the *Acta2*^{-/-} mice. These studies were complicated by the fact that sugar water was used to dissolve the bitter tasting doxycycline, and this increased the weight of the treated mice and the size of their aortas.

We failed to control for the increased weight by giving the control mice sugar water.

Furthermore, the study was most likely underpowered to determine differences between the groups.

Next, I hypothesized that development of aortic disease in *Acta2*^{-/-} mice was hindered by hypotension. I showed that making them normotensive with a combination of L-NAME and high salt diet drastically accelerated and exacerbated the phenotype over time. To further assess the role of biomechanical forces in driving the disease, we attempted to use constriction of the thoracic aorta to increase biomechanical forces on the ascending aorta (see methods for details) on the *Acta2*^{-/-} mice (unpublished data). However, we were unable to get results from this study because the majority of the *Acta2*^{-/-} mice died when they were anesthetized for surgery, including in sham operated mice. The high death rate is most likely due to the hypotension in the *Acta2*^{-/-} mice. We also had increased peri-operative mortality with the TAC procedure in *Agtr1a*^{-/-} mice, which are also hypotensive. I conclude that hypotensive mouse models are unable to survive the stress associated with anesthesia and surgery.

In the end, I was able to show that disrupting SM α -actin sensitizes the aortic SMC to exogenous AngII by increasing ROS and NF κ B signaling, leading to an increase in the expression of *Agtr1a*. I confirmed this pathway is also activated using pharmacologic disruption of SM α -actin filaments *in vitro* (data not shown) (11). Blocking both ROS production with NAC and the AT1R with losartan attenuated aortic growth in the *Acta2*^{-/-} mice. Based on the signaling pathways identified in these studies, blocking NF- κ B signaling

should also block aortic growth, and these pathways may also be effective therapeutic targets in other patients with disruption in SM α -actin filament formation.

**Chapter 4 – Pharmacological manipulation of AngII signaling in the TAC mouse model of
thoracic aortic aneurysm formation**

4.1 Introduction

As mentioned earlier, the major risk for thoracic aortic aneurysms and dissections is hypertension. In fact, any condition that increases biomechanical forces on the ascending aorta increases the risk for thoracic aortic disease. Uncontrolled essential hypertension is the most concerning risk factor, but other conditions that increase blood pressure also predispose to aortic disease such as cocaine or stimulant use, weight lifting, the Valsalva maneuver, and congenital defects that constrict the aorta like aortic coarctation (32). While Chapter 3 has addressed altered genes that predispose to the disease, hypertension can lead to earlier onset thoracic aortic disease in individuals with and without a genetic predisposition.

I have adopted a mouse model of an acute increase in biomechanical forces to assess how increased biomechanical stress leads to aortic enlargement. A transverse aortic constriction (TAC) is created by constricting the aorta between the first two major vessels branching off the aorta, the innominate and left common carotid (Section 2.3) (52). The model has been used extensively to study pressure-induced cardiac hypertrophy due to hypertension or aortic stenosis. With the acute constriction of the transverse aorta, the blood pressure increases proximally on the heart, ascending aorta, and right carotid artery. The increased pressures lead to hypertrophy of the left ventricle within two weeks after placement of the constriction (93). Subsequently, the left ventricle dilates, and congestive heart failure ensues (66, 94). TAC results may vary due to different surgeons, anesthesia

and surgical techniques, and various other factors such as suture migration (94-96). Hence, the precise phenotype present in each of these models is open to interpretation.

Before mice develop heart failure after TAC, increased left ventricular pressure and hypertrophy of the heart produces significant increase in biomechanical forces on the ascending aortic wall proximal to the site of constriction. Therefore, I used this model to study aortic remodeling due to increased biomechanical forces on the ascending aorta and limited all analyses to two weeks after constriction so that forces continuously increased on the aorta and our results were not complicated by heart failure. After two weeks, the ascending aorta dilates and there is thickening of the medial and adventitial layers in the aortic wall. The medial layer thickens due to widening between the elastin layers without evidence of hyperplasia, suggesting SMC hypertrophy. The adventitial layer increases in area and cell density due to accumulation of collagen, myofibroblasts, and macrophages. Inflammatory markers are increased, including interleukin-6 (IL6) and monocyte chemoattractant protein 1 (MCP-1), and remodeling factors like matrix metalloproteinase 2 (MMP2) and matrix metalloproteinase 9 (MMP9) also increase in expression (52).

The pathologic changes associated with aortic remodeling with TAC are similar to the pathologic changes in the aorta associated with AngII infusion (28, 30, 57). This suggests that AngII signaling may drive the hypertension-associated remodeling. We hypothesized that utilizing an ARB, losartan, would alter the response and prevent the observed pathologic changes and aortic enlargement. The administration of losartan 3 days prior to TAC and for two weeks post operatively eliminated the vascular inflammatory

response, including the macrophage accumulation. Losartan partially rescues the TAC-induced adventitial hyperplasia, collagen accumulation, and ascending aortic dilatation. Therefore, I concluded that signaling through the AT1R was completely responsible for the vascular inflammation and partially responsible for the TAC-induced aortic remodeling.

At the outset of these studies, the signaling downstream of AT1R was the interest. It is well established that there are different intracellular pathways associated with the AT1R, only some of which are ligand-dependent (97). I was specifically interested in the ligand independent pathways that had been investigated in the heart. Known to play a part in load induced hypertrophy, it was shown *in vivo* and *in vitro* that stimulation of the AT1R independently of AngII leads to translocation of G-proteins into the cytosol via Janus kinase 2. This activation was inhibited by another ARB, candesartan (64). Later, it was shown *ex vivo* that mechanical stretch mediates a conformation change in β -arrestin, driving signaling consistent with ligand mediated AT1R signaling. Hearts from mice lacking β -arrestin or the AT1R did not respond to the mechanical stress (85). The ligand-independent activation of AT1R in vascular SMCs has also been investigated. Mechanical signaling of the Agtr1a to activate SMC's in mesenteric and renal arteries did not rely on ion channels TRPC6 or KCNQ3, 4, or 5 for SMC (98). However, in *Fbn*^{C1039G/+} mice, studies suggested that β -arrestin contributed to thoracic aortic aneurysm formation in Marfan syndrome (99). Hence, we wanted to investigate the ligand independent activation of the AT1R in our TAC model.

At the initiation of these studies, we sought to confirm whether the remodeling is due to an increase in circulating AngII levels or if ligand-independent signaling is a more important driver of disease. To test this hypothesis, we administrated an ACE inhibitor to

block conversion of angiotensin I to angiotensin II to see if it prevented hyper-acute aortic remodeling in our TAC model.

4.2 Results

4.2.1 Treatment with captopril fails to rescue remodeling associated with TAC

Wildtype C57BL6/J male mice (12 weeks of age) underwent TAC or sham surgeries with or without treatment with either losartan or captopril to determine if captopril could prevent pathologic remodeling as effectively as losartan. All treatments were started ~72 hours prior to surgery with losartan and captopril given via drinking water at 600 mg/L or 75 mg/L, respectively. Initial experiments showed a significant decrease in survival with captopril treatment (**Figure 4.1 A**) despite the fact that the losartan mice were significantly more constricted than the captopril treated group (**Figure 4.1 B**). Necropsy results from our preliminary study showed multiple deaths due to aortic rupture or dissection in the ascending aorta. I first noted that only mice treated with captopril were acutely dying post-operatively for no apparent reason. Prior TAC studies performed by this surgeon did not result in similar deaths, so I began to investigate whether and how captopril might be causing death. I performed surgery on a second group of mice and monitored survival rates closely, with necropsy performed on any non-surviving mice. Closer examination indicated that only mice treated with captopril were acutely dying outside of what we considered the perioperative window. Therefore, I began to monitor the mice more closely in the second preliminary group and the monitored survival rates after post-op day five were consistent

with our first group and necropsies were routinely performed. Two mice treated with captopril following TAC specifically stood out. Prior to echocardiography on day 14, one mouse exhibited behaviors consistent with significant discomfort and pain. Necropsy revealed an intramural hematoma in this mouse (**Figure 4.1 C**). Another visibly healthy mouse acutely died after post-op day five, and gross examination of the ascending aorta indicated a dissection that started in the ascending aorta. Histologic examination of the same mouse indicated that blood was present in the vessel wall near the pulmonary artery (**Figure 4.1 D & E**).

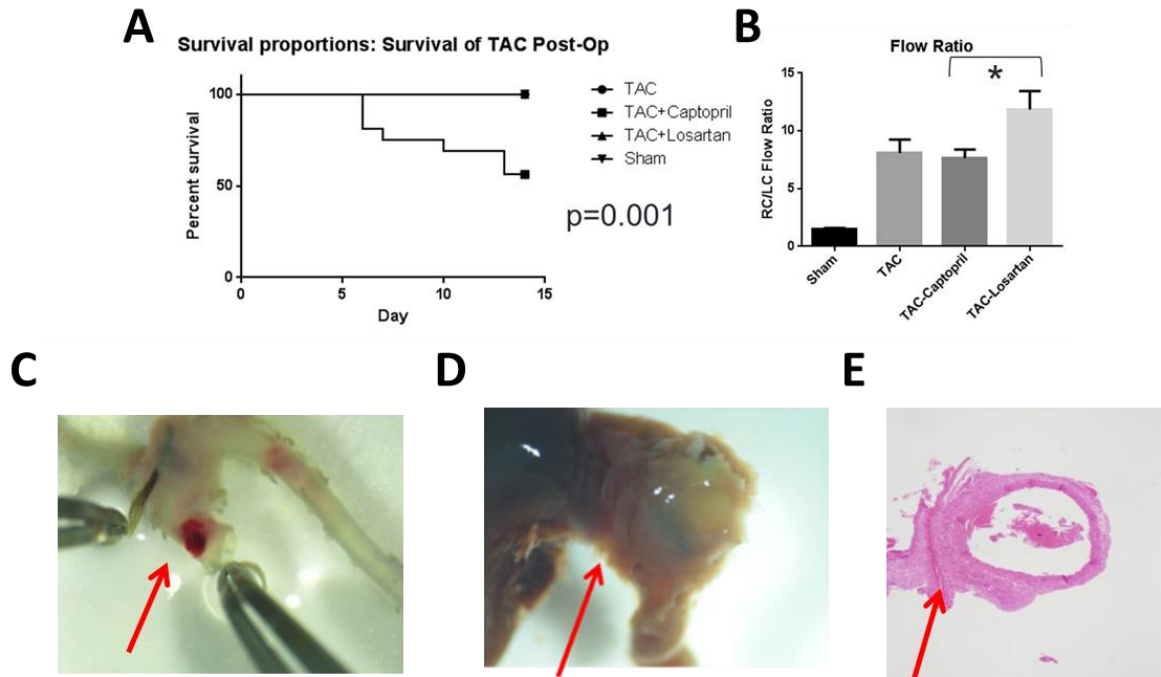


Figure 4.1 – A) The survival curve after TAC and treatment with either losartan or captopril. Only mice treated with captopril died after TAC. B) The increased deaths of the mice treatment with captopril were not due to increased constriction as measured by RCCA/LCCA ratio. C) Prior to echocardiography on day 14, this mouse exhibited behaviors consistent with significant discomfort. After necropsy, thorough cleaning of the aorta revealed and intramural hematoma (red arrow). D) Gross examination of the ascending aorta of another mouse who on necropsy who died acutely indicated a dissection that started in the ascending aorta (red arrow). Histologic examination of the same mouse, (F) indicated that blood was present in the vessel wall (red arrow) near the pulmonary artery. * indicates $p \leq 0.05$.

These initial experiments were repeated by a different surgeon performing the TAC. There was a significant increase in the ascending aorta and aortic root diameter between the WT sham controls and WT TAC mice (**Figure 4.2 A, B, & C**). As in my previous study, aortic growth was attenuated by losartan treatment compared to untreated TAC mice in the ascending aorta and aortic root. Captopril treatment, on the other hand, was unable to attenuate the increase in size of the ascending aorta or aortic root in these mice to the

same extent as the losartan treatment. In contrast to the previous studies, none of the captopril treated mice died after the five day peri-operative period.

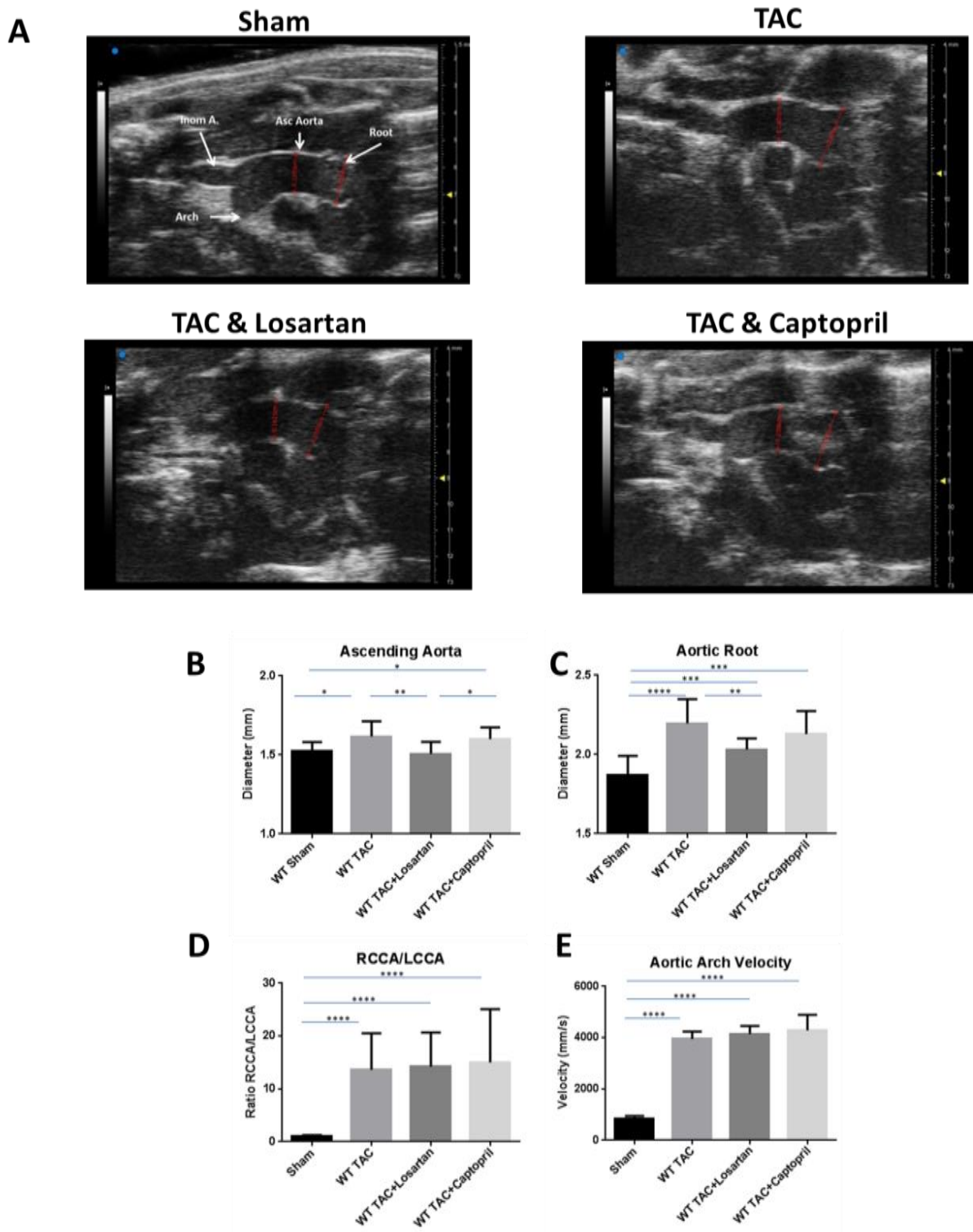


Figure 4.2 – A) In our third set of studies, echoes from the four different groups were obtained in our WT sham, TAC, TAC+captopril, and TAC+losartan treated groups. The approximate locations of the measurements are indicated in the sham image. B & C) The

increase in the ascending aorta and in the aortic root size was significant in the untreated TAC mouse compared to sham. Losartan was able to attenuate the increase in size as previously observed. However, TAC mice treated with captopril was not attenuated. D) As previously, the level of constriction was verified via Doppler flow studies indicating successful constriction in all TAC mice. E) Successful constriction in TAC mice were also verified by measuring blood flow across the constriction in the transverse aorta. * indicates $p \leq 0.05$, ** indicates $p \leq 0.01$, *** indicates $p \leq 0.001$, and **** indicates $p \leq 0.0001$. (Andrew M. Peters, Zhen Zhou, Jiyuan Chen, Alexandra Janda, Corey L. Reynolds, Shao-Qing Kuang, Shanzhi Wang, Siddharth Prakash, GenTAC Consortium, Callie S. Kwartler, Dianna M. Milewicz Pharmacologic Manipulation of the Angiotensin System Affects Aortic Remodeling and Aneurysm Development: Cautions for Clinical Practice, Submitted 2017) See reference (77).

The level of constriction was accessed by comparing the ratio of Doppler velocities between the right common carotid artery (RCCA) and the left common carotid artery (LCCA) (RCCA/LCCA). In my original studies, a successful constriction was considered a ratio between 5-10 which was also consistent with what was seen in literature and our preliminary studies (52, 66). It is important to note that the ratios in the constricted groups were consistently above 10 without a decrease in survival rates (**Figure 4.2 D**), which was higher than the ratio in our previous studies (**Figure 4.1 B**). We also assessed blood flow across the aortic constriction in these mice as this has been reported to be another method to assess the level of constriction (100). It was significantly elevated in all the TAC groups compared to the sham, and there was no significant difference between the TAC groups (**Figure 4.2 E**).

Histologic analysis of the TAC mice showed that the increase in vascular and adventitial area was similar between the losartan and captopril treated groups (**Figure 4.3 A, B, & C**). These results reflected the observations in my first study, but my earlier

histopathologic measurements were too underpowered to indicate a significant difference between the medial area in these groups (data not shown). The adventitial cell density decreased significantly in the captopril treated group compared to the non-treated TAC group and sham control (**Figure 4.3 D**), and the medial cell density significantly decreased in both TAC and TAC + Captopril groups compared to the sham controls (**Figure 4.3 E**). Additionally, inflammatory markers including *IL6*, *MCP-1*, *MMP2*, and *MMP9* remained elevated under captopril treatment compared to WT sham (data not shown), but this was difficult to assess given these markers were nearly undetectable in my WT sham cohort. The changes in the structure of the aortic wall were consistent with our previous TAC studies with an increased distance between the elastic lamellae increased number of Mac-2 positive cells in untreated and captopril treated TAC mice (**Figure 4.4 A**). The increase in distance between the lamellae coupled with the significant decrease in medial cell density could indicate that there is significant SMC hypertrophy. The expansion of the adventitia also appeared to consist largely of proteoglycans along with inflammatory cells. In the media, we verified that there was a significant increase in elastin breaks in the mice undergoing TAC that was not attenuated with captopril treatment (**Figure 4.4 B**). We also observed a significant increase in the proteoglycans in the medial layer in addition to what we observed in the adventitia (**Figure 4.4 C**). Cell counting confirmed that there was a significant increase in inflammatory cells that was not reversed with captopril treatment (**Figure 4.4 D**).

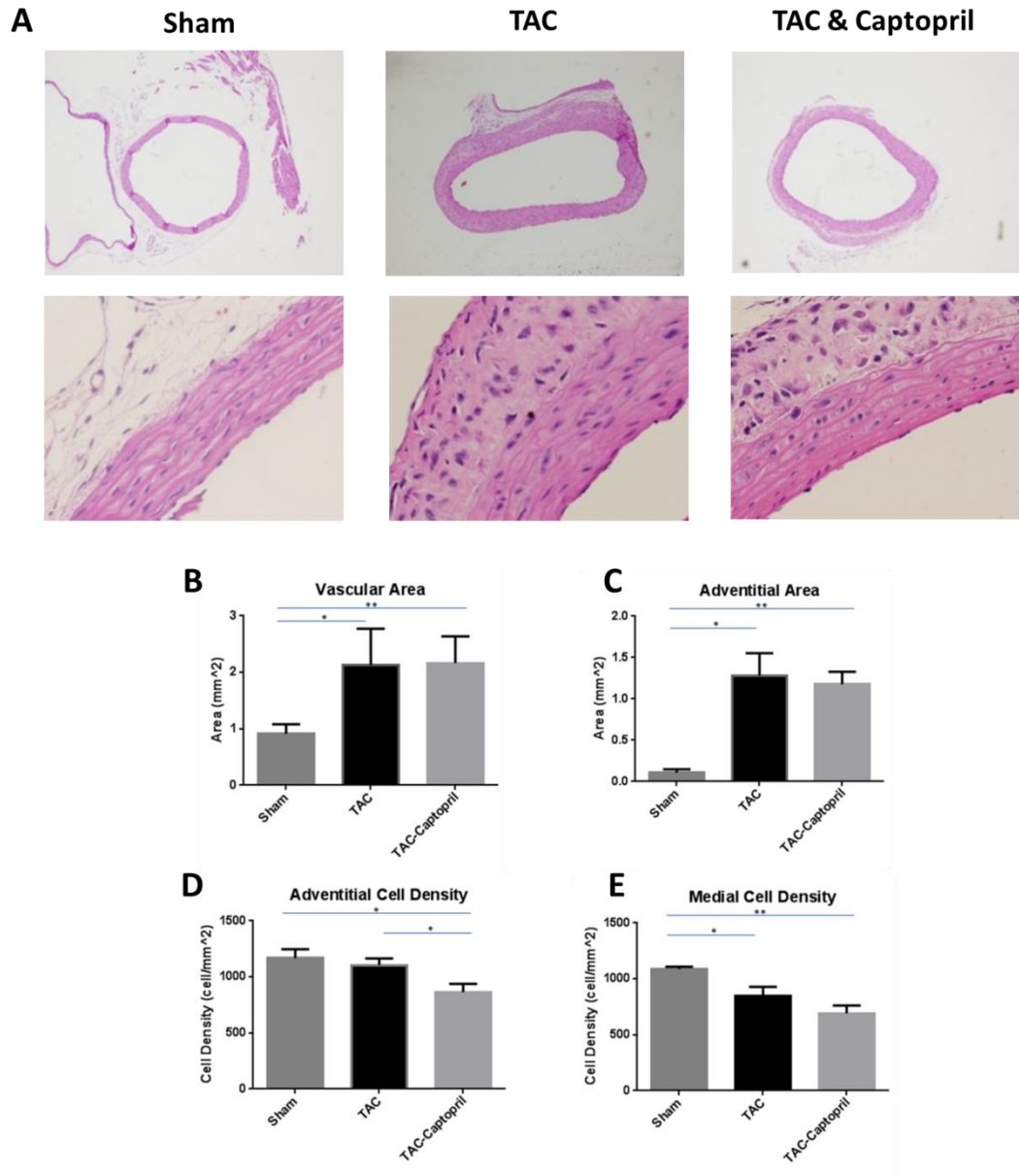


Figure 4.3 – A, B, & C) H&E stains showing that captopril did not alter the increase in vascular or adventitial area. D) Treatment with captopril in TAC mice increased adventitial cell density compare to both the sham and TAC controls. E) Medial cell density was also significantly decreased in the TAC and TAC + captopril mice compared to sham controls. * indicates $p \leq 0.05$, ** indicates $p \leq 0.01$, *** indicates $p \leq 0.001$, and **** indicates $p \leq 0.0001$. (Andrew M. Peters, Zhen Zhou, Jiyan Chen, Alexandra Janda, Corey L. Reynolds, Shao-Qing Kuang, Shanzhi Wang, Siddharth Prakash, GenTAC Consortium, Callie S. Kwartler, Dianna M. Milewicz Pharmacologic Manipulation of the Angiotensin System Affects Aortic Remodeling and Aneurysm Development: Cautions for Clinical Practice, Submitted 2017) See reference (77).

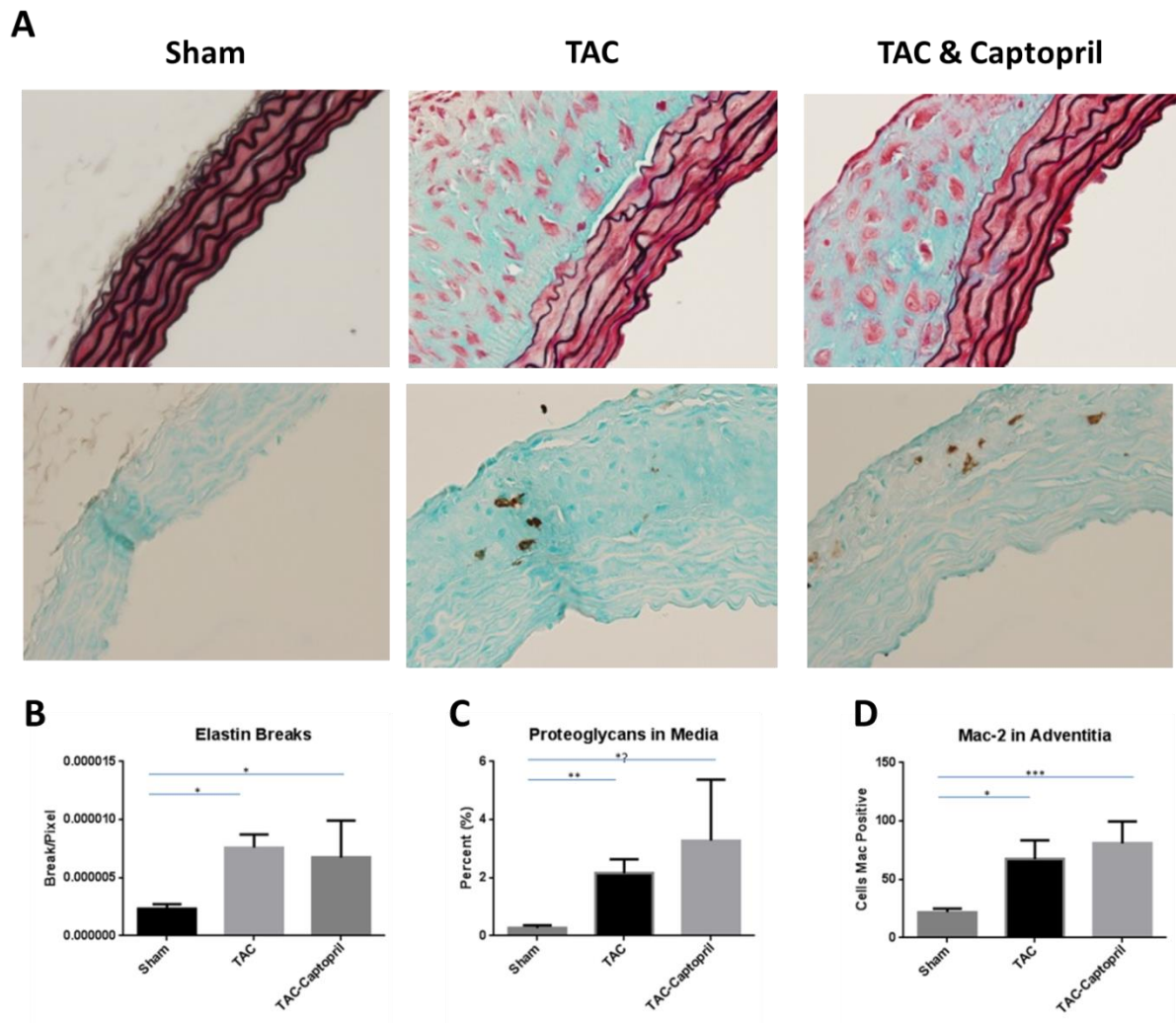


Figure 4.4 – A) Movat stains (top) show the changes in the structure of the aortic wall were consistent with my previous TAC studies showing an increased distance between the elastic lamellae increased number of Mac-2 positive staining cells in untreated and treated TAC mice. B) There was significant increase in elastin breaks in the mice undergoing TAC, and C) increase in the proteoglycan in the medial layer. D) Cell counting confirmed that there was a significant increase in inflammatory cells that was not reversed with captopril treatment. * indicates $p \leq 0.05$, ** indicates $p \leq 0.01$, and *** indicates $p \leq 0.001$. (Andrew M. Peters, Zhen Zhou, Jiyuan Chen, Alexandra Janda, Corey L. Reynolds, Shao-Qing Kuang, Shanzhi Wang, Siddharth Prakash, GenTAC Consortium, Callie S. Kwartler, Dianna M. Milewicz Pharmacologic Manipulation of the Angiotensin System Affects Aortic Remodeling and Aneurysm Development: Cautions for Clinical Practice, Submitted 2017) See reference (77).

4.2.2 C21 is beneficial in biomechanical stress model

There are additional receptors involved in that angiotensin system other than the ligand dependent or independent signaling of the AT1R (See section 1.3, pg. 10). Therefore, I sought to characterize the role of the AT2R and Mas receptor in the captopril treated TAC mice by treating with agonists for these receptors: compound 21 (C21) is an agonist for the AT2R while AVE0991 is an agonist for the Mas receptor. I focused on the physiologic changes associated with treatment. Ultrasound examination of the ascending aorta and the aortic root again showed a significant increase in aortic size in the ascending aorta, which was not attenuated with captopril. Co-treatment with C21 was able to eliminate the increase in the ascending aortic diameter, but it only attenuated the increase in size in the aortic root. Meanwhile co-treatment with AVE0991 with captopril had no effect on the ascending aorta or aortic root compared to untreated or captopril treated mice and remained significantly elevated compared to mice treated with both captopril and C21 (**Figure 4.5 A & B**). As with previous studies, I verified the level of constriction using the ratio between the left and right carotid (RCCA/LCCA) and flow across the constriction site (**Figure 4.6 C & D**).

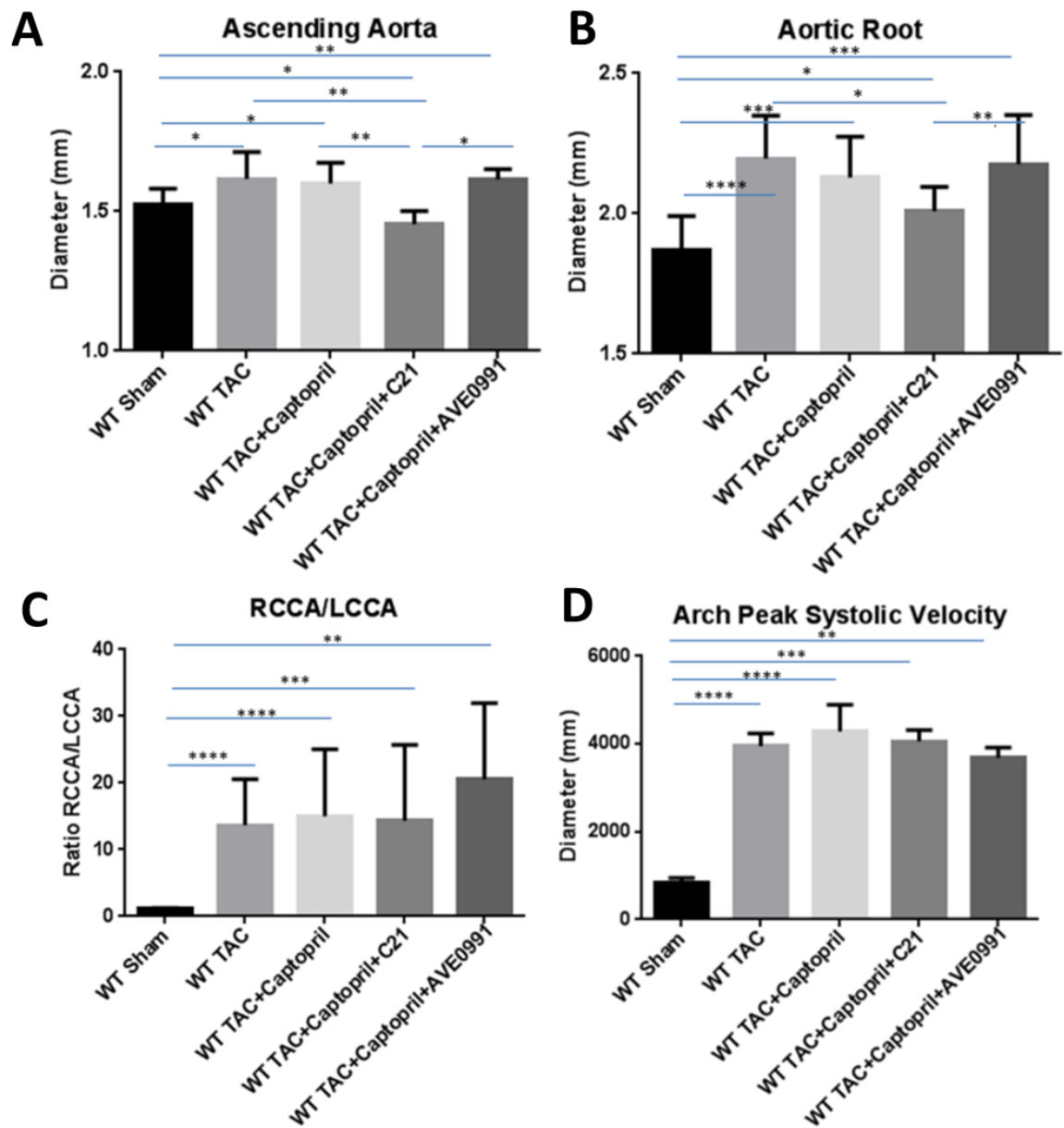


Figure 4.5 – A & B) Echoes of the ascending aorta and the aortic root again showed a significant increase in the ascending aorta size which was not attenuated with captopril. Co-treatment with C21 was able to eliminate the change in the ascending aorta and attenuate it in the root. Meanwhile co-treatment with AVE0991 and captopril had no effect compared to untreated mice. C & D) We verified that the constriction in the untreated and treated mice were similar between groups using two methods. * indicates $p \leq 0.05$, ** indicates $p \leq 0.01$, *** indicates $p \leq 0.001$, and **** indicates $p \leq 0.0001$. (Andrew M. Peters, Zhen Zhou, Jiyuan Chen, Alexandra Janda, Corey L. Reynolds, Shao-Qing Kuang, Shanzhi Wang, Siddharth Prakash, GenTAC Consortium, Callie S. Kwartler, Dianna M. Milewicz

In our original publication on aortic remodeling with TAC, we did not assess blood pressure (52). For the studies reported here, I assessed blood pressure and pulse pressure in the ascending aorta by inserting a catheter into the right carotid artery and advancing it to the ascending aorta. There was a significant increase in systolic blood pressure in the TAC mice, and systolic blood pressure was significantly decreased in both treatment groups. In contrast, the diastolic blood pressure was not different between the TAC and sham group. However, the losartan and captopril treated mice both had significantly lower diastolic blood pressure (DBP) compared to sham and TAC controls in the ascending aorta (**Figures 4.6 A & B**). There was no difference in pulse pressure between any of the treated or untreated in mice that underwent TAC (**Figure 4.6 C**), which was interesting since cyclic strain has been directly correlated with vascular disease in the carotid arteries (101).

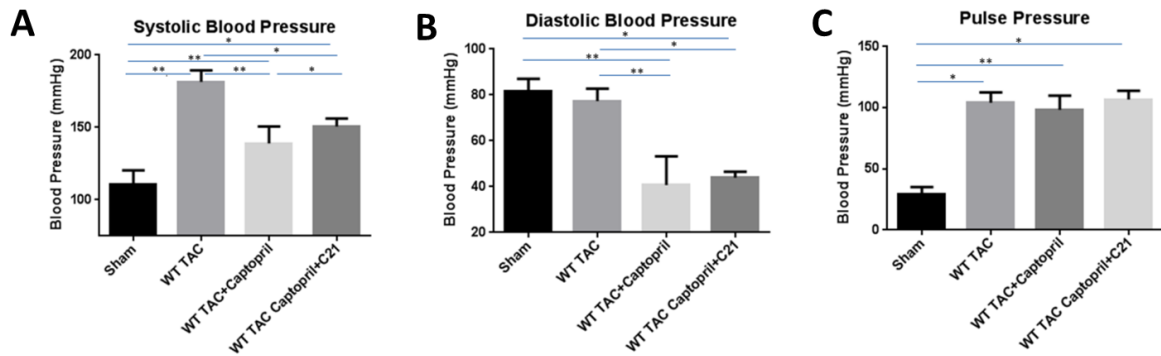


Figure 4.6 – With an intraluminal catheter, we directly measured the A) systolic and B) diastolic blood pressure in the groups. C) Pulse pressure was then calculated. All TAC mice had significantly increased systolic blood pressure, but the blood pressure in mice treated with losartan and captopril were significantly lower. The losartan and captopril treated mice also had significantly decreased diastolic blood pressure compared to both sham and untreated TAC mice, but the pulse pressure was consistent in all mice treated with TAC. * indicates $p \leq 0.05$ and ** indicates $p \leq 0.01$. (Andrew M. Peters, Zhen Zhou, Jiyuan Chen, Alexandra Janda, Corey L. Reynolds, Shao-Qing Kuang, Shanzhi Wang, Siddharth Prakash, GenTAC Consortium, Callie S. Kwartler, Dianna M. Milewicz Pharmacologic Manipulation of the Angiotensin System Affects Aortic Remodeling and Aneurysm Development: Cautions for Clinical Practice, Submitted 2017) See reference (77).

Lastly, mice undergoing TAC were treated with C21 alone, which was able to decrease the ascending aorta similar to the captopril and C21 treated mice but not the aortic root when compared to the untreated TAC mice (**Figure 4.7**). As expected, direct measurement of the systolic blood pressure (SBP) in the ascending aorta and aortic root was significantly increased in all mice that underwent TAC. Any combination of the pharmaceutical agents was capable of decreasing the SBP however, all remained elevated compared to WT sham mice. While diastolic blood pressure (DBP) remained normal in the untreated TAC mice, all treated TAC mice had a significant decrease in DBP compared to sham and control mice (**Figure 4.8**). These results are consistent with our earlier study,

which indicated TAC mice had increased pulse pressure with or without any pharmaceutical manipulation.

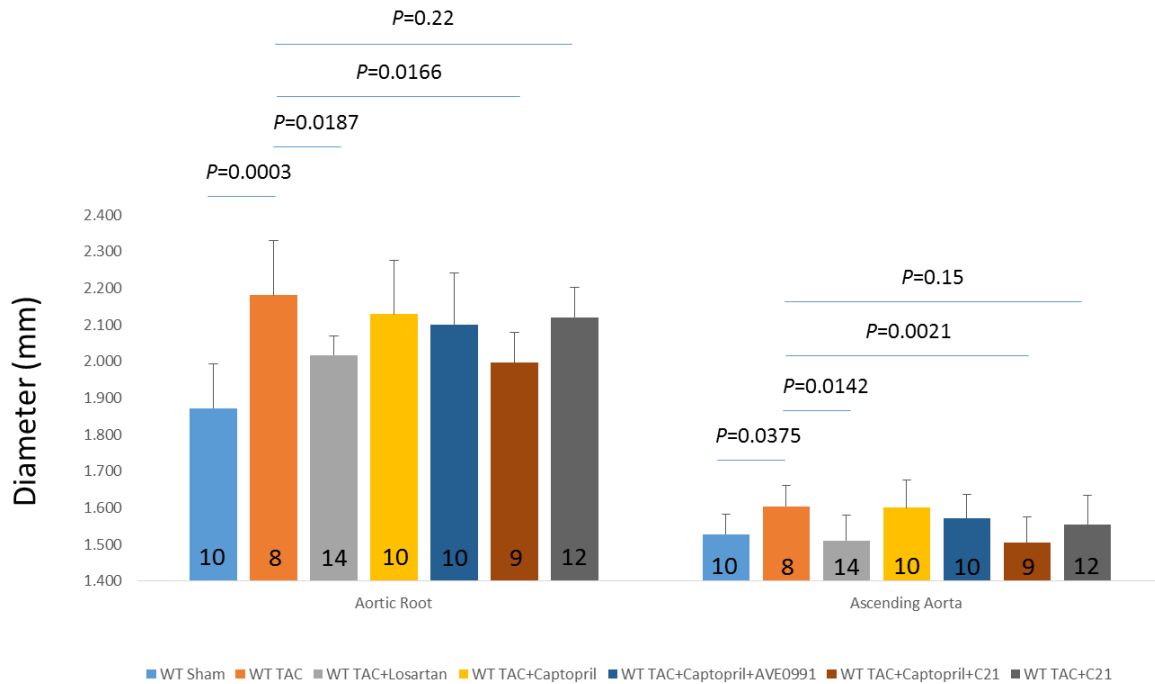


Figure 4.7 – Ultrasound assessments of the aortic root and ascending aortic diameters in WT sham, TAC, TAC + losartan, TAC + captopril, TAC + captopril + AVE0991, TAC + captopril+ C21, and TAC + C21. The number of observations for each group is listed at the bottom of each graph, and significant p values are listed above. As expected TAC mice had an increase in the size of the aortic root and ascending aorta compared to sham mice, and losartan was able to attenuate these changes. Captopril alone was not able to attenuate the increase, and the combination with AVE0991 did not show any significant changes compared to the untreated mice. Captopril in combination with C21 was able to significantly decrease the increase in aortic size. Alone, C21 was only able to decrease the ascending aorta when compared to the untreated TAC mice. (Andrew M. Peters, Zhen Zhou, Jiyuan Chen, Alexandra Janda, Corey L. Reynolds, Shao-Qing Kuang, Shanzhi Wang, Siddharth Prakash, GenTAC Consortium, Callie S. Kwartler, Dianna M. Milewicz Pharmacologic Manipulation of the Angiotensin System Affects Aortic Remodeling and Aneurysm Development: Cautions for Clinical Practice, Submitted 2017) See reference (77).

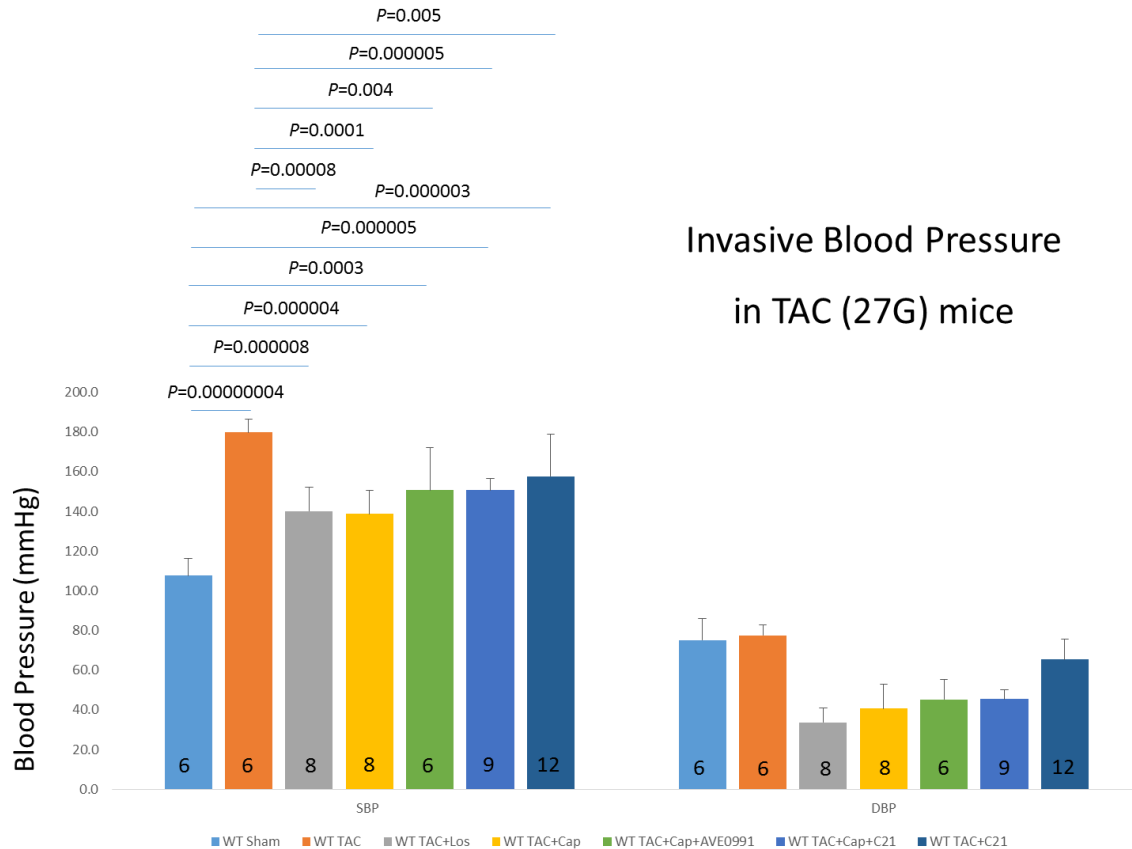


Figure 4.8 – As expected, direct measurement of the systolic blood pressure (SBP) in the ascending aorta and aortic root was significantly increased in all mice that underwent TAC. Any combination of the pharmaceutical agents was capable of decreasing the SBP, but they all remained elevated compared to WT sham mice. While diastolic blood pressure (DBP) remained normal in the untreated TAC mice, all treated TAC mice had a significant decrease in DBP compared to sham and control mice. (Andrew M. Peters, Zhen Zhou, Jiyuan Chen, Alexandra Janda, Corey L. Reynolds, Shao-Qing Kuang, Shanzhi Wang, Siddharth Prakash, GenTAC Consortium, Callie S. Kwartler, Dianna M. Milewicz Pharmacologic Manipulation of the Angiotensin System Affects Aortic Remodeling and Aneurysm Development: Cautions for Clinical Practice, Submitted 2017) See reference (77).

The aortic pathology was also assessed in these aortas from animals treated with losartan, captopril, and captopril plus the agonists. The pathologic changes in the adventitia in the losartan and captopril treatment were consistent with what was

previously shown (**Figure 4.3**). Interestingly, there appeared to be little change in the adventitia with co-treatment of captopril and C21 or C21 alone. However, treatment with captopril and AVE0991 decreased both the medial and adventitial area with an increase in adventitial cell density and decrease in medial cell density (**Figure 4.9**). There was significant proteoglycan deposition in the adventitia in all groups.

Next, vascular inflammation was assessed by Mac-2 staining for macrophages in the adventitia. TAC causes significant increases macrophage positive cells in the adventitia, and losartan completely blocks the accumulation of Mac-2 positive cells in the adventitia. However, captopril and co-treatment with C21 or C21 alone do not appear to decrease this accumulation of Mac-2 cells in the adventitia. In contrast, co-treatment of captopril and AVE0991 completely eliminate Mac-2 positive cells the inflammatory response in the adventitia (**Figure 4.11**). Sirius red staining for collagen deposition indicated a significant increase in the adventitial fibrotic response with TAC. This response was attenuated with losartan but remained elevated with captopril treatment and C21 with and without captopril. Interestingly, AVE0991 treatment with captopril significantly decreases the amount of collagen in the adventitia (**Figure 4.12**).

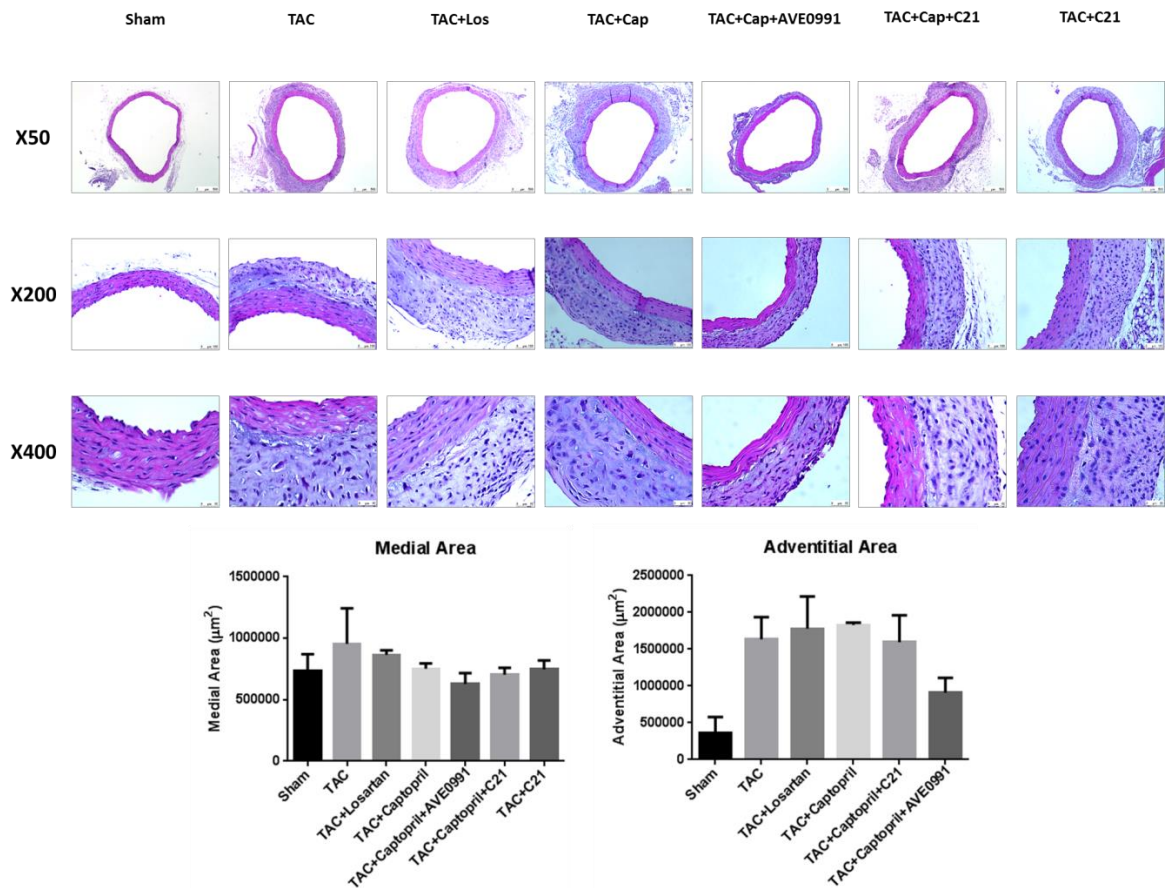


Figure 4.9 – Preliminary H&E stains (n=2) confirming what was previously observed in all of our earlier published and unpublished studies. TAC increased medial and adventitial thickening, and losartan treatment was able to attenuate it. Losartan was able to attenuate the changes. While captopril attenuated the changes in the medial layer, it appeared to not do so in the adventitial layer, and the pathologic changes in the adventitia observed in these mice were consistent with what was previously shown. There appeared to be little change with co-treatment of captopril and C21 or C21 alone, but treatment with captopril and AVE0991 appeared to significantly both medial and adventitial area. There also appeared to be an increase in adventitial cell density. Note that p values not calculated. (Andrew M. Peters, Zhen Zhou, Jiyuan Chen, Alexandra Janda, Corey L. Reynolds, Shao-Qing Kuang, Shanzhi Wang, Siddharth Prakash, GenTAC Consortium, Callie S. Kwartler, Dianna M. Milewicz Pharmacologic Manipulation of the Angiotensin System Affects Aortic Remodeling and Aneurysm Development: Cautions for Clinical Practice, Submitted 2017) See reference (77).

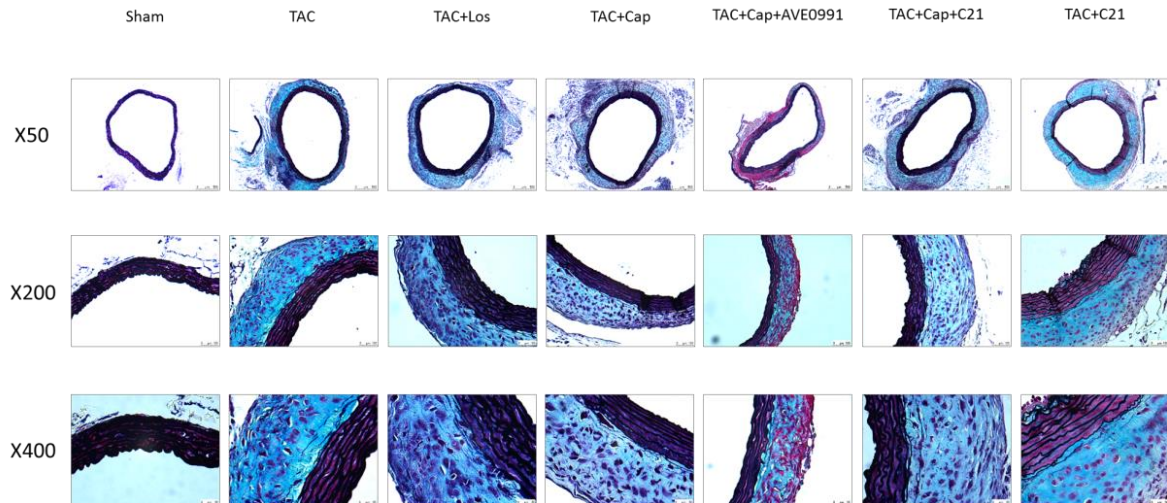


Figure 4.10 – Movat staining (n=2) shows increased proteoglycan deposition in the adventitial layer. There was an increase in the distance between the elastic lamellae in TAC mice, and significant proteoglycan deposition in the adventitia. These observations appeared slightly attenuated in the losartan treated mice, but was absent in the captopril and AVE0991 treated mice. While the adventitia appears larger compared to the WT sham controls, there appears to be less proteoglycan deposition and more cells in the wall. Note that p values not calculated. (Andrew M. Peters, Zhen Zhou, Jiyuan Chen, Alexandra Janda, Corey L. Reynolds, Shao-Qing Kuang, Shanzhi Wang, Siddharth Prakash, GenTAC Consortium, Callie S. Kwartler, Dianna M. Milewicz Pharmacologic Manipulation of the Angiotensin System Affects Aortic Remodeling and Aneurysm Development: Cautions for Clinical Practice, Submitted 2017) See reference (77).

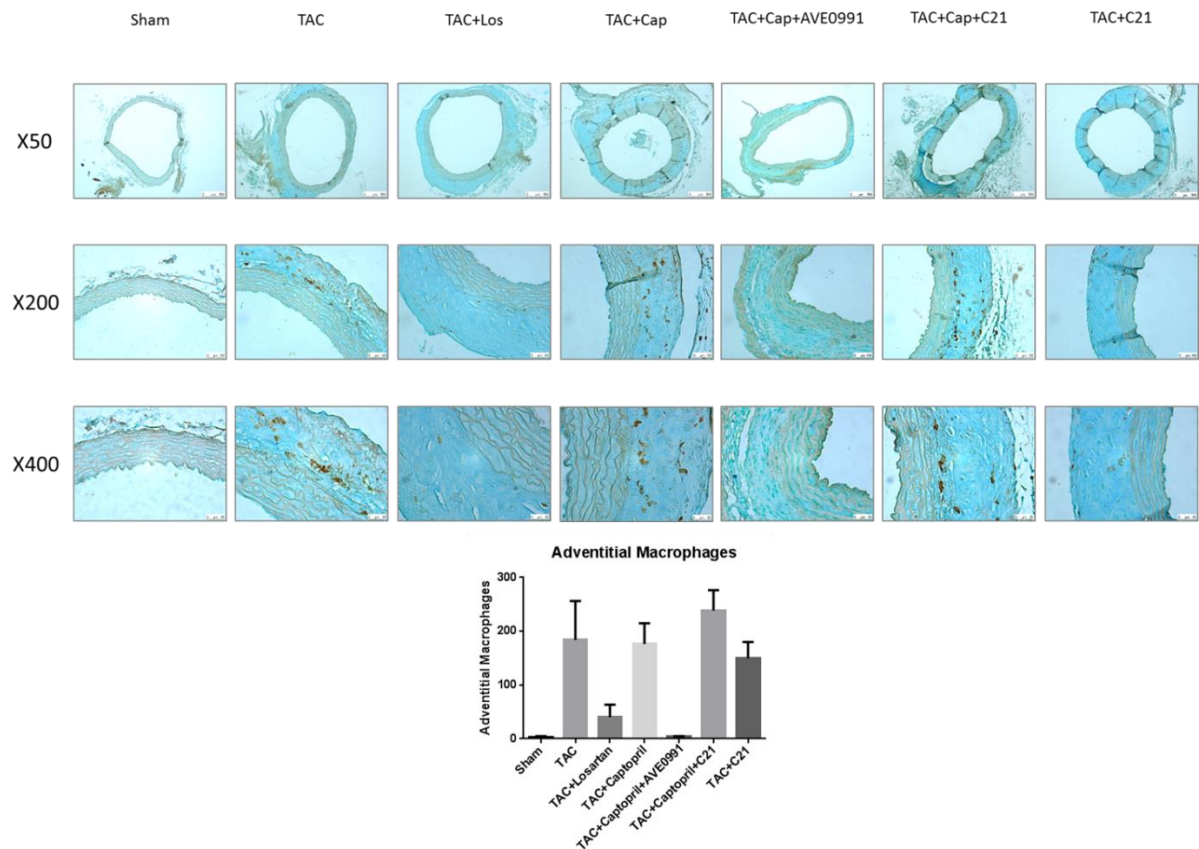


Figure 4.11 – Mac-2 staining of the aortas (n=2). TAC significant increases macrophage positive cells in the adventitia, and losartan attenuates it. Captopril and co-treatment with C21 or C21 alone do not appear to decrease this inflammatory response. Co-treatment of captopril and AVE0991 appeared to completely eliminate the inflammatory response in the adventitia. Note that p values not calculated. (Andrew M. Peters, Zhen Zhou, Jiyuan Chen, Alexandra Janda, Corey L. Reynolds, Shao-Qing Kuang, Shanzhi Wang, Siddharth Prakash, GenTAC Consortium, Callie S. Kwartler, Dianna M. Milewicz Pharmacologic Manipulation of the Angiotensin System Affects Aortic Remodeling and Aneurysm Development: Cautions for Clinical Practice, Submitted 2017) See reference (77).

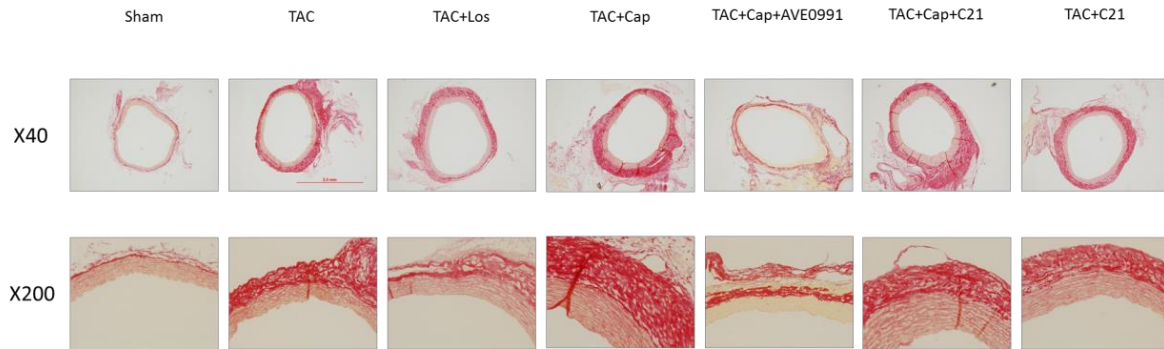


Figure 4.12 – Sirius red staining (n=2) in the cells indicated a significant increase in the adventitial fibrotic response, and it was attenuated with losartan but remained elevated with captopril treatment. It appears to be slight decreased with C21 with and without captopril. AVE0991 treatment with captopril and TAC significantly decrease the amount of collagen in the adventitia. Note the absence of p values. (Andrew M. Peters, Zhen Zhou, Jiyuan Chen, Alexandra Janda, Corey L. Reynolds, Shao-Qing Kuang, Shanzhi Wang, Siddharth Prakash, GenTAC Consortium, Callie S. Kwartler, Dianna M. Milewicz Pharmacologic Manipulation of the Angiotensin System Affects Aortic Remodeling and Aneurysm Development: Cautions for Clinical Practice, Submitted 2017) See reference (77).

4.2.3 Knock out of *Agtr1a* fails to alter vascular inflammation

Given the effectiveness of losartan in previous studies (61, 65), I set out early to try to perform TAC in *Agtr1a*^{-/-} mice. We expected results similar to those observed in pharmaceutically treated mice in *Agtr1a*^{-/-} mice. The *Agtr1a*^{-/-} mice are hypotensive compared to WT controls (**Figure 4.13**). My early results indicated a significantly decreased peri-operative survival rate making my study difficult. Because of my concerns regarding possible flaws in my original study, this was repeated with two different surgeons. After the peri-operative period, surviving *Agtr1a*^{-/-} mice were not significantly different than the WT untreated TAC mice. Vascular and adventitial area remained elevated in WT and *Agtr1a*^{-/-} untreated mice. Investigation of inflammatory markers such as Mac-2 indicated that inflammation was attenuated in *Agtr1a*^{-/-} TAC mice (**Figure 4.14**). Therefore, we

investigated the difference between the WT and *Agtr1a*^{-/-} mice. *Agtr1a*^{-/-} mice have decreased medial area compared to WT mice, but the medial area is significantly increased compared to *Agtr1a*^{-/-} mice after TAC. Vascular and adventitial expansion are still present in *Agtr1a*^{-/-} TAC mice compared with both WT and *Agtr1a*^{-/-} sham controls (**Figure 4.15**). TAC *Agtr1a*^{-/-} mice show increased distance between the elastic lamellae, but *Agtr1a*^{-/-} mice appear to have more elastic lamellae, and early results in other studies have indicated that they are less developed.

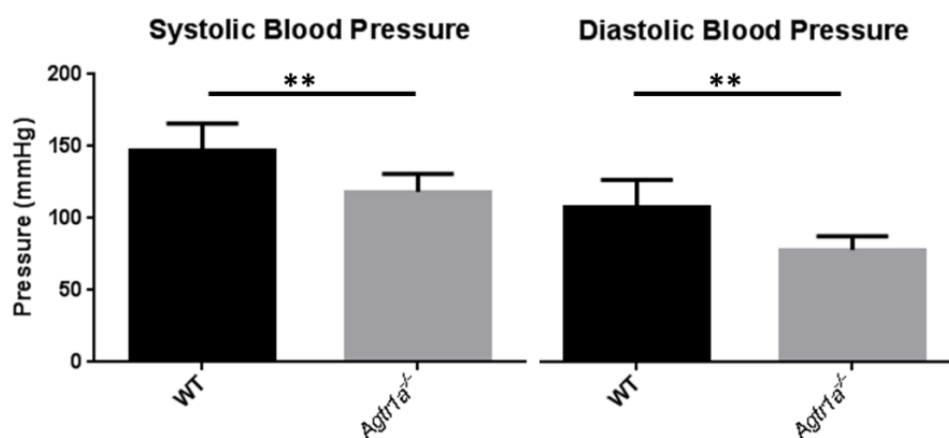


Figure 4.13 – SBP and DBP measurement taking in WT and *Agtr1a*^{-/-} mice to verify their decreased blood pressure. All measurements taken by tail cuff following the protocol previously mentioned (Section 2.5). ** indicates $p \leq 0.01$.

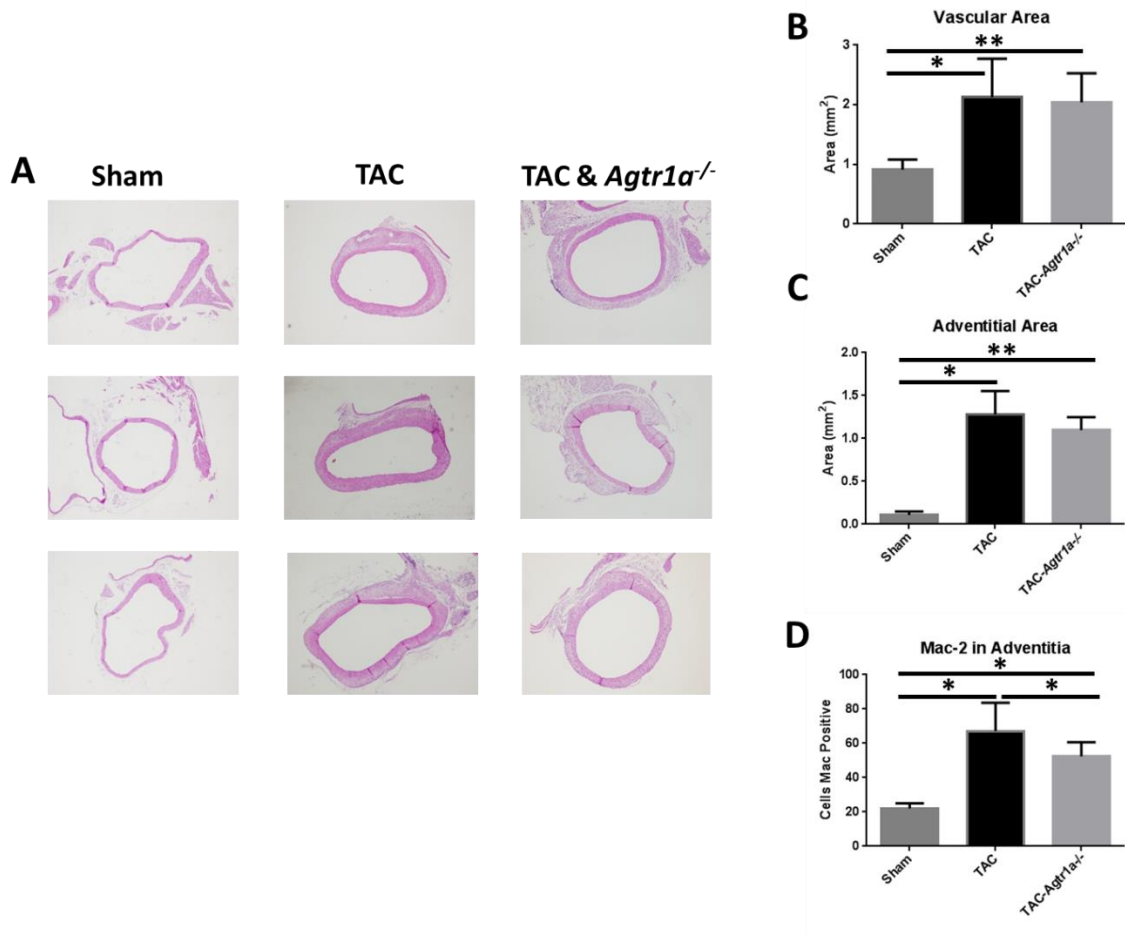


Figure 4.14 – My preliminary studies in mice deficient in *Agtr1a* did not have the same effect as while type mice treated with losartan. A, B, & C) Vascular and adventitial area remain elevated in WT and *Agtr1a*^{-/-} treated mice. D) While inflammation appeared to be attenuated in these mice, the number of Mac-2 positive cells was only attenuated in *Agtr1a*^{-/-} mice.

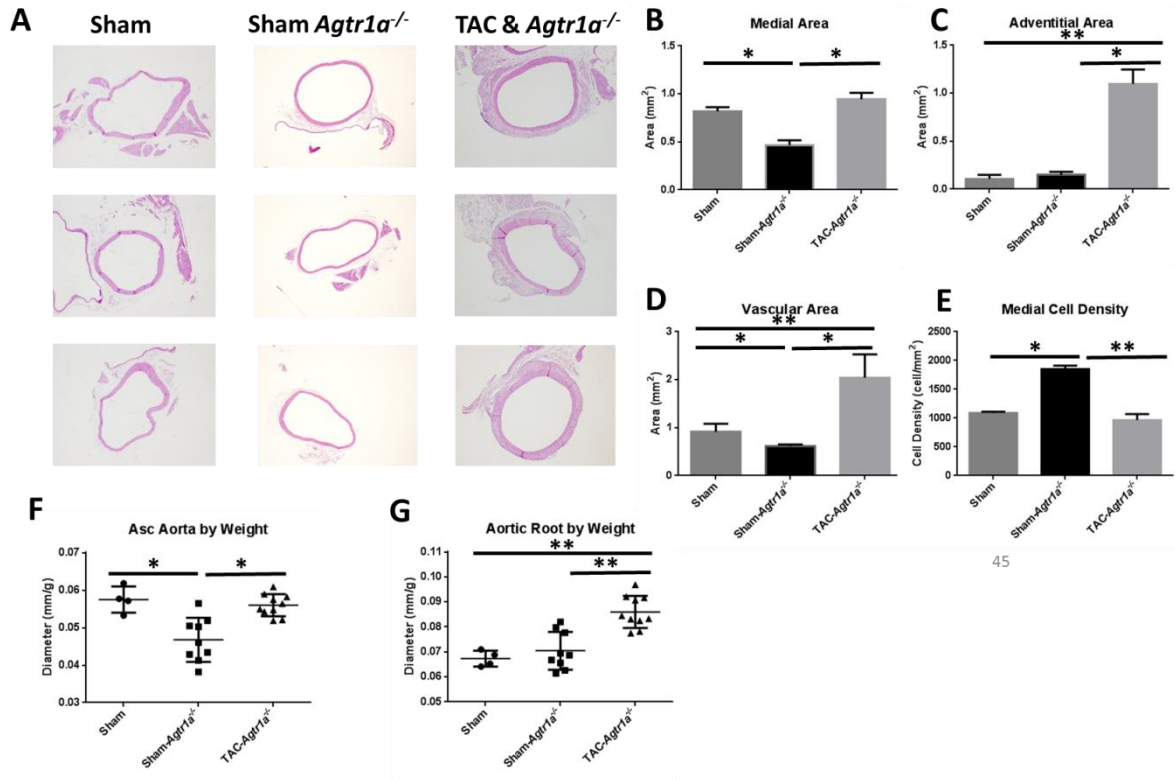


Figure 4.15 – A, B, & C) *Agtr1a*^{-/-} mice have decreased medial area compared to WT mice, but the medial area is significantly increased compared to *Agtr1a*^{-/-} mice after TAC. C & D) Significant vascular and adventitial expansion is still present in *Agtr1a*^{-/-} mice compare to both sham controls. E) There is a significant increase in SMCs in the media under control conditions. F & G) When analyzed by weight, the ascending aorta is significantly lower in the sham mice compared to WT sham, but there is no difference between the two in the aortic root.

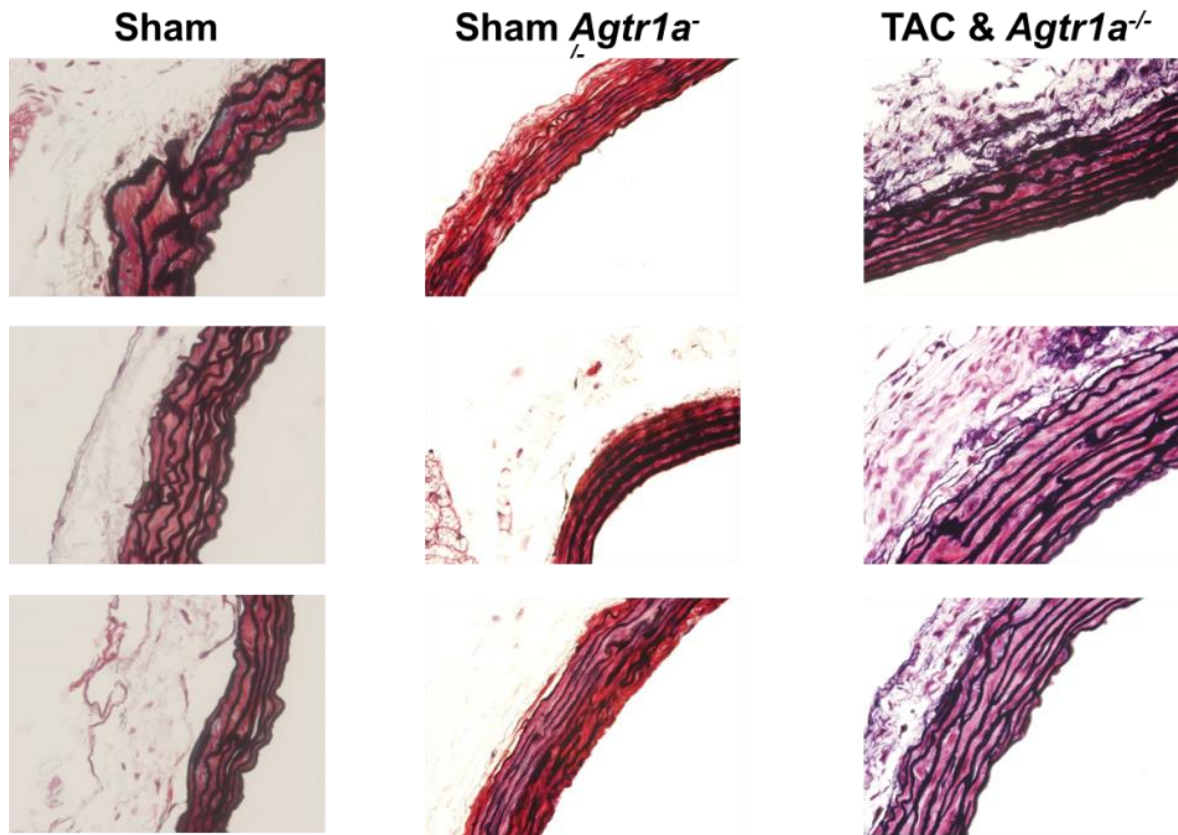


Figure 4.16 – Significant adventitial expansion remains in the TAC *Agtr1a*^{-/-} compared to WT and *Agtr1a*^{-/-} mice who underwent sham surgery. TAC *Agtr1a*^{-/-} mice show increased distance between the elastic lamellae, but *Agtr1a*^{-/-} mice appear to have more elastic lamellae and early results appear less developed.

4.3 Discussion

We have previously shown that signaling through the AT1R is responsible for a significant portion of the aortic remodeling that occurs with TAC. A prominent component of TAC-induced aortic remodeling is vascular inflammation characterized by increased *Il6* and *Mcp1* expression and recruitment of macrophages to the adventitia, and these changes are completely blocked when signaling through the AT1R is prevented by

treatment with losartan. Other changes are only partially blocked, including ascending aortic dilatation, adventitial cellular hyperplasia and collagen accumulation. I initially hypothesized that the AT1R activation was not due to increased AngII in aortic tissue, but rather mechanical stretch activation of the AT1R, which has been described in cardiomyocytes and SMCs (64, 85, 98, 99). Furthermore, it has been shown that inverse agonists of the AT1R can block this activation of the AT1R (102). Although losartan is not an AT1R inverse agonist, EXP3174, an active metabolite of losartan, can act as an inverse agonist in the inositol phosphate (IP) production assay based on studies involving a constitutively active AT₁-N111G mutant (103). To begin to investigate whether AT1R activation with TAC-induced aortic remodeling was ligand independent, I blocked the production of AngII using captopril. Indeed, captopril did not block the aortic dilatation and vascular remodeling associated with TAC, supporting the conclusion that the AT1R activation in SMC with TAC is ligand independent. At the same time, the initial experiments suggested that captopril had a negative effect on aortic remodeling, leading to increased deaths due to aortic rupture.

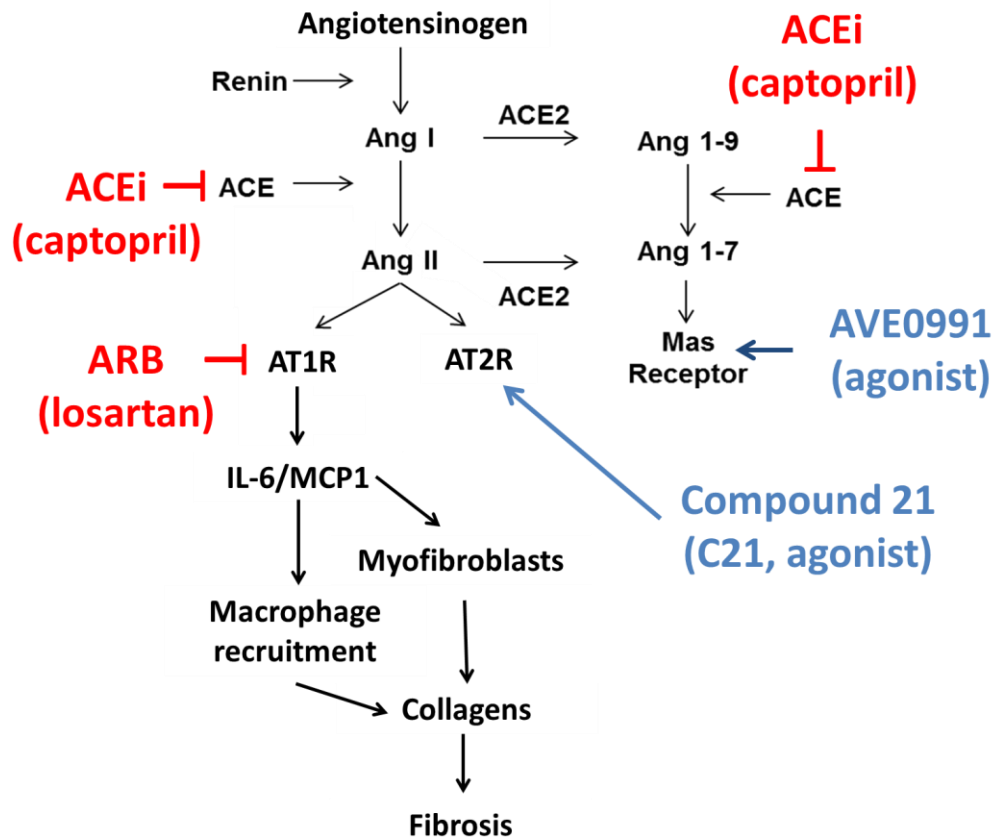


Figure 4.17 – Working model indicating my points of interest in the angiotensin system. The questions remaining are the influence of the AT2R and Mas receptor in our hyper-acute model specifically in the ascending aorta and how they could modulate the ligand independent signaling.

I sought to determine the role of signaling through other receptors in the angiotensin system with TAC when all AngII signaling is blocked and aortic remodeling is dependent on mechanical stimulation. AT2R receptors are present in vascular SMCs, and have been reported to comprise approximately 30% of the AngII receptors in the rat aorta (104). It is feasible that AT1R activation proceeds unchecked when all the receptors are blocked but selective activation of AT2R could block aortic enlargement to the same extent

as losartan treatment alone. As stated above (Section 1.3), the AT2R has been known to counter the effects of the AT1R downstream in multiple systems. In the vascular SMCs, the AT1R increases proliferation, fibrosis, MMP2, and MMP9 expression (52), while the AT2R decreases proliferation, fibrosis, and MMP9 and MMP2 expression (48, 105). However, in some models the AT2R has been thought to affect smooth muscle cell apoptosis (53, 54)

Another ACEi, enalapril, was used to reinforce the importance of the AT2 receptor. A cross between the *Fbln*^{C1039G/+} with mice deficient in AT2R, *Agtr2*^{-/-} (106), actually increased aneurysm formation and made losartan less effective (48). Their results indicated the AT2R decreases pERK signaling, cell proliferation, fibrosis, and MMP9 signaling. Their results were reinforced by other labs, which showed that antagonists of the AT2R are detrimental in abdominal aortic models. In *ApoE*^{-/-} mice infused with AngII, the antagonist of the AT2R, PD123319, leads to an increase in atherosclerosis and AngII induced vascular pathology (107). However, they later showed PD123319 could work by an AT2R independent mechanism, which complicates interpretation of their results (108). Still, the independent beneficial effects of the AT2R could possibly explain why captopril was not just ineffective but detrimental.

Ang1-7 is a peptide mainly generated from AngII by angiotensin converting enzyme 2 (ACE2), but which can also be made from AngI via neutral endopeptidase activity. Ang1-7 binds to the G protein-coupled receptor Mas. In SMCs, Mas receptor signaling is considered an antagonist of AngII signaling. Mas receptor signaling is vasodilatory and blocks hypertrophy and migration of SMCs. Importantly, Ang1-7 blocks the pro-inflammatory

response triggered by AngII in primary human SMCs in culture by blocking NF- κ B signaling and inducible nitric oxide synthase induction. With exposure to AngII, SMCs activate NF- κ B signaling, and Ang1-7 markedly inhibits this activation and the associated inflammatory changes (109). Specifically, Ang1-7 suppresses superoxide anion levels and NADPH oxidase activity that occurs in SMCs with exposure to AngII (110), but does not have these effects on SMCs in the absence of AngII exposure. In our studies of TAC-induced aortic remodeling and blocking angiotensin signaling through the major receptors, selective activation of the Mas receptor agonist completely blocked vascular inflammation based on decreased *Il6* and *Mcp1* expression and lack of macrophage accumulation in the adventitia. At the same time, aortic enlargement was not rescued and the aortic pathology was adversely affected. The Mas agonist prevented SMC hypertrophy and instead caused SMC loss in the aortic media and decreased fibrosis in the adventitial layer. The loss of SMCs is in contrast to a protective role of the Mas receptor in other cells types.

Ang1-7 has been studied extensively in multiple systems. In the kidney, its activation has been associated with decreased matrix protein production and improved renal function and its inhibition associated with increased collagen deposition, TGF- β , Smad2/3, ERK1/2, and NFK β (55). In rat models, Ang 1-7 was shown to improve heart function by reducing cardiomyocyte hypertrophy, fibrosis and inflammatory cell infiltration with short term administration. In the cerebrovasculature, in a study of intracerebral hemorrhagic stroke with C57BL/6 mice, it was shown to modulate NF- κ B signaling by decreasing TNF- α , MCP-1, and IL-8 (111). Of interest to me, another group utilized mice deficient in ACE2, *Ace2*^{-/-} (112) and the AngII infusion model to study the thoracic aorta.

They were able to find ACE2 deficiency worsened the AngII mediated inflammation model with enhanced AKT phosphorylation, increased ERK1/2, and increased endothelial nitric oxide synthase. These results could be reversed with an ARB, irbesartan, that prevented inflammation by suppressing the Akt-ERK-eNOS signaling pathway (113). Therefore, the loss of SMCs and other adverse pathologic changes with TAC when the Mas receptor is activated suggests that ROS generation with TAC plays a protective role in aortic SMCs.

While our focus is on the angiotensin system, we must remember the kinin system also influences the vascular disease. Kininogen is metabolized by kallikrein into bradykinin. Bradykinin, a fundamental part of the kinin system, has been a well-established vasodilator helping to control blood pressure. It has also been associated with increased vasodilation, vascular permeability, inflammation, and pain. ACE is one of the major vasopeptidases regulating bradykinin signaling as it metabolizes bradykinin into its inactive forms. Subsequently, ACEi use has been shown to increase nitric oxide and vasorelaxation (114). Hence, the kinin system may play a role in the results I observed with captopril. While inhibiting both AT1R and AT2R, we may have left bradykinin uninhibited resulting in our increased inflammation observed with captopril treated mice compared to losartan treated mice.

Finally, I sought to determine how TAC-induced aortic remodeling would occur with loss of the AT1R. These studies were complicated by the fact that the *Agtr1a*^{-/-} mice are significantly hypotensive and appear underdeveloped ascending aortas. Interestingly deletion of *Agtr1a*^{-/-} in mice has been associated with a variety of factors including

increased life expectancy (115, 116), but diminished growth, vascular thickening, and atrophy of the inner renal medulla (117). Despite these issues with the aorta, it was still surprising that TAC induced medial wall thickening, adventitial thickening, and vascular inflammation were present in the *Agtr1a*^{-/-} mice. We expected our results to be similar to the mice treated with losartan. Based on the pharmacologic manipulation of aortic remodeling with TAC, these changes are proposed to be in part due to ligand independent activation of AT1R. Despite this conclusion, it is clear that mechanical forces are still able to cause remodeling in the absence of the *Agtr1a*. It is notable that not all TAC-induced remodeling is blocked by losartan (52), but the influence of deleting a gene in a highly variable system is difficult to predict. In such a dynamic system, there is no guarantee that another signaling pathway does not become more dominant or compensates for the loss of the *Agtr1a* receptor. Humans only have one isoform of the AT1R, but mice have two, and in the kidney the absence of one can be compensated by the other isoform (117). In this model, *Agtr1b* is still present, and it is yet unknown how it might affect the cell types in the ascending aorta and whether it can compensate for the loss of *Agtr1a*. Others have found *Agtr1b* to be more mechanosensitive in vascular SMC myogenic vasoconstriction (118). This model would need to be studied more extensively to verify the role of *Agtr1b* in TAC-induced remodeling of *Agtr1a*^{-/-} mice.

Chapter 5 – Discussion and Conclusions

5.1 Introduction

I hypothesized that angiotensin II signaling through the AT1R contributes to thoracic aortic aneurysm formation in multiple model systems of disease, but that blocking related receptors in addition to the AT1R, such as the AT2R and Mas receptor, may have negative consequences. In the *Acta2*^{-/-} mouse model, I found an increased sensitivity of cells to AT1R signaling without exogenous AngII was due to increased ROS and NF-KB signaling. *Acta2*^{-/-} mice develop dilated aortas over time, and the dilation is partially blocked with an ARB, losartan, but blocking the formation of the ligand with an ACEi, captopril, was insufficient to attenuate disease. In TAC, I again found that ARB treatment attenuated the physiologic and pathophysiologic changes I observed, but captopril did not. The combination of captopril and C21 had the same physiologic affect as an ARB. However, the results did not coincide with the pathophysiologic changes.

Angiotensin signaling was initially identified as a system to manage the blood pressure in response to different environmental stimuli. As described in Chapter 1, angiotensinogen is converted to angiotensin I by renin which is then converted to the ligand AngII by ACE (24). Investigations into AngII signaling were at first primarily focused on the renal response to manage blood pressure, but over time research has been expanded to identify a role for angiotensin signaling in other systems, such as the heart and aorta (50, 51).

In addition to its function in regulating blood pressure, the renin angiotensin system is also known to be involved in triggering inflammation and fibrosis during remodeling of

multiple organ systems including the kidneys and the heart. In the kidneys, the renin-angiotensin-aldosterone-system plays a role in both hypertensive and end-stage kidney disease (119). The invasion of fibroblasts and the fibrotic response eventually lead to the destruction of nephrons and the interstitium of the kidney, resulting in kidney failure (120). In patients, the administration of ARBs has been shown to improve proteinuria, indicating improved kidney function and reinforcing the beneficial aspects of ARBs and their relationship to fibrosis (121). In the heart, a similar fibrotic response has been observed. It has been well established that angiotensin signaling and downstream aldosterone signaling have been associated with increased collagen synthesis and deposition (122). They have also been associated with degenerative remodeling of the heart, restricted blood flow, and heart failure (103). In investigations of these models, data has consistently shown that these changes involved TGF- β signaling in the fibrotic response (75).

5.2 Role of angiotensin signaling in TAA

The work presented in this dissertation furthers understanding of the role of angiotensin signaling in thoracic aortic remodeling and disease. First, we addressed the role of blocking all angiotensin receptors using an ACE inhibitor, captopril. Previous studies had shown another ACE inhibitor, enalapril, was not as effective as losartan in preventing aortic growth in the Marfan mouse model (48). Interestingly, in the *Fbln4*^{-/-} mouse model, captopril was as effective as losartan in preventing many of pathologic changes associated with the disease such as an increase in vascular area (65). I found that captopril actually increased aortic growth in both the aortic root and ascending aorta of the *Acta2*^{-/-} mouse

model and worsened elastin breaks compared with no treatment. In our TAC model of acute hypertension, treatment with captopril did not prevent aortic enlargement and vascular inflammation, whereas treatment with losartan did. These results provide additional data to support that ACE inhibitors are not equivalent to ARBs in terms of treating thoracic aortic disease.

In the *Acta2*^{-/-} mouse model, we identified that the source of increased AngII signaling in the aorta was not an increase in ligand. Rather, there was a significantly increased sensitivity of the AT1R to endogenous levels of AngII due to ROS increasing NF-κB signaling, which drives increased expression of AT1R (11). It is important to note that the *Fbn1*^{-/-} mice may also have increased AT1R expression since these mice also show increased ROS in SMCs and aortic tissues.

We intended to use the data from the TAC captopril trial to show that TAC-induced AT1R signaling in the ascending aorta and aortic root was not dependent on the ligand, AngII. Surprisingly, our original captopril trials gave an overwhelmingly poor outcome with 50% of the mice dying. Replication of the study by a different surgeon did not demonstrate the increased death rates. However, captopril did not rescue the aortic remodeling induced by TAC. Markers of vascular inflammation remained elevated in the captopril treated TAC mice, and the aortic root and ascending aorta enlarged despite decreased systolic pressures in the ascending aorta. These results support our hypothesis that ligand-independent AT1R signaling is important in driving aortic disease but also raised the

question of whether other components of the angiotensin system may play a role in the remodeling.

5.3 Angiotensin signaling through AT1R

In the past 10 years, angiotensin signaling through AT1R has emerged as a potential therapeutic target to prevent thoracic aortic disease. Initially, losartan was used to block canonical TGF- β signaling in the Marfan mouse model. Additional studies showed that losartan could block thoracic aortic disease in multiple mouse models, including our own studies of aortic enlargement in the *Acta2*^{-/-} mice (52, 61). Since blocking TGF- β signaling using losartan was so effective in the Marfan mouse model, the use of an ARB as a receptor blocker to prevent aortic disease in Marfan patients has been tested in multiple clinical trials (123). Many of these trials compared ARB treatment to β -adrenergic blocking agents which are considered the gold standard for treatment of aortic disease under the belief that it reduces stress on the aorta by reducing left ventricular ejection fraction and heart rate (123, 124). These studies focused on aortic growth rates but included other endpoints including aortic surgery and acute aortic dissection.

5.4 Clinical relevance

At least eight randomized clinical trials of losartan in patients with MFS were initiated worldwide. The first prospective trial completed was the Dutch *COMPARE trial*, which assessed 233 MFS patient over the age of 18 years who met diagnostic criteria for MFS and were assigned to receive losartan or no additional medications beyond “usual therapy”, which commonly included a β -blocker. After a mean follow up of 3.1 years,

losartan significantly reduced the rate of aortic root dilation when compared with “usual therapy” with the caveat that more patients in the losartan group than in the “usual care” group took β -blockers (125). Importantly, a sub study analyzed the 117 MFS patients with characterized *FBN1* mutations and determined that only individuals with haploinsufficiency mutations (n=38, 32.5%), but not individuals with missense mutations (n=79, 67.5%), had a reduction in the rate of aortic root dilation with losartan treatment (126). Other outcomes beyond rate of aortic root dilation have not been reported for the COMPARE trial.

The *US Pediatric Heart Network Trial* was the largest losartan trial (127). It enrolled 608 patients with MFS between the ages of 6 months and 25 years who met Ghent criteria and had significant aortic root enlargement (defined by a Z score > 3.0). The two arms of the randomized trial were atenolol (started at 0.5mg/kg/day and increased on the basis of hemodynamic response to a maximum of 4mg/kg/ day) and losartan (started at 0.4 mg/kg/day and increased on the basis of hemodynamic response to a maximum of 1.4 mg/kg/day). The “mean” dose for young adults was 151 mg atenolol per day and 85 mg of losartan per day. The main outcome of the trial did not show any significant difference in the rate of aortic root growth between the groups. Similarly, two other double blind clinical trials testing losartan against atenolol (128) or against placebo (129) showed no effect of losartan in limiting aortic dilatation. In contrast, a small open label pilot study in 28 patients with MFS found reduced rate of aortic dilation with losartan added on to β -blockade therapy (130). Other clinical studies are still ongoing and results have not been published.

Although the US Pediatric Heart Network trial was designed to examine rate of aortic root growth as the primary outcome and there was no difference between groups, a

combined secondary endpoint (death, dissection, aortic root surgery) was reached over the 3 years clinical trial period in 10 of 268 atenolol-treated patients and in 19 of 267 Losartan-treated patients. This event rate was almost 2-fold higher in the losartan treated patients, but did not reach statistical significance (p value = 0.07). The study was not sufficiently powered to examine clinical endpoints of dissection, death, and aortic root surgery, in part due to the fact that these events are fortunately very rare in a young cohort like the Pediatric Heart Network study. Assuming a similar cohort of MFS patient and the same statistical parameters as used for the US Pediatric Heart Network study with an 85% power to detect a difference at the level of significance of 0.05, a sample size of 760 patients may have reached a statistically significant increase for combined secondary endpoints of dissection, aortic surgery, or death in the losartan-treated group. However, this is speculative, and extrapolation of the observed event rate in the US Pediatric Heart Network trial is uncertain since it occurred exceedingly rarely. But the results from this trial raise the important point that future clinical studies cannot focus on aortic dilatation alone, and must include clinically important outcomes such as dissection and need for aortic surgery. The p-value of 0.07 indicates that there is a 93% chance that the increased combined frequency of dissection, death, and aortic root surgery in the losartan-treated MFS patients in the US Pediatric Heart Network trial did not occur randomly. Importantly, other smaller clinical trials comparing β -blockade to losartan did not have increased events in individuals treated with losartan.

5.5 The fibrotic response

These results bring up an interesting question: is it possible that the fibrotic response seen in many of the models may not be detrimental but beneficial? Angiotensin II blockade with enalapril was recently reported to reduce the progression of cardiac fibrosis in patients with Duchenne and Becker muscle dystrophy in a small randomized clinical trial (131, 132). While reduced cardiac or renal fibrosis might improve the functions of these organs, it could be of disadvantage for the aorta, where tensile strength is required to withstand the force of pulsatile blood flow. Biomechanical studies show that the wall increases in thickness to better distribute the hoop stress in response to an increase in pulse pressure (25). We also know that AngII signaling drives a fibrotic response in the thoracic aorta stimulating fibroblast and myofibroblast proliferation and recruiting macrophages and monocytes. Eventually, this leads to adventitial thickening and deposition of increased extracellular matrix (28, 30). The thickening of the medial and adventitial layer and increased fibrosis with TAC is a physiologic response to increased wall stress.

Hence, blocking aortic fibrosis driven by TGF- β or AngII signaling may not be the correct pharmacological target to block aneurysm growth. This view is supported by multiple observations. First, mutations in genes encoding proteins in the TGF- β canonical signaling pathway lead to decreased TGF- β signaling in smooth muscle cells but actually cause heritable thoracic aortic disease (8). It is counter-intuitive to further block TGF- β signaling in these individuals to prevent aortic disease. Second, blocking TGF- β signaling in

the MFS mouse model through knockout of the TGF- β type II receptor or knockdown of TGF- β 2 increases aneurysm formation (133, 134). Third, blocking TGF- β signaling in another mouse model for aortic aneurysms, AngII infusion, increases the penetrance and severity of aneurysms and deaths due to aortic rupture (135). Finally, loss of function mutation of lysyl oxidase, an enzyme mediating collagen crosslinking and strongly linked to mechanical stability of extracellular matrix and fibrosis, were recently identified as causative for familial thoracic aortic aneurysms and dissections (136, 137). Blocking TGF- β signaling or blocking proper collagen maturation disrupts the integrity of the thoracic aorta.

AngII signaling also drives fibrosis in the adventitial layer of the thoracic aorta. AngII stimulates aortic adventitial fibroblasts to recruit monocytes via secretion of MCP-1, and the recruited monocytes further activate the fibroblasts/myofibroblasts to proliferate and deposit extracellular matrix, leading to adventitial thickening (28, 105). Although this process occurs as part of aneurysm formation associated with AngII infusion, the same vascular inflammation and adventitial fibrosis occurs when the forces are increased on the aorta by thoracic aortic constriction and this hypertensive remodeling is attenuated by losartan (52). Therefore, aortic adventitial remodeling driven by signaling through the AT1R can be physiologic to adapt to increased pressures or pathologic and associated with aneurysms. The unanswered question is whether blocking this adventitial fibrotic remodeling through the use of losartan will increase the risk for aortic dissection or rupture.

5.6 Angiotensin signaling through AT2R

I asked whether signaling through the AT2R or the Mas receptor might be important in TAC-induced aortic remodeling. Dramatic differences in terms of aortic growth and aortic pathology were found when agonists of the AT2R or the Mas receptor were used with captopril in TAC mice. The AT2R agonist, C21, in combination with captopril was able to prevent aortic enlargement but not vascular inflammation in this model system. Almost the exact opposite was found when the Mas receptor agonist was used – aortic enlargement was not rescued but vascular inflammation and much of the associated adventitial fibrosis was completely blocked. These results support that additional studies must now focus on the use of AT2R agonists as potential therapeutics to help prevent thoracic aortic disease. Although the Mas receptor agonists have shown to be beneficial in skeletal and heart diseases, the profound aortic pathologic changes, including collapse of the aortic media with SMC loss, and the continued enlargement of the aorta indicate that activation of the Mas receptor is not a target for thoracic aortic disease.

5.7 Study limitations

Several limitations of my studies should be kept in mind when considering my conclusions. First, in many experiments there was insufficient statistical power. Furthermore, I did not account for the Bonferroni correction in any of my calculations. This may have altered some of the statistical significance in my results. Second, all of my studies focused on aneurysm formation but did not effectively investigate the risk for dissections and how they relate to the angiotensin system in these models. Ideally, a model that more

consistently causes aortic dissection should be utilized for future studies. While some of my necropsy studies indicated possible dissections, the frequency of the finding was not consistent enough to draw conclusions. Our lab is currently attempting to define better mouse models for aortic dissection. Once those models are established, one of the first goals should be to assess whether changes in the fibrotic or inflammatory responses associated with the angiotensin pathway may hinder or exacerbate dissection.

5.8 Future directions

Moving forward, we should pay closer attention to the difference between the ascending aorta and the aortic root. We know that they are derived from distinct developmental origins (3), but how does that specifically affect their different responses to the same stimulus? Recent results have also indicated an inducible nitric oxide synthase was potential therapeutic target (88), and it would be interesting to determine how the AT2R or Mas could play a role in this system. Finally, I would also be interested in going back and to address my original question about which intracellular pathway downstream of the AT1R is activated in the ascending aorta in response to biomechanical stress.

My goal at the start of this project was to identify pathways that might improve the treatment of thoracic aortic aneurysms. I believe that the results of my studies contribute, in a small way, to our understanding of therapeutic strategies targeting the angiotensin system. While ARBs are considered the therapeutic with the highest potential of all the pharmaceutical manipulations of the angiotensin system, the angiotensin system is far more complicated and dynamic than most would have ever anticipated. Much more time

needs to be invested in our understanding of the angiotensin system in thoracic aortic disease, and we should not assume that blocking particular receptors or pathways in other systems, such as the kidneys or heart, will also be beneficial in the thoracic aorta. We must carefully choose our experimental designs to better investigate disease pathologies and possible therapeutic strategies.

Bibliography

1. Weinsaft JW, Devereux RB, Preiss LR, Feher A, Roman MJ, Basson CT, Geevarghese A, Ravekes W, Dietz HC, Holmes K, Habashi J, Pyeritz RE, Bavaria J, Milewski K, LeMaire SA, Morris S, Milewicz DM, Prakash S, Maslen C, Song HK, Silberbach GM, Shohet RV, McDonnell N, Hendershot T, Eagle KA, Asch FM, Investigators GR. Aortic Dissection in Patients With Genetically Mediated Aneurysms: Incidence and Predictors in the GenTAC Registry. *Journal of the American College of Cardiology*. 2016;67(23):2744-54.
2. Netter FH, Hansen JT. *Atlas of human anatomy*. 3rd ed. Teterboro, N.J.: Icon Learning Systems; 2003.
3. Jiang X, Rowitch DH, Soriano P, McMahon AP, Sucov HM. Fate of the mammalian cardiac neural crest. *Development*. 2000;127(8):1607-16.
4. Majesky MW. Developmental basis of vascular smooth muscle diversity. *Arteriosclerosis, thrombosis, and vascular biology*. 2007;27(6):1248-58.
5. Milewicz DM, Guo DC, Tran-Fadulu V, Lafont AL, Papke CL, Inamoto S, Kwartler CS, Pannu H. Genetic basis of thoracic aortic aneurysms and dissections: focus on smooth muscle cell contractile dysfunction. *Annu Rev Genomics Hum Genet*. 2008;9:283-302.
6. Wolinsky H, Glagov S. A lamellar unit of aortic medial structure and function in mammals. *Circulation research*. 1967;20(1):99-111.
7. Milewicz DM, Kwartler CS, Papke CL, Regalado ES, Cao J, Reid AJ. Genetic variants promoting smooth muscle cell proliferation can result in diffuse and diverse vascular

diseases: evidence for a hyperplastic vasculomyopathy. *Genetics in medicine : official journal of the American College of Medical Genetics*. 2010;12(4):196-203.

8. Milewicz DM, Prakash SK, Ramirez F. Therapeutics Targeting Drivers of Thoracic Aortic Aneurysms and Acute Aortic Dissections: Insights from Predisposing Genes and Mouse Models. *Annu Rev Med*. 2017;68:51-67.

9. Papke CL, Cao J, Kwartler CS, Villamizar C, Byanova KL, Lim SM, Sreenivasappa H, Fischer G, Pham J, Rees M, Wang M, Chaponnier C, Gabbiani G, Khakoo AY, Chandra J, Trache A, Zimmer W, Milewicz DM. Smooth muscle hyperplasia due to loss of smooth muscle alpha-actin is driven by activation of focal adhesion kinase, altered p53 localization and increased levels of platelet-derived growth factor receptor-beta. *Human molecular genetics*. 2013;22(15):3123-37.

10. Li DY, Faury G, Taylor DG, Davis EC, Boyle WA, Mecham RP, Stenzel P, Boak B, Keating MT. Novel arterial pathology in mice and humans hemizygous for elastin. *The Journal of clinical investigation*. 1998;102(10):1783-7.

11. Chen J, Peters AM, Papke CL, Villamizar C, Ringuette LJ, Cao JM, Wang S, Ma S, Gong L, Byanova K, Xiong J, Zhu MX, Madonna R, Kee P, Geng YJ, Brasier A, Davis EC, Prakash SK, Kwartler CS, Milewicz DM. Loss of Smooth Muscle alpha-actin Leads to NF-kappaB-Dependent Increased Sensitivity to Angiotensin II in Smooth Muscle Cells and Aortic Enlargement. *Circulation research*. 2017.

12. Belz GG. Elastic properties and Windkessel function of the human aorta. *Cardiovasc Drugs Ther*. 1995;9(1):73-83.

13. Wagenseil JE, Mecham RP. Vascular extracellular matrix and arterial mechanics. *Physiol Rev.* 2009;89(3):957-89.
14. Davis EC. Smooth muscle cell to elastic lamina connections in developing mouse aorta. Role in aortic medial organization. *Lab Invest.* 1993;68(1):89-99.
15. Sainz J, Al Haj Zen A, Caligiuri G, Demerens C, Urbain D, Lemitre M, Lafont A. Isolation of "side population" progenitor cells from healthy arteries of adult mice. *Arteriosclerosis, thrombosis, and vascular biology.* 2006;26(2):281-6.
16. Psaltis PJ, Puranik AS, Spoon DB, Chue CD, Hoffman SJ, Witt TA, Delacroix S, Kleppe LS, Mueske CS, Pan S, Gulati R, Simari RD. Characterization of a resident population of adventitial macrophage progenitor cells in postnatal vasculature. *Circulation research.* 2014;115(3):364-75.
17. Majesky MW, Dong XR, Hoglund V, Daum G, Mahoney WM, Jr. The adventitia: a progenitor cell niche for the vessel wall. *Cells, tissues, organs.* 2012;195(1-2):73-81.
18. Majesky MW, Dong XR, Hoglund V, Mahoney WM, Jr., Daum G. The adventitia: a dynamic interface containing resident progenitor cells. *Arteriosclerosis, thrombosis, and vascular biology.* 2011;31(7):1530-9.
19. Majesky MW, Mummery CL. Smooth muscle diversity from human pluripotent cells. *Nature biotechnology.* 2012;30(2):152-4.
20. Hoffman GS, Weyand CM. *Inflammatory diseases of blood vessels.* New York: Marcel Dekker; 2002. xvi, 815 p. p.
21. LeMaire SA, Russell L. Epidemiology of thoracic aortic dissection. *Nat Rev Cardiol.* 2011;8(2):103-13.

22. Milewicz DM. Stopping a killer: improving the diagnosis, treatment, and prevention of acute ascending aortic dissections. *Circulation*. 2011;124(18):1902-4.
23. Bojar RM, Mathisen DJ, Warner KG. Manual of perioperative care in cardiac and thoracic surgery. 2nd ed. Boston: Blackwell Scientific; 1994. x, 584 p. p.
24. Andreoli TE, Cecil RL. Andreoli and Carpenter's Cecil essentials of medicine. 8th ed. Philadelphia, PA: Saunders/Elsevier; 2010. xxvii, 1282 p. p.
25. Humphrey JD, Schwartz MA, Tellides G, Milewicz DM. Role of mechanotransduction in vascular biology: focus on thoracic aortic aneurysms and dissections. *Circulation research*. 2015;116(8):1448-61.
26. Busch A, Grimm C, Hartmann E, Paloschi V, Kickuth R, Lengquist M, Otto C, Eriksson P, Kellersmann R, Lorenz U, Maegdefessel L. Vessel wall morphology is equivalent for different artery types and localizations of advanced human aneurysms. *Histochem Cell Biol*. 2017.
27. Guo DC, Papke CL, He R, Milewicz DM. Pathogenesis of thoracic and abdominal aortic aneurysms. *Ann N Y Acad Sci*. 2006;1085:339-52.
28. Tieu BC, Lee C, Sun H, Lejeune W, Recinos A, 3rd, Ju X, Spratt H, Guo DC, Milewicz D, Tilton RG, Brasier AR. An adventitial IL-6/MCP1 amplification loop accelerates macrophage-mediated vascular inflammation leading to aortic dissection in mice. *The Journal of clinical investigation*. 2009;119(12):3637-51.
29. Zhang X, Shen YH, LeMaire SA. Thoracic aortic dissection: are matrix metalloproteinases involved? *Vascular*. 2009;17(3):147-57.

30. Tieu BC, Ju X, Lee C, Sun H, Lejeune W, Recinos A, 3rd, Brasier AR, Tilton RG. Aortic adventitial fibroblasts participate in angiotensin-induced vascular wall inflammation and remodeling. *Journal of vascular research*. 2011;48(3):261-72.
31. Kuang SQ, Medina-Martinez O, Guo DC, Gong L, Regalado ES, Reynolds CL, Boileau C, Jondeau G, Prakash SK, Kwartler CS, Zhu LY, Peters AM, Duan XY, Bamshad MJ, Shendure J, Nickerson DA, Santos-Cortez RL, Dong X, Leal SM, Majesky MW, Swindell EC, Jamrich M, Milewicz DM. FOXE3 mutations predispose to thoracic aortic aneurysms and dissections. *The Journal of clinical investigation*. 2016;126(3):948-61.
32. Hiratzka LF, Bakris GL, Beckman JA, Bersin RM, Carr VF, Casey DE, Jr., Eagle KA, Hermann LK, Isselbacher EM, Kazerooni EA, Kouchoukos NT, Lytle BW, Milewicz DM, Reich DL, Sen S, Shinn JA, Svensson LG, Williams DM, American College of Cardiology Foundation/American Heart Association Task Force on Practice G, American Association for Thoracic S, American College of R, American Stroke A, Society of Cardiovascular A, Society for Cardiovascular A, Interventions, Society of Interventional R, Society of Thoracic S, Society for Vascular M. 2010 ACCF/AHA/AATS/ACR/ASA/SCA/SCAI/SIR/STS/SVM guidelines for the diagnosis and management of patients with Thoracic Aortic Disease: a report of the American College of Cardiology Foundation/American Heart Association Task Force on Practice Guidelines, American Association for Thoracic Surgery, American College of Radiology, American Stroke Association, Society of Cardiovascular Anesthesiologists, Society for Cardiovascular Angiography and Interventions, Society of Interventional Radiology, Society of Thoracic Surgeons, and Society for Vascular Medicine. *Circulation*. 2010;121(13):e266-369.

33. Biddinger A, Rocklin M, Coselli J, Milewicz DM. Familial thoracic aortic dilatations and dissections: a case control study. *J Vasc Surg.* 1997;25(3):506-11.
34. Coady MA, Davies RR, Roberts M, Goldstein LJ, Rogalski MJ, Rizzo JA, Hammond GL, Kopf GS, Elefteriades JA. Familial patterns of thoracic aortic aneurysms. *Arch Surg.* 1999;134(4):361-7.
35. Albornoz G, Coady MA, Roberts M, Davies RR, Tranquilli M, Rizzo JA, Elefteriades JA. Familial thoracic aortic aneurysms and dissections--incidence, modes of inheritance, and phenotypic patterns. *The Annals of thoracic surgery.* 2006;82(4):1400-5.
36. Milewicz DM, Chen H, Park ES, Petty EM, Zaghi H, Shashidhar G, Willing M, Patel V. Reduced penetrance and variable expressivity of familial thoracic aortic aneurysms/dissections. *The American journal of cardiology.* 1998;82(4):474-9.
37. Shalhoub S, Black JH, 3rd, Cecchi AC, Xu Z, Griswold BF, Safi HJ, Milewicz DM, McDonnell NB. Molecular diagnosis in vascular Ehlers-Danlos syndrome predicts pattern of arterial involvement and outcomes. *J Vasc Surg.* 2014;60(1):160-9.
38. LeMaire SA, McDonald ML, Guo DC, Russell L, Miller CC, 3rd, Johnson RJ, Bekheirnia MR, Franco LM, Nguyen M, Pyeritz RE, Bavaria JE, Devereux R, Maslen C, Holmes KW, Eagle K, Body SC, Seidman C, Seidman JG, Isselbacher EM, Bray M, Coselli JS, Estrera AL, Safi HJ, Belmont JW, Leal SM, Milewicz DM. Genome-wide association study identifies a susceptibility locus for thoracic aortic aneurysms and aortic dissections spanning FBN1 at 15q21.1. *Nat Genet.* 2011;43(10):996-1000.
39. Boileau C, Guo DC, Hanna N, Regalado ES, Detaint D, Gong L, Varret M, Prakash SK, Li AH, d'Indy H, Braverman AC, Grandchamp B, Kwartler CS, Gouya L, Santos-Cortez RL,

- Abifadel M, Leal SM, Muti C, Shendure J, Gross MS, Rieder MJ, Vahanian A, Nickerson DA, Michel JB, National Heart L, Blood Institute Go Exome Sequencing P, Jondeau G, Milewicz DM. TGFBR2 mutations cause familial thoracic aortic aneurysms and dissections associated with mild systemic features of Marfan syndrome. *Nat Genet.* 2012;44(8):916-21.
40. Inamoto S, Kwartler CS, Lafont AL, Liang YY, Fadulu VT, Duraisamy S, Willing M, Estrera A, Safi H, Hannibal MC, Carey J, Wiktorowicz J, Tan FK, Feng XH, Pannu H, Milewicz DM. TGFBR2 mutations alter smooth muscle cell phenotype and predispose to thoracic aortic aneurysms and dissections. *Cardiovascular research.* 2010;88(3):520-9.
41. Guo DC, Pannu H, Tran-Fadulu V, Papke CL, Yu RK, Avidan N, Bourgeois S, Estrera AL, Safi HJ, Sparks E, Amor D, Ades L, McConnell V, Willoughby CE, Abuelo D, Willing M, Lewis RA, Kim DH, Scherer S, Tung PP, Ahn C, Buja LM, Raman CS, Shete SS, Milewicz DM. Mutations in smooth muscle alpha-actin (ACTA2) lead to thoracic aortic aneurysms and dissections. *Nat Genet.* 2007;39(12):1488-93.
42. Guo DC, Papke CL, Tran-Fadulu V, Regalado ES, Avidan N, Johnson RJ, Kim DH, Pannu H, Willing MC, Sparks E, Pyeritz RE, Singh MN, Dalman RL, Grotta JC, Marian AJ, Boerwinkle EA, Frazier LQ, LeMaire SA, Coselli JS, Estrera AL, Safi HJ, Veeraraghavan S, Muzny DM, Wheeler DA, Willerson JT, Yu RK, Shete SS, Scherer SE, Raman CS, Buja LM, Milewicz DM. Mutations in smooth muscle alpha-actin (ACTA2) cause coronary artery disease, stroke, and Moyamoya disease, along with thoracic aortic disease. *American journal of human genetics.* 2009;84(5):617-27.
43. Kuang SQ, Kwartler CS, Byanova KL, Pham J, Gong L, Prakash SK, Huang J, Kamm KE, Stull JT, Sweeney HL, Milewicz DM. Rare, nonsynonymous variant in the smooth muscle-

specific isoform of myosin heavy chain, MYH11, R247C, alters force generation in the aorta and phenotype of smooth muscle cells. *Circulation research*. 2012;110(11):1411-22.

44. Wang L, Guo DC, Cao J, Gong L, Kamm KE, Regalado E, Li L, Shete S, He WQ, Zhu MS, Offermanns S, Gilchrist D, Elefteriades J, Stull JT, Milewicz DM. Mutations in myosin light chain kinase cause familial aortic dissections. *American journal of human genetics*. 2010;87(5):701-7.

45. Guo DC, Gong L, Regalado ES, Santos-Cortez RL, Zhao R, Cai B, Veeraraghavan S, Prakash SK, Johnson RJ, Muilenburg A, Willing M, Jondeau G, Boileau C, Pannu H, Moran R, Debacker J, GenTac Investigators NHL, Blood Institute Go Exome Sequencing P, Montalcino Aortic C, Bamshad MJ, Shendure J, Nickerson DA, Leal SM, Raman CS, Swindell EC, Milewicz DM. MAT2A mutations predispose individuals to thoracic aortic aneurysms. *American journal of human genetics*. 2015;96(1):170-7.

46. Lyubarova R, Gosmanova EO. Mineralocorticoid Receptor Blockade in End-Stage Renal Disease. *Curr Hypertens Rep*. 2017;19(5):40.

47. Maning J, Negussie S, Clark MA, Lymperopoulos A. Biased agonism/antagonism at the AngII-AT1 receptor: Implications for adrenal aldosterone production and cardiovascular therapy. *Pharmacological research : the official journal of the Italian Pharmacological Society*. 2017.

48. Habashi JP, Doyle JJ, Holm TM, Aziz H, Schoenhoff F, Bedja D, Chen Y, Modiri AN, Judge DP, Dietz HC. Angiotensin II type 2 receptor signaling attenuates aortic aneurysm in mice through ERK antagonism. *Science*. 2011;332(6027):361-5.

49. Senbonmatsu T, Ichihara S, Price E, Jr., Gaffney FA, Inagami T. Evidence for angiotensin II type 2 receptor-mediated cardiac myocyte enlargement during in vivo pressure overload. *The Journal of clinical investigation*. 2000;106(3):R25-9.
50. Hannan RE, Widdop RE. Vascular angiotensin II actions mediated by angiotensin II type 2 receptors. *Curr Hypertens Rep*. 2004;6(2):117-23.
51. Widdop RE, Jones ES, Hannan RE, Gaspari TA. Angiotensin AT2 receptors: cardiovascular hope or hype? *British journal of pharmacology*. 2003;140(5):809-24.
52. Kuang SQ, Geng L, Prakash SK, Cao JM, Guo S, Villamizar C, Kwartler CS, Peters AM, Brasier AR, Milewicz DM. Aortic remodeling after transverse aortic constriction in mice is attenuated with AT1 receptor blockade. *Arteriosclerosis, thrombosis, and vascular biology*. 2013;33(9):2172-9.
53. Yamamoto Y, Watari Y, Brydun A, Yoshizumi M, Akishita M, Horiuchi M, Chayama K, Oshima T, Ozono R. Role of the angiotensin II type 2 receptor in arterial remodeling after wire injury in mice. *Hypertens Res*. 2008;31(6):1241-9.
54. Nagashima H, Sakomura Y, Aoka Y, Uto K, Kameyama K, Ogawa M, Aomi S, Koyanagi H, Ishizuka N, Naruse M, Kawana M, Kasanuki H. Angiotensin II type 2 receptor mediates vascular smooth muscle cell apoptosis in cystic medial degeneration associated with Marfan's syndrome. *Circulation*. 2001;104(12 Suppl 1):I282-7.
55. Simoes e Silva AC, Silveira KD, Ferreira AJ, Teixeira MM. ACE2, angiotensin-(1-7) and Mas receptor axis in inflammation and fibrosis. *British journal of pharmacology*. 2013;169(3):477-92.

56. Papinska AM, Mordwinkin NM, Meeks CJ, Jadhav SS, Rodgers KE. Angiotensin-(1-7) administration benefits cardiac, renal and progenitor cell function in db/db mice. *British journal of pharmacology*. 2015.
57. Daugherty A, Rateri DL, Charo IF, Owens AP, Howatt DA, Cassis LA. Angiotensin II infusion promotes ascending aortic aneurysms: attenuation by CCR2 deficiency in apoE^{-/-} mice. *Clinical science*. 2010;118(11):681-9.
58. Owens AP, 3rd, Subramanian V, Moorlegghen JJ, Guo Z, McNamara CA, Cassis LA, Daugherty A. Angiotensin II induces a region-specific hyperplasia of the ascending aorta through regulation of inhibitor of differentiation 3. *Circulation research*. 2010;106(3):611-9.
59. Carta L, Pereira L, Arteaga-Solis E, Lee-Arteaga SY, Lenart B, Starcher B, Merkel CA, Sukoyan M, Kerkis A, Hazeki N, Keene DR, Sakai LY, Ramirez F. Fibrillins 1 and 2 perform partially overlapping functions during aortic development. *J Biol Chem*. 2006;281(12):8016-23.
60. Bunton TE, Biery NJ, Myers L, Gayraud B, Ramirez F, Dietz HC. Phenotypic alteration of vascular smooth muscle cells precedes elastolysis in a mouse model of Marfan syndrome. *Circulation research*. 2001;88(1):37-43.
61. Habashi JP, Judge DP, Holm TM, Cohn RD, Loeys BL, Cooper TK, Myers L, Klein EC, Liu G, Calvi C, Podowski M, Neptune ER, Halushka MK, Bedja D, Gabrielson K, Rifkin DB, Carta L, Ramirez F, Huso DL, Dietz HC. Losartan, an AT1 antagonist, prevents aortic aneurysm in a mouse model of Marfan syndrome. *Science*. 2006;312(5770):117-21.

62. Judge DP, Biery NJ, Keene DR, Geubtner J, Myers L, Huso DL, Sakai LY, Dietz HC. Evidence for a critical contribution of haploinsufficiency in the complex pathogenesis of Marfan syndrome. *The Journal of clinical investigation*. 2004;114(2):172-81.
63. Yang HH, Kim JM, Chum E, van Breemen C, Chung AW. Effectiveness of combination of losartan potassium and doxycycline versus single-drug treatments in the secondary prevention of thoracic aortic aneurysm in Marfan syndrome. *The Journal of thoracic and cardiovascular surgery*. 2010;140(2):305-12 e2.
64. Zou Y, Akazawa H, Qin Y, Sano M, Takano H, Minamino T, Makita N, Iwanaga K, Zhu W, Kudoh S, Toko H, Tamura K, Kihara M, Nagai T, Fukamizu A, Umemura S, Iiri T, Fujita T, Komuro I. Mechanical stress activates angiotensin II type 1 receptor without the involvement of angiotensin II. *Nature cell biology*. 2004;6(6):499-506.
65. Huang J, Yamashiro Y, Papke CL, Ikeda Y, Lin Y, Patel M, Inagami T, Le VP, Wagenseil JE, Yanagisawa H. Angiotensin-converting enzyme-induced activation of local angiotensin signaling is required for ascending aortic aneurysms in fibulin-4-deficient mice. *Science translational medicine*. 2013;5(183):183ra58, 1-11.
66. deAlmeida AC, van Oort RJ, Wehrens XH. Transverse aortic constriction in mice. *Journal of visualized experiments : JoVE*. 2010(38).
67. Schildmeyer LA, Braun R, Taffet G, DeBiasi M, Burns AE, Bradley A, Schwartz RJ. Impaired vascular contractility and blood pressure homeostasis in the smooth muscle alpha-actin null mouse. *FASEB journal : official publication of the Federation of American Societies for Experimental Biology*. 2000;14(14):2213-20.

68. Xiong W, Knispel RA, Dietz HC, Ramirez F, Baxter BT. Doxycycline delays aneurysm rupture in a mouse model of Marfan syndrome. *J Vasc Surg.* 2008;47(1):166-72; discussion 72.
69. Najjar SM, Ledford KJ, Abdallah SL, Paus A, Russo L, Kaw MK, Ramakrishnan SK, Muturi HT, Raphael CK, Lester SG, Heinrich G, Pierre SV, Benndorf R, Kleff V, Jaffa AA, Levy E, Vazquez G, Goldberg IJ, Beauchemin N, Scalia R, Ergun S. Ceacam1 deletion causes vascular alterations in large vessels. *Am J Physiol Endocrinol Metab.* 2013;305(4):E519-29.
70. Regalado ES, Guo DC, Prakash S, Benseid TA, Flynn K, Estrera A, Safi H, Liang D, Hyland J, Child A, Arno G, Boileau C, Jondeau G, Braverman A, Moran R, Morisaki T, Morisaki H, Montalcino Aortic C, Pyeritz R, Coselli J, LeMaire S, Milewicz DM. Aortic Disease Presentation and Outcome Associated With ACTA2 Mutations. *Circ Cardiovasc Genet.* 2015;8(3):457-64.
71. Morisaki H, Akutsu K, Ogino H, Kondo N, Yamanaka I, Tsutsumi Y, Yoshimuta T, Okajima T, Matsuda H, Minatoya K, Sasaki H, Tanaka H, Ishibashi-Ueda H, Morisaki T. Mutation of ACTA2 gene as an important cause of familial and nonfamilial nonsyndromic thoracic aortic aneurysm and/or dissection (TAAD). *Hum Mutat.* 2009;30(10):1406-11.
72. Disabella E, Grasso M, Gambarin FI, Narula N, Dore R, Favalli V, Serio A, Antoniazzi E, Mosconi M, Pasotti M, Odero A, Arbustini E. Risk of dissection in thoracic aneurysms associated with mutations of smooth muscle alpha-actin 2 (ACTA2). *Heart.* 2011;97(4):321-6.
73. Renard M, Callewaert B, Baetens M, Campens L, MacDermot K, Fryns JP, Bonduelle M, Dietz HC, Gaspar IM, Cavaco D, Stattin EL, Schrander-Stumpel C, Coucke P, Loeys B, De

- Paepe A, De Backer J. Novel MYH11 and ACTA2 mutations reveal a role for enhanced TGFbeta signaling in FTAAD. *International journal of cardiology*. 2013;165(2):314-21.
74. El-Hamamsy I, Yacoub MH. Cellular and molecular mechanisms of thoracic aortic aneurysms. *Nat Rev Cardiol*. 2009;6(12):771-86.
75. Peters H, Border WA, Noble NA. Angiotensin II blockade and low-protein diet produce additive therapeutic effects in experimental glomerulonephritis. *Kidney Int*. 2000;57(4):1493-501.
76. Moltzer E, Essers J, van Esch JH, Roos-Hesselink JW, Danser AH. The role of the renin-angiotensin system in thoracic aortic aneurysms: clinical implications. *Pharmacol Ther*. 2011;131(1):50-60.
77. Peters AM ZZ, Chen J, Janda A, Reynolds CL, Kuang SQ, Wang S, Prakash S, GenTAC Consortium, Kwartler CS, Milewicz DM. Pharmacologic Manipulation of the Angiotensin System Affects Aortic Remodeling and Aneurysm Development: Cautions for Clinical Practice. Submitted 2017.
78. Cui R, Tieu B, Recinos A, Tilton RG, Brasier AR. RhoA mediates angiotensin II-induced phospho-Ser536 nuclear factor kappaB/RelA subunit exchange on the interleukin-6 promoter in VSMCs. *Circulation research*. 2006;99(7):723-30.
79. Lyss G, Knorre A, Schmidt TJ, Pahl HL, Merfort I. The anti-inflammatory sesquiterpene lactone helenalin inhibits the transcription factor NF-kappaB by directly targeting p65. *J Biol Chem*. 1998;273(50):33508-16.

80. Lyss G, Schmidt TJ, Merfort I, Pahl HL. Helenalin, an anti-inflammatory sesquiterpene lactone from Arnica, selectively inhibits transcription factor NF-kappaB. *Biol Chem*. 1997;378(9):951-61.
81. Lyle AN, Deshpande NN, Taniyama Y, Seidel-Rogol B, Pounkova L, Du P, Papaharalambus C, Lassegue B, Griendling KK. Poldip2, a novel regulator of Nox4 and cytoskeletal integrity in vascular smooth muscle cells. *Circulation research*. 2009;105(3):249-59.
82. Datla SR, McGrail DJ, Vukelic S, Huff LP, Lyle AN, Pounkova L, Lee M, Seidel-Rogol B, Khalil MK, Hilenski LL, Terada LS, Dawson MR, Lassegue B, Griendling KK. Poldip2 controls vascular smooth muscle cell migration by regulating focal adhesion turnover and force polarization. *American journal of physiology Heart and circulatory physiology*. 2014;307(7):H945-57.
83. Barman SA, Chen F, Su Y, Dimitropoulou C, Wang Y, Catravas JD, Han W, Orfi L, Szantai-Kis C, Keri G, Szabadkai I, Barabutis N, Rafikova O, Rafikov R, Black SM, Jonigk D, Giannis A, Asmis R, Stepp DW, Ramesh G, Fulton DJ. NADPH oxidase 4 is expressed in pulmonary artery adventitia and contributes to hypertensive vascular remodeling. *Arteriosclerosis, thrombosis, and vascular biology*. 2014;34(8):1704-15.
84. Manea A, Tanase LI, Raicu M, Simionescu M. Transcriptional regulation of NADPH oxidase isoforms, Nox1 and Nox4, by nuclear factor-kappaB in human aortic smooth muscle cells. *Biochem Biophys Res Commun*. 2010;396(4):901-7.

85. Rakesh K, Yoo B, Kim IM, Salazar N, Kim KS, Rockman HA. beta-Arrestin-biased agonism of the angiotensin receptor induced by mechanical stress. *Science signaling*. 2010;3(125):ra46.
86. Griendling KK, Minieri CA, Ollerenshaw JD, Alexander RW. Angiotensin II stimulates NADH and NADPH oxidase activity in cultured vascular smooth muscle cells. *Circulation research*. 1994;74(6):1141-8.
87. Weber DS, Rocic P, Mellis AM, Laude K, Lyle AN, Harrison DG, Griendling KK. Angiotensin II-induced hypertrophy is potentiated in mice overexpressing p22phox in vascular smooth muscle. *American journal of physiology Heart and circulatory physiology*. 2005;288(1):H37-42.
88. Oller J, Mendez-Barbero N, Ruiz EJ, Villahoz S, Renard M, Canelas LI, Briones AM, Alberca R, Lozano-Vidal N, Hurle MA, Milewicz D, Evangelista A, Salaices M, Nistal JF, Jimenez-Borreguero LJ, De Backer J, Campanero MR, Redondo JM. Nitric oxide mediates aortic disease in mice deficient in the metalloprotease Adamts1 and in a mouse model of Marfan syndrome. *Nat Med*. 2017;23(2):200-12.
89. Guo DC, Regalado E, Casteel DE, Santos-Cortez RL, Gong L, Kim JJ, Dyack S, Horne SG, Chang G, Jondeau G, Boileau C, Coselli JS, Li Z, Leal SM, Shendure J, Rieder MJ, Bamshad MJ, Nickerson DA, Gen TACRC, National Heart L, Blood Institute Grand Opportunity Exome Sequencing P, Kim C, Milewicz DM. Recurrent gain-of-function mutation in PRKG1 causes thoracic aortic aneurysms and acute aortic dissections. *American journal of human genetics*. 2013;93(2):398-404.

90. Brooke BS, Bayes-Genis A, Li DY. New insights into elastin and vascular disease. *Trends Cardiovasc Med*. 2003;13(5):176-81.
91. Pober BR, Johnson M, Urban Z. Mechanisms and treatment of cardiovascular disease in Williams-Beuren syndrome. *The Journal of clinical investigation*. 2008;118(5):1606-15.
92. Faury G, Pezet M, Knutsen RH, Boyle WA, Heximer SP, McLean SE, Minkes RK, Blumer KJ, Kovacs A, Kelly DP, Li DY, Starcher B, Mecham RP. Developmental adaptation of the mouse cardiovascular system to elastin haploinsufficiency. *The Journal of clinical investigation*. 2003;112(9):1419-28.
93. Rockman HA, Ross RS, Harris AN, Knowlton KU, Steinhilber ME, Field LJ, Ross J, Jr., Chien KR. Segregation of atrial-specific and inducible expression of an atrial natriuretic factor transgene in an in vivo murine model of cardiac hypertrophy. *Proceedings of the National Academy of Sciences of the United States of America*. 1991;88(18):8277-81.
94. Mohammed SF, Storlie JR, Oehler EA, Bowen LA, Korinek J, Lam CS, Simari RD, Burnett JC, Jr., Redfield MM. Variable phenotype in murine transverse aortic constriction. *Cardiovasc Pathol*. 2012;21(3):188-98.
95. Martin TP, Robinson E, Harvey AP, MacDonald M, Grieve DJ, Paul A, Currie S. Surgical optimization and characterization of a minimally invasive aortic banding procedure to induce cardiac hypertrophy in mice. *Experimental physiology*. 2012;97(7):822-32.
96. Lygate CA, Schneider JE, Hulbert K, ten Hove M, Sebag-Montefiore LM, Cassidy PJ, Clarke K, Neubauer S. Serial high resolution 3D-MRI after aortic banding in mice: band

internalization is a source of variability in the hypertrophic response. Basic research in cardiology. 2006;101(1):8-16.

97. Aplin M, Bonde MM, Hansen JL. Molecular determinants of angiotensin II type 1 receptor functional selectivity. Journal of molecular and cellular cardiology. 2009;46(1):15-24.
98. Schleifenbaum J, Kassmann M, Szijarto IA, Hercule HC, Tano JY, Weinert S, Heidenreich M, Pathan AR, Anistan YM, Alenina N, Rusch NJ, Bader M, Jentsch TJ, Gollasch M. Stretch-activation of angiotensin II type 1a receptors contributes to the myogenic response of mouse mesenteric and renal arteries. Circulation research. 2014;115(2):263-72.
99. Wisler JW, Harris EM, Raisch M, Mao L, Kim J, Rockman HA, Lefkowitz RJ. The role of beta-arrestin2-dependent signaling in thoracic aortic aneurysm formation in a murine model of Marfan syndrome. American journal of physiology Heart and circulatory physiology. 2015;309(9):H1516-27.
100. Wu J, You J, Li L, Ma H, Jia J, Jiang G, Chen Z, Ye Y, Gong H, Bu L, Ge J, Zou Y. Early estimation of left ventricular systolic pressure and prediction of successful aortic constriction in a mouse model of pressure overload by ultrasound biomicroscopy. Ultrasound in medicine & biology. 2012;38(6):1030-9.
101. Eberth JF, Gresham VC, Reddy AK, Popovic N, Wilson E, Humphrey JD. Importance of pulsatility in hypertensive carotid artery growth and remodeling. J Hypertens. 2009;27(10):2010-21.

102. Wang S, Gong H, Jiang G, Ye Y, Wu J, You J, Zhang G, Sun A, Komuro I, Ge J, Zou Y. Src is required for mechanical stretch-induced cardiomyocyte hypertrophy through angiotensin II type 1 receptor-dependent beta-arrestin2 pathways. *PloS one*. 2014;9(4):e92926.
103. Miura S, Saku K, Karnik SS. Molecular analysis of the structure and function of the angiotensin II type 1 receptor. *Hypertens Res*. 2003;26(12):937-43.
104. Chang RS, Lotti VJ. Angiotensin receptor subtypes in rat, rabbit and monkey tissues: relative distribution and species dependency. *Life Sci*. 1991;49(20):1485-90.
105. Brassard P, Amiri F, Schiffrin EL. Combined angiotensin II type 1 and type 2 receptor blockade on vascular remodeling and matrix metalloproteinases in resistance arteries. *Hypertension*. 2005;46(3):598-606.
106. Ichiki T, Labosky PA, Shiota C, Okuyama S, Imagawa Y, Fogo A, Niimura F, Ichikawa I, Hogan BL, Inagami T. Effects on blood pressure and exploratory behaviour of mice lacking angiotensin II type-2 receptor. *Nature*. 1995;377(6551):748-50.
107. Daugherty A, Manning MW, Cassis LA. Antagonism of AT2 receptors augments angiotensin II-induced abdominal aortic aneurysms and atherosclerosis. *British journal of pharmacology*. 2001;134(4):865-70.
108. Daugherty A, Rateri DL, Howatt DA, Charnigo R, Cassis LA. PD123319 augments angiotensin II-induced abdominal aortic aneurysms through an AT2 receptor-independent mechanism. *PloS one*. 2013;8(4):e61849.
109. Villalobos LA, San Hipolito-Luengo A, Ramos-Gonzalez M, Cercas E, Vallejo S, Romero A, Romacho T, Carraro R, Sanchez-Ferrer CF, Peiro C. The Angiotensin-(1-7)/Mas

- Axis Counteracts Angiotensin II-Dependent and -Independent Pro-inflammatory Signaling in Human Vascular Smooth Muscle Cells. *Front Pharmacol.* 2016;7:482.
110. Zhang F, Ren X, Zhao M, Zhou B, Han Y. Angiotensin-(1-7) abrogates angiotensin II-induced proliferation, migration and inflammation in VSMCs through inactivation of ROS-mediated PI3K/Akt and MAPK/ERK signaling pathways. *Sci Rep.* 2016;6:34621.
 111. Bihl JC, Zhang C, Zhao Y, Xiao X, Ma X, Chen Y, Chen S, Zhao B, Chen Y. Angiotensin-(1-7) counteracts the effects of Ang II on vascular smooth muscle cells, vascular remodeling and hemorrhagic stroke: Role of the NFsmall ka, CyrillicB inflammatory pathway. *Vascul Pharmacol.* 2015;73:115-23.
 112. Crackower MA, Sarao R, Oudit GY, Yagil C, Kozieradzki I, Scanga SE, Oliveira-dos-Santos AJ, da Costa J, Zhang L, Pei Y, Scholey J, Ferrario CM, Manoukian AS, Chappell MC, Backx PH, Yagil Y, Penninger JM. Angiotensin-converting enzyme 2 is an essential regulator of heart function. *Nature.* 2002;417(6891):822-8.
 113. Jin HY, Song B, Oudit GY, Davidge ST, Yu HM, Jiang YY, Gao PJ, Zhu DL, Ning G, Kassiri Z, Penninger JM, Zhong JC. ACE2 deficiency enhances angiotensin II-mediated aortic profilin-1 expression, inflammation and peroxynitrite production. *PloS one.* 2012;7(6):e38502.
 114. Daull P, Jeng AY, Battistini B. Towards triple vasopeptidase inhibitors for the treatment of cardiovascular diseases. *J Cardiovasc Pharmacol.* 2007;50(3):247-56.
 115. Benigni A, Corna D, Zoja C, Sonzogni A, Latini R, Salio M, Conti S, Rottoli D, Longaretti L, Cassis P, Morigi M, Coffman TM, Remuzzi G. Disruption of the Ang II type 1

receptor promotes longevity in mice. *The Journal of clinical investigation*. 2009;119(3):524-30.

116. Cassis P, Conti S, Remuzzi G, Benigni A. Angiotensin receptors as determinants of life span. *Pflugers Arch*. 2010;459(2):325-32.

117. Oliverio MI, Kim HS, Ito M, Le T, Audoly L, Best CF, Hiller S, Kluckman K, Maeda N, Smithies O, Coffman TM. Reduced growth, abnormal kidney structure, and type 2 (AT2) angiotensin receptor-mediated blood pressure regulation in mice lacking both AT1A and AT1B receptors for angiotensin II. *Proceedings of the National Academy of Sciences of the United States of America*. 1998;95(26):15496-501.

118. Blodow S, Schneider H, Storch U, Wizemann R, Forst AL, Gudermann T, Mederos y Schnitzler M. Novel role of mechanosensitive AT1B receptors in myogenic vasoconstriction. *Pflugers Arch*. 2014;466(7):1343-53.

119. Michel MC, Brunner HR, Foster C, Huo Y. Angiotensin II type 1 receptor antagonists in animal models of vascular, cardiac, metabolic and renal disease. *Pharmacol Ther*. 2016;164:1-81.

120. Nogueira A, Pires MJ, Oliveira PA. Pathophysiological Mechanisms of Renal Fibrosis: A Review of Animal Models and Therapeutic Strategies. *In Vivo*. 2017;31(1):1-22.

121. Liu D, Wang LN, Li HX, Huang P, Qu LB, Chen FY. Pentoxifylline plus ACEIs/ARBs for proteinuria and kidney function in chronic kidney disease: a meta-analysis. *J Int Med Res*. 2017;45(2):383-98.

122. Munoz-Durango N, Fuentes CA, Castillo AE, Gonzalez-Gomez LM, Vecchiola A, Fardella CE, Kalergis AM. Role of the Renin-Angiotensin-Aldosterone System beyond Blood

Pressure Regulation: Molecular and Cellular Mechanisms Involved in End-Organ Damage during Arterial Hypertension. *Int J Mol Sci.* 2016;17(7).

123. Chun AS, Elefteriades JA, Mukherjee SK. Medical treatment for thoracic aortic aneurysm - much more work to be done. *Prog Cardiovasc Dis.* 2013;56(1):103-8.

124. Shores J, Berger KR, Murphy EA, Pyeritz RE. Progression of aortic dilatation and the benefit of long-term beta-adrenergic blockade in Marfan's syndrome. *The New England journal of medicine.* 1994;330(19):1335-41.

125. Groenink M, den Hartog AW, Franken R, Radonic T, de Waard V, Timmermans J, Scholte AJ, van den Berg MP, Spijkerboer AM, Marquering HA, Zwinderman AH, Mulder BJ. Losartan reduces aortic dilatation rate in adults with Marfan syndrome: a randomized controlled trial. *European heart journal.* 2013;34(45):3491-500.

126. Franken R, den Hartog AW, Radonic T, Micha D, Maugeri A, van Dijk FS, Meijers-Heijboer HE, Timmermans J, Scholte AJ, van den Berg MP, Groenink M, Mulder BJ, Zwinderman AH, de Waard V, Pals G. Beneficial Outcome of Losartan Therapy Depends on Type of FBN1 Mutation in Marfan Syndrome. *Circulation Cardiovascular genetics.* 2015;8(2):383-8.

127. Lacro RV, Dietz HC, Sleeper LA, Yetman AT, Bradley TJ, Colan SD, Pearson GD, Selamet Tierney ES, Levine JC, Atz AM, Benson DW, Braverman AC, Chen S, De Backer J, Gelb BD, Grossfeld PD, Klein GL, Lai WW, Liou A, Loeys BL, Markham LW, Olson AK, Paridon SM, Pemberton VL, Pierpont ME, Pyeritz RE, Radojewski E, Roman MJ, Sharkey AM, Stylianou MP, Wechsler SB, Young LT, Mahony L, Pediatric Heart Network I. Atenolol versus

losartan in children and young adults with Marfan's syndrome. The New England journal of medicine. 2014;371(22):2061-71.

128. Forteza A, Evangelista A, Sanchez V, Teixido-Tura G, Sanz P, Gutierrez L, Gracia T, Centeno J, Rodriguez-Palomares J, Rufilanchas JJ, Cortina J, Ferreira-Gonzalez I, Garcia-Dorado D. Efficacy of losartan vs. atenolol for the prevention of aortic dilation in Marfan syndrome: a randomized clinical trial. Eur Heart J. 2016;37(12):978-85.

129. Milleron O, Arnoult F, Ropers J, Aegerter P, Detaint D, Delorme G, Attias D, Tubach F, Dupuis-Girod S, Plauchu H, Barthelet M, Sassolas F, Pangaud N, Naudion S, Thomas-Chabaneix J, Dulac Y, Edouard T, Wolf JE, Faivre L, Odent S, Basquin A, Habib G, Collignon P, Boileau C, Jondeau G. Marfan Sartan: a randomized, double-blind, placebo-controlled trial. European heart journal. 2015;36(32):2160-6.

130. Chiu HH, Wu MH, Wang JK, Lu CW, Chiu SN, Chen CA, Lin MT, Hu FC. Losartan added to beta-blockade therapy for aortic root dilation in Marfan syndrome: a randomized, open-label pilot study. Mayo Clinic proceedings. 2013;88(3):271-6.

131. McNally EM. Cardiomyopathy in Muscular Dystrophy: When to Treat? JAMA cardiology. 2017;2(2):199.

132. Silva MC, Magalhaes TA, Meira ZM, Rassi CH, Andrade AC, Gutierrez PS, Azevedo CF, Gurgel-Giannetti J, Vainzof M, Zatz M, Kalil-Filho R, Rochitte CE. Myocardial Fibrosis Progression in Duchenne and Becker Muscular Dystrophy: A Randomized Clinical Trial. JAMA cardiology. 2017;2(2):190-9.

133. Lindsay ME, Schepers D, Bolar NA, Doyle JJ, Gallo E, Fert-Bober J, Kempers MJ, Fishman EK, Chen Y, Myers L, Bjeda D, Oswald G, Elias AF, Levy HP, Anderlid BM, Yang MH,

Bongers EM, Timmermans J, Braverman AC, Canham N, Mortier GR, Brunner HG, Byers PH, Van Eyk J, Van Laer L, Dietz HC, Loeys BL. Loss-of-function mutations in TGFB2 cause a syndromic presentation of thoracic aortic aneurysm. *Nature genetics*. 2012;44(8):922-7.

134. Wei H, Hu JH, Angelov SN, Fox K, Yan J, Enstrom R, Smith A, Dichek DA. Aortopathy in a Mouse Model of Marfan Syndrome Is Not Mediated by Altered Transforming Growth Factor beta Signaling. *Journal of the American Heart Association*. 2017;6(1).

135. Wang Y, Ait-Oufella H, Herbin O, Bonnin P, Ramkhelawon B, Taleb S, Huang J, Offenstadt G, Combadiere C, Renia L, Johnson JL, Tharaux PL, Tedgui A, Mallat Z. TGF-beta activity protects against inflammatory aortic aneurysm progression and complications in angiotensin II-infused mice. *The Journal of clinical investigation*. 2010;120(2):422-32.

136. Guo DC, Regalado ES, Gong L, Duan X, Santos-Cortez RL, Arnaud P, Ren Z, Cai B, Hostetler EM, Moran R, Liang D, Estrera A, Safi HJ, University of Washington Center for Mendelian G, Leal SM, Bamshad MJ, Shendure J, Nickerson DA, Jondeau G, Boileau C, Milewicz DM. LOX Mutations Predispose to Thoracic Aortic Aneurysms and Dissections. *Circulation research*. 2016;118(6):928-34.

137. Grau-Bove X, Ruiz-Trillo I, Rodriguez-Pascual F. Origin and evolution of lysyl oxidases. *Scientific reports*. 2015;5:10568.

Vita

Andrew Milton Peters was born in Hondo, Texas on January 13, 1987. He is the son of Mary Jo (Rummel) Peters and Douglas Andrew Peters, grandson of Kenneth and Carolyn Rummel and Russell and Frances Peters. After graduating valedictorian at Hondo High School in 2005, he followed his heart to Texas A&M University as a fourth generation Texas Aggie. He graduated Summa Cum Laude with a Bachelor of Science in Biomedical Engineering in May 2009. Ten days later he started in the MD/PhD Program at the University of Texas Medical School at Houston as a Cullen Fellow. The program would eventually be known by the partnership between the McGovern Medical School and the University of Texas MD Anderson Cancer Center UTHHealth School of Graduate School of Biomedical Sciences.